Scanning and statistical evaluation of polymer product surface quality

Bc. Karel Schuch

Master thesis
2012

Tomas Bata University in Zlín
Faculty of Technology

Univerzita Tomáše Bati ve Zlíně

Fakulta technologická

Ústav výrobního inženýrství

akademický rok: 2011/2012

ZADÁNÍ DIPLOMOVÉ PRÁCE

(PROJEKTU, UMĚLECKÉHO DÍLA, UMĚLECKÉHO VÝKONU)

Jméno a příjmení: **Bc. Karel SCHUCH**

Osobní číslo: **T10387**

Studijní program: **N 3909 Procesní inženýrství**

Studijní obor: **Konstrukce technologických zařízení**

Téma práce: **Snímání a statistické hodnocení jakosti povrchu polymerního výrobku**

Zásady pro vypracování:

1) Vypracování problematiky hodnocení jakosti povrchu
2) Popis měřících metod
3) Skenování povrchu polymerního výrobku
4) Volba vhodných parametrů pro vyhodnocení získaných dat
5) Statistické hodnocení získaných dat

Rozsah diplomové práce:

Rozsah příloh:

Forma zpracování diplomové práce: **tištěná/elektronická**

Seznam odborné literatury:

THOMAS, R. Tom. Rough Surfaces. 2nd edition. Imperial College (London) : Imperial College Press, 1999. 278 s. ISBN 1-86094-100-1
WHITEHOUSE, David. Surfaces and their measurement. 1st edition. Hermes Penton Science (London) : Hermes Penton Science, 2002. 425 s. ISBN 1-9039-9601-5
BUMBÁLEK, B.; ODVODY, V.; OŠŤÁDAL, B. Drnost povrchu. Praha : Nakladatelství technické literatury, 1989. 340 s. ISBN 04-252-89
WILEY, John. Fractal Geometry : Mahematical foundations and Applications. 2nd edition. Cornwall (Great Britain) : John Wiley & Sons, 2003. 337 s. ISBN 0-470-84862-6

Vedoucí diplomové práce: **doc. Dr. Ing. Vladimír Pata**
                                Ústav výrobního inženýrství
Datum zadání diplomové práce: **13. února 2012**
Termín odevzdání diplomové práce: **18. května 2012**

Ve Zlíně dne 2. února 2012

doc. Ing. Roman Čermák, Ph.D.   prof. Ing. Berenika Hausnerová, Ph.D.
děkan   *ředitel ústavu*

Příjmení a jméno: …SCHUCH KAREL………………………   Obor: ……KTZ…………

PROHLÁŠENÍ

Prohlašuji, že

- beru na vědomí, že odevzdáním diplomové/bakalářské práce souhlasím se zveřejněním své práce podle zákona č. 111/1998 Sb. o vysokých školách a o změně a doplnění dalších zákonů (zákon o vysokých školách), ve znění pozdějších právních předpisů, bez ohledu na výsledek obhajoby [1];
- beru na vědomí, že diplomová/bakalářská práce bude uložena v elektronické podobě v univerzitním informačním systému dostupná k nahlédnutí, že jeden výtisk diplomové/bakalářské práce bude uložen na příslušném ústavu Fakulty technologické UTB ve Zlíně a jeden výtisk bude uložen u vedoucího práce;
- byl/a jsem seznámen/a s tím, že na moji diplomovou/bakalářskou práci se plně vztahuje zákon č. 121/2000 Sb. o právu autorském, o právech souvisejících s právem autorským a o změně některých zákonů (autorský zákon) ve znění pozdějších právních předpisů, zejm. § 35 odst. 3 [2];
- beru na vědomí, že podle § 60 [3] odst. 1 autorského zákona má UTB ve Zlíně právo na uzavření licenční smlouvy o užití školního díla v rozsahu § 12 odst. 4 autorského zákona;
- beru na vědomí, že podle § 60 [3] odst. 2 a 3 mohu užít své dílo – diplomovou/bakalářskou práci nebo poskytnout licenci k jejímu využití jen s předchozím písemným souhlasem Univerzity Tomáše Bati ve Zlíně, která je oprávněna v takovém případě ode mne požadovat přiměřený příspěvek na úhradu nákladů, které byly Univerzitou Tomáše Bati ve Zlíně na vytvoření díla vynaloženy (až do jejich skutečné výše);
- beru na vědomí, že pokud bylo k vypracování diplomové/bakalářské práce využito softwaru poskytnutého Univerzitou Tomáše Bati ve Zlíně nebo jinými subjekty pouze ke studijním a výzkumným účelům (tedy pouze k nekomerčnímu využití), nelze výsledky diplomové/bakalářské práce využít ke komerčním účelům;
- beru na vědomí, že pokud je výstupem diplomové/bakalářské práce jakýkoliv softwarový produkt, považují se za součást práce rovněž i zdrojové kódy, popř. soubory, ze kterých se projekt skládá. Neodevzdání této součásti může být důvodem k neobhájení práce.

Ve Zlíně …2.5.2012………

…………………………………

[1] zákon č. 111/1998 Sb. o vysokých školách a o změně a doplnění dalších zákonů (zákon o vysokých školách), ve znění pozdějších právních předpisů, § 47 Zveřejňování závěrečných prací:

(1) Vysoká škola nevýdělečně zveřejňuje disertační, diplomové, bakalářské a rigorózní práce, u kterých proběhla obhajoba, včetně posudků oponentů a výsledku obhajoby prostřednictvím databáze kvalifikačních prací, kterou spravuje. Způsob zveřejnění stanoví vnitřní předpis vysoké školy.

(2) Disertační, diplomové, bakalářské a rigorózní práce odevzdané uchazečem k obhajobě musí být též nejméně pět pracovních dnů před konáním obhajoby zveřejněny k nahlížení veřejnosti v místě určeném vnitřním předpisem vysoké školy nebo není-li tak určeno, v místě pracoviště vysoké školy, kde se má konat obhajoba práce. Každý si může ze zveřejněné práce pořizovat na své náklady výpisy, opisy nebo rozmnoženiny.

(3) Platí, že odevzdáním práce autor souhlasí se zveřejněním své práce podle tohoto zákona, bez ohledu na výsledek obhajoby.

[2] zákon č. 121/2000 Sb. o právu autorském, o právech souvisejících s právem autorským a o změně některých zákonů (autorský zákon) ve znění pozdějších právních předpisů, § 35 odst. 3:

(3) Do práva autorského také nezasahuje škola nebo školské či vzdělávací zařízení, užije-li nikoli za účelem přímého nebo nepřímého hospodářského nebo obchodního prospěchu k výuce nebo k vlastní potřebě dílo vytvořené žákem nebo studentem ke splnění školních nebo studijních povinností vyplývajících z jeho právního vztahu ke škole nebo školskému či vzdělávacího zařízení (školní dílo).

[3] zákon č. 121/2000 Sb. o právu autorském, o právech souvisejících s právem autorským a o změně některých zákonů (autorský zákon) ve znění pozdějších právních předpisů, § 60 Školní dílo:

(1) Škola nebo školské či vzdělávací zařízení mají za obvyklých podmínek právo na uzavření licenční smlouvy o užití školního díla (§ 35 odst. 3). Odpírá-li autor takového díla udělit svolení bez vážného důvodu, mohou se tyto osoby domáhat nahrazení chybějícího projevu jeho vůle u soudu. Ustanovení § 35 odst. 3 zůstává nedotčeno.

(2) Není-li sjednáno jinak, může autor školního díla své dílo užít či poskytnout jinému licenci, není-li to v rozporu s oprávněnými zájmy školy nebo školského či vzdělávacího zařízení.

(3) Škola nebo školské či vzdělávací zařízení jsou oprávněny požadovat, aby jim autor školního díla z výdělku jím dosaženého v souvislosti s užitím díla či poskytnutím licence podle odstavce 2 přiměřeně přispěl na úhradu nákladů, které na vytvoření díla vynaložily, a to podle okolností až do jejich skutečné výše; přitom se přihlédne k výši výdělku dosaženého školou nebo školským či vzdělávacím zařízením z užití školního díla podle odstavce 1.

ABSTRAKT

Cílem této práce je popsat problematiku vyhodnocování jakosti povrchu u polymerních materiálů. Teoretická část předkládá obsáhlý popis drsnosti povrchu, jejích charakteristik a současně přináší krátký úvod do teorie fraktálů ve spojitosti s řešením povrchové jakosti, popis metod replikace a výpis statistických veličin. Poznatky z Teoretické části jsou následně zúročeny v části Praktické, která popisuje vyhodnocení jednoho z naměřených vzorků společně s detailní diskuzí výsledných hodnot.

Klíčová slova: Povrch, kvalita, drsnost povrchu, 3D měření, 3D snímání, Gaussův filtr, Robustní Gaussův filtr, měřící zařízení, Talysurf, Talymap, polymer, fraktál, polykarbonát, statistické vyhodnocení, Minitab, zatékavost taveniny, replikace povrchu

ABSTRACT

This work's goal is to describe the issues of surface quality evaluation for polymeric materials. The Theoretical part provides a comprehensive description of the surface roughness characterization, its measuring and evaluating, altogether with brief introduction to the fractals in connection with surface assessment, description of surface replication methods and list of statistical variables. Knowledge from the Theoretical part is applied in the Analysis part which describes the evaluation of one of the samples together with detailed discussion of the resulting data.

Keywords: Surface, quality, roughness, 3D measurement, 3D scanning, Gauss filter, Robust Gauss filter, measuring devices, Taysurf, Talymap, polymer, fractal, polycarbonate, statistical evaluation, Minitab, melt fluidity, surface replication
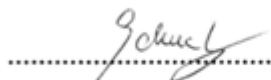
ACKNOWLEDGEMENTS

First of all I would like to thank to my supervisor doc. Vladimir Pata for the time, care and knowledge he passed on me. His support was really important for me and not only in case of this Master thesis. My thanks also go to doc. Anežka Lengálová for her intensive help during the creation of this work and also for all the time she spent with correction of the text from the Theoretical part.

Finally, I would like to thank to every member of my family – for their care and love far more greater than I deserved; my friends and colleagues for all the great times we enjoyed together during the studies. And at last, but the most to our Lord Jesus Christ for everything I have, for everything I am.

I hereby declare that the print version of my Master's thesis and the electronic version of my thesis deposited in the IS/STAG system are identical.

In Zlin

....
Signature of the graduate

CONTENTS

INTRODUCTION

Evaluation of surface quality in recent years has developed into an operation that, because of its importance, determines production parameters and expenses. Surface roughness controlling has become an ordinary part of the output control in manufacturing and an essential element for production drawings. However, this assessment includes mostly metal parts. It is because roughness measurement was originally developed primarily for the evaluation of metallic surfaces. In case of polymer materials, which are increasingly used in manufacturing nowadays, the method of surface roughness evaluation has not been sufficiently adjusted yet. For the specification of polymer product surface roughness construction engineers/producers refer in most cases to surface quality of the forming tool or they do not state the roughness at all.

The aim of this work is to describe the designed methodology of surface roughness measuring of an injection molded polymeric (polycarbonate) product and comment in detail an assessment of surface quality of the polymeric part together with statistical evaluation of the retrieved data.

For this purpose, the Theoretical part embraces the surface roughness issues from the variables description up for filtering and measuring methods as well as slight introduction to the theory of fractals in connection with surface quality evaluation, and description of surface scanning device - Taylor & Hobson's Talysurf 500, which was used for measurement. Furthermore, it mentions the ways of surface replication, and at the end of the Theoretical part is enclosed the list of statistical variables for basic statistical evaluation.

The Analysis part contains, among the others, detailed description of samples preparation with thorough commentary on the measurement assumptions, which explains individual decisions that were made during the evaluation. This section is followed by comprehensive description of one of the samples data, which were gathered by evaluation software Talysurf 5, in connection with final results processing, where measured data of individual samples are compared among themselves by time series plots created in statistical software Minitab 14. For this comparison Ra, Rz, Rt variables and fractal dimension were used.

I. THEORY

1   SURFACE ROUGHNESS

Nowadays, it is well known that not all surfaces are strictly flat as they look. Actually, when using a microscope, rough valleys and peaks can be seen instead of simple planar surface. It is a result of mechanical machining, corrosion, wear of material and of course it is also the natural state of all surfaces. The most important for manufacturing process is roughness obtained from mechanical machining – its measuring is the crucial part of output control in production.

1.1   Importance of surface roughness quality

The surface roughness affects a very wide spectrum of technical activity. Surface quality is important in tribology, production engineering, aircraft engineering, bioengineering and many other fields of science and technology.

Surface metrology has two important roles. It helps to control manufacture - manufacturing process and the machine tool, and also helps to optimize the function. The result of these roles has a great impact on quality. Control of manufacture supports repeatability and also the quality of conformance. Functional optimization contributes to quality of design. Surface texture sometimes influences the function positively but in many cases it can be detrimental. For example, in tribology where the peak to valley height of the roughness must by lower than the thickness of oil layer. Otherwise the result will be metal to metal contact. [2, 8]

It would be ideal to test functionality (resistance to wear, friction, etc.) of the surface by imitating its function in terms of loads, speeds and materials. However this is not possible because of the spread of parameter values and too many configurations. Instead of this direct approach, an indirect method is used – the alternative is to measure the quality of the surface and with use of experience and available theory the likely performance of the surface is estimated. [1, 2]

1.2   Types of surfaces

As already mentioned, the surface roughness in production is a result of the manufacturing process and applied tool. Table 1 shows the variety of surface roughness resulting from different processes. It displays the range of 0,05μm to 25μm.

Tab. 1 – Typical roughness values obtained by different finishing process [2]

Process	Roughness (Ra) [µm]									
	0,05	0,1	0,2	0,4	0,8	1,6	3,6	6,3	12,5	25
Superfinishing	▓	▓								
Lapping	▓	▓	▓							
Polishing		▓	▓							
Honing		▓	▓	▓						
Grinding		▓	▓	▓	▓					
Boring				▓	▓	▓	▓			
Turning				▓	▓	▓	▓			
Drilling						▓	▓			
Extruding					▓	▓				
Drawing					▓	▓				
Milling					▓	▓	▓			
Shaping					▓	▓	▓	▓	▓	
Planing					▓	▓	▓	▓	▓	

When using microscope it can be seen that surfaces are very different not only by heights of peaks and valleys but also by their shapes. For example grinding or milling generates rather symmetrical shape (*Fig. 1*). On contrary, honing surface appears as asymmetrical (*Fig. 2*). [1, 2, 19]
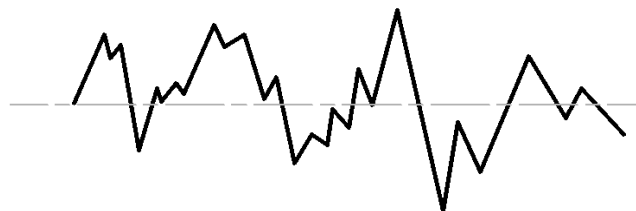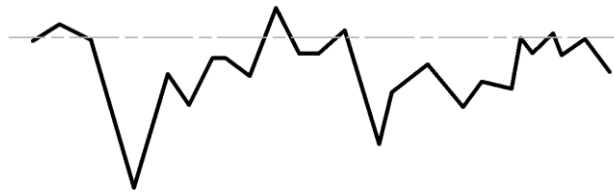

Fig. 1 – Symmetrical surface

Fig. 2 – Asymmetrical surface

These types of distribution of material are very important and must be included in the evaluation of the surface. It is because of a different approach in measuring – asymmetrical surface has large valleys, but almost no peaks in response to the mean line. According to this fact, it can be evaluated in two ways. An improper way is to ignore these geometrical properties, the result will be quite rough surface, similar to surfaces machined by grinding or milling. The proper way takes in account the shape of surface and in evaluation uses other surface characteristic than Ra. This problem will be discussed later in more detail.

Another problematic surface is that with hidden features (*Fig. 3*), which can be found within porous and composite materials and also cast iron. In these cases the X – rays or ultrasonic techniques are used. It is important to say that these hidden features are not involved in contact applications but are useful in the area of lubrication and plating. [1, 2, 7, 19]
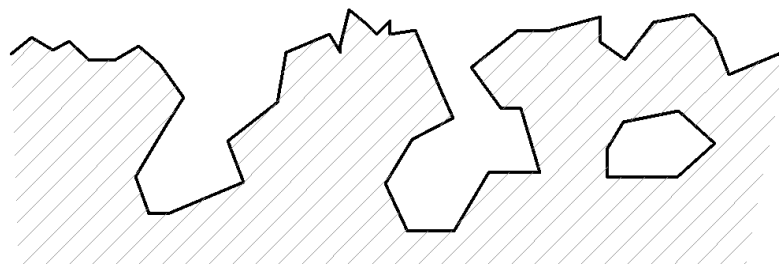

Fig. 3 – Cross section inside surface skin of porous material

2 SURFACE PARAMETERS

To evaluate the measured surface, it is important to take into account a number of surface characteristics and properties. There are many parameters that are used to describe surface and in many cases it is not simple to decide which one to use to get a reliable result. It starts from filtering roughness, waviness and form to get an assessable result. For acquired profile it is needed to find corresponding parameters as are Ra, Rz, Rt etc.. Important also are spacing parameters, amplitude parameters and other special (hybrid).

2.1 Roughness, waviness, form

Measured surface is during manufacture effected by the process and by the tool. These influences are projected on the machined surface as roughness and waviness. Roughness is a result of the machining process and has a short wavelength. Waviness, on the other hand, is an avoidable consequence of vibrations caused by stiffness or balance problems. It has a long wavelength. In addition to roughness and waviness, the weight deflections or long thermal effects cause errors in general shape of machined part. [2, 8, 16, 19]
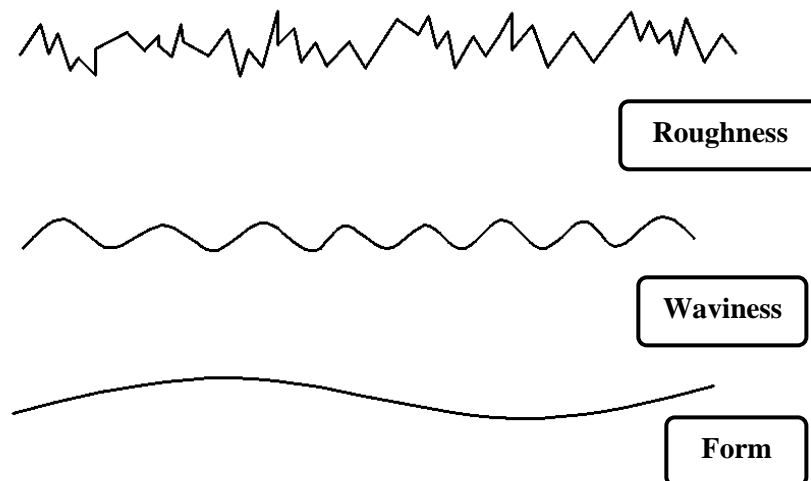

Fig. 4 – Breakdown of surface

A special type of assessed surfaces are the stratified one. They are created by more than just one machining operation and the result is a multi-texture surface. Most of these surfaces are even asymmetrical and cannot be evaluated by common techniques and parameters. The measured surface must be processed by a robust filter (e.g. robust Gaussian filter), and frequency parameters such as Rsk, Rku, RMR and RMS must be used for evaluation. Above that, measurement must be repeated several times. [16, 17, 19]

2.2 Filtering

The filtering is used for separation of roughness, waviness and form. This is one of the most important operations needed for effective surface evaluation. By separating surface profile into these forms, it is also possible to map the frequency spectrum of these to the manufacturing process that generated it. [3, 16]

To obtain roughness, other wavelengths (waviness and form) must be blocked. Transformed wavelengths then constitute mean lines in the filtered profile. [2] Mean line for roughness profile (*Fig. 5*) is line, that is corresponding to wavelength get from profile filter λ_c. On the other hand, the mean line for waviness profile is line, that is corresponding to wavelength get from profile filter λ_f. Finally, the mean line for primary profile is line determined by fitting a least – squares line of nominal form through the primary profile. [4, 5, 16]
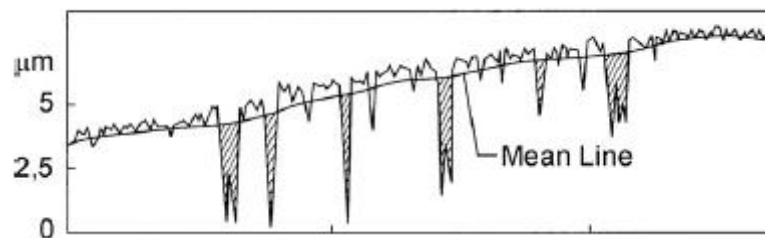
Fig. 5 – Unfiltered profile

2.2.1 Gaussian filter

The Gaussian filter is the most used filter to derive data from surface roughness measurement. It is described in ISO 11562 and ASME B46.1. The principle of this linear filter is in replacing of every point on the profile or surface by a weighted average of points in its neighborhood. [3, 4, 6, 16]


*Fig. 6 – Use of Gaussian filter [4]*

The Gaussian filter has a linear phase and 50% transmission at the cut – off, the waviness can be calculated by simple subtraction of roughness from the measured profile. The main shortcomings of this filter, however, are presence of edge effects and resulting limitation in the use of the first and last cut – off, and poor performance on surfaces with deep valleys. Because of the elimination of the first and last cuts, the Gaussian filter is not applicable for measuring of very short profiles. [3, 6]

2.2.2 Robust Gaussian filter

The purpose of the robust filter is to suppress disadvantages of the simple Gaussian filter. The robust Gaussian filter is non-linear and generates a mean line which is not affected by deep valleys or problematic features of the profile. The robust solution of Gaussian filter is defined by ISO TS 16610 – 31 and for result computations uses iterative statistical method. Thus the robust Gaussian filter can be used for assessing of asymmetrical surfaces and for surfaces machined by more than one technology – stratified surfaces. Comparison of simple and robust Gaussian filters (*Fig. 7*) shows the plain deflection of the mean line in case of the simple Gaussian filter, while the mean line of the robust Gaussian filter remains unaffected by deep valley of the measured profile. [4, 7, 17, 19]
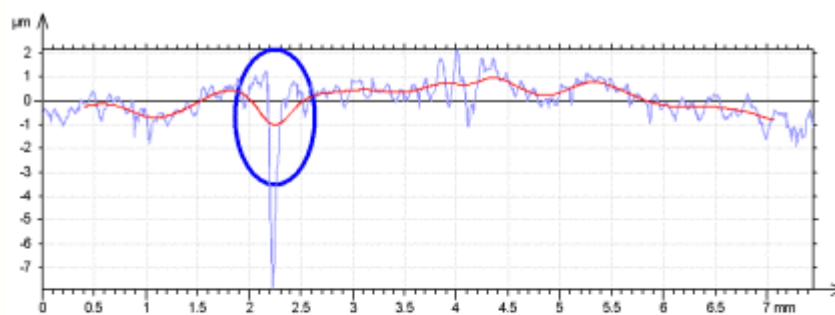
Gaussian filter
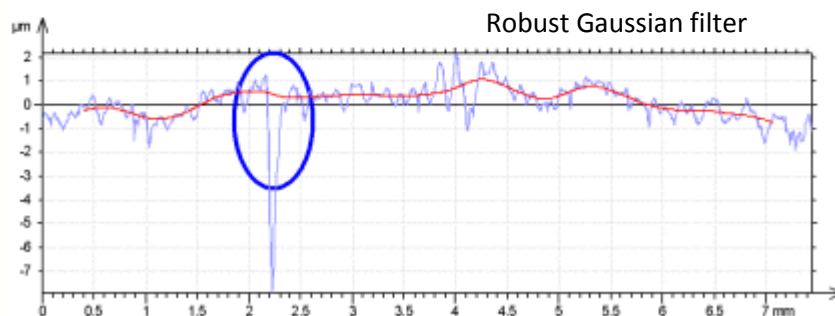
Robust Gaussian filter

Fig. 7 – Comparison of simple Gaussian filter and robust Gaussian filter [4]

2.3   Profile parameters

Profile parameters can be calculated respectively on the raw profile, or after filtering: on the roughness profile, or on the waviness profile. For each parameter is defined type of filter and cut – off. The result is that for one parameter there can be several occurrences with different settings. The parameters from ISO 4287 standard are defined on sampling or evaluation length. Parameters estimated on sampling length are averaged on all the measured sampling lengths (indicated in ISO 4288 standard). [4, 18, 20]

2.3.1   Sampling length

"Sampling length is the length on which surface finish parameters are calculated. On a filtered roughness or waviness profile, the sampling length is equivalent to the length of the cut-off. On a raw profile, the sampling length is equivalent to the total length of the profile called evaluation length. The ISO 4288 standard indicates that a parameter calculated on a sampling length is called assessed parameter (or parameter evaluator). The parameters are calculated on each sampling length and are then expressed as the average on the number of sampling lengths used."[4]

The purpose of sampling length is in including enough surface within it for evaluation of its parameters, and in precluding the waviness of the measured surface. Hence, the decision of the dimension of sampling length is very important for further evaluation. It is usual to arrange five sampling lengths within one assessment length (the length over which surface data are acquired and assessed). In case of surface generated by more than just one process where it is difficult or impossible to separate all the components, it is important to choose an adequate sampling length to cover all the effects of machining process. As displayed in *Fig. 8*, the common sampling length L1 (0,8mm) is too short in this case and does not includes the deep valleys of the measured surface. Therefore, the sampling length L2 is more suitable because the deep valleys will be always included in this longer dimension (its size moves from 0,8 to 2,5mm). [2, 4, 18, 20]
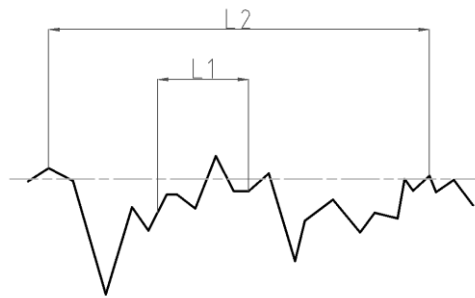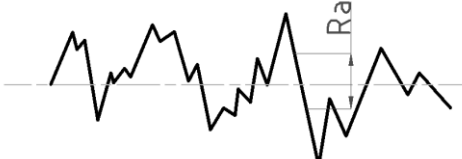
Fig. 8 – A multi-process surface

2.3.2 Amplitude parameters

Amplitude parameters describe the distribution of heights of the assessed profile. They are normalized by ISO 4287 standard. The reference plane for their evaluation serves the mean plane of the measured surface. [4]

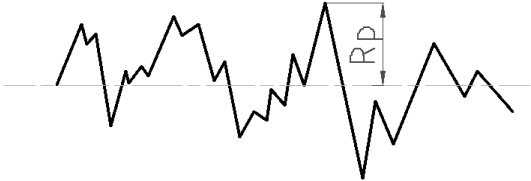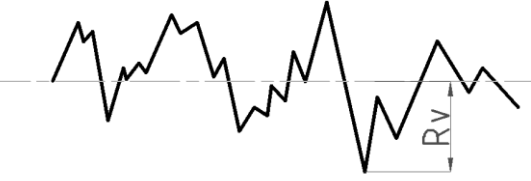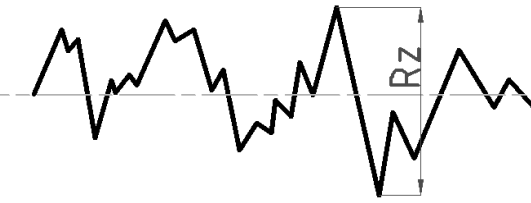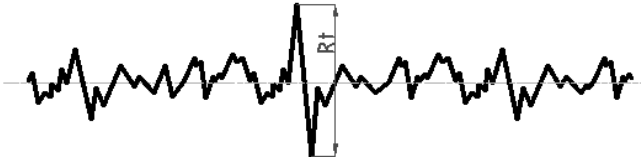Amplitude parameters can be divided into these groups [1]:

‒ Average parameters (Rq, Ra)

Tab. 2 – Amplitude parameters – average parameters [4, 18, 20]

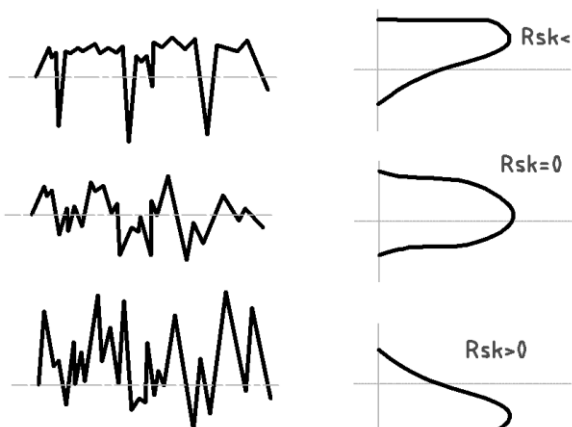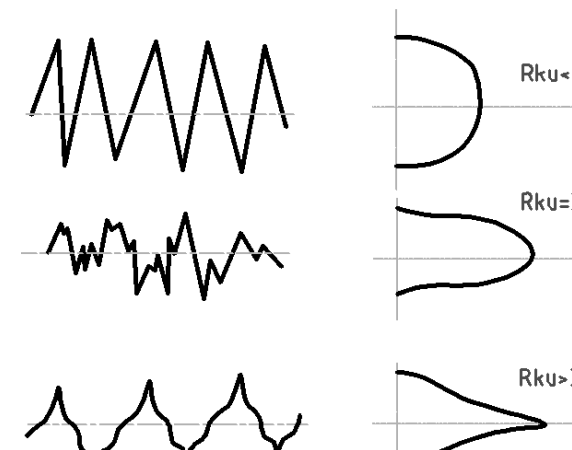| Parameter name	Mark	Explanation
Arithmetic mean deviation of the assessed profile	Ra	$$Ra = \frac{1}{L} \times \int_{0}^{L} |z(x)| d(x)$$
Root-Mean-Square (RMS) deviation of the assessed profile	Rq	Parameter Rq differs from parameter Ra by use of different type of measuring device. For Ra AC signal is passed through the rectifier to charge up the capacitor. In case of Rq is electrical signal passed through an AC voltmeter [1]. Rq means Root mean square average of the roughness profile ordinates. $$Rq = \sqrt{\frac{1}{L} \times \int_{0}^{L} |z^2(x)| d(x)}$$

– Extreme – value parameters (Rt, Rp, Rv, Rz) are, unlike the average parameters, unaffected by mathematical operations and have a direct informative value.

Tab. 3 – Amplitude parameters – extreme-value parameters[4, 18, 20]

Parameter name	Mark	Explanation
Maximum profile peak height within a sampling length	Rp	
Maximum profile valley depth within a sampling length	Rv	
Maximum height of the profile within sampling length	Rz	
Mean height of the elements of the profile, inside a sampling length	Rc	Parameter Rc expressed on a sampling length determined by segments with interval between two growing zero crossings.
Total height of the profile on the evaluation length	Rt	This parameter is very sensible to abnormal points included on the evaluated surface (deep holes or extreme peaks).

– Height distribution parameters (Rsk, Rku); the importance of these parameters is in description of surface roughness shape.
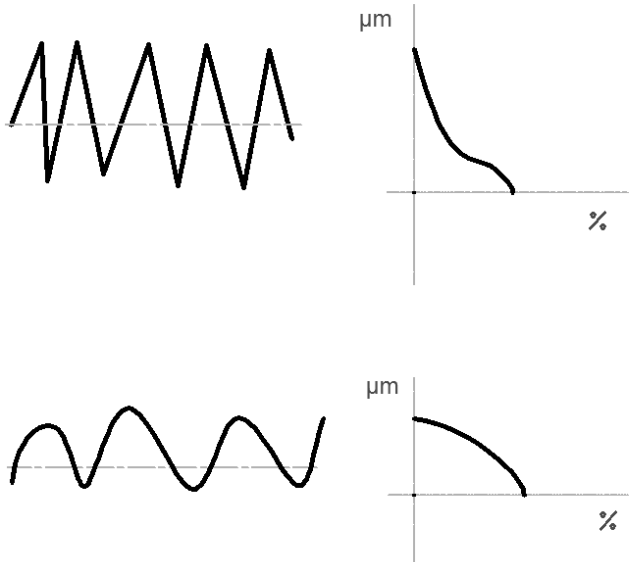
Tab. 4 – Amplitude parameters – height distribution parameters [4, 18, 20]

Parameter name	Mark	Explanation
Skewness (asymmetry) of the assessed profile	Rsk	Skewness parameter describes how much the surface roughness profile is symmetrical to the mean line of the roughness profile. Three types of the parameter are distinguished:
Kurtosis of the assessed profile	Rku	Kurtosis parameter describes the shape of roughness profile according to its sharp and blunt shapes and their distribution along the mean line of the roughness profile

2.3.3 Material ratio parameters

The main parameter of this type is relative material ratio parameter - sometimes called bearing ratio. This parameter is very important because it expresses "*the sum of the lengths of individual plateaus at a particular height, normalized by the total assessment length"[1]*. Information obtained from this parameter is useful for detailed description of measured surfaces – especially of asymmetrical surfaces with big valleys and almost no peaks. In case of components used with tribological interactions the material ratio parameter is one of crucial surface roughness characteristics. [1, 2]

Tab. 5 – Material ratio parameters [4, 18, 20]

Parameter name	Mark	Explanation
Relative material ratio	Rmr	Ratio of the material-filled length to the evaluation length at the profile section level expressed in percent. Material ratio curve (Abbott-Firestone curve) shows the material ratio Rmr as a function of the profile section level.
Profile section height difference	Rdc	Expresses vertical distance between two cut levels given by their bearing ratio.

2.3.4 Spacing parameters

Spacing parameters are used for description of measured surface distribution along the sampling length. The most used spacing parameter is Rsm parameter. With this parameter it is possible to find the mean width dimension of the surface elements. [11]

Tab. 6 – Spacing parameters [4, 11]

Parameter name	Mark	Explanation
Mean width of profile elements, within a sampling length	Rsm	Arithmetic mean of widths R_s on sampling length.
Root-Mean-Square (RMS) slope of the profile within a sampling length	Rdq	Result of RMS, expressed in degrees.

2.3.5 Peak parameters

Tab. 7 – Peak parameters [4]

Parameter name	Mark	Explanation
Peak count	RPc	Expresses number of peaks per centimeter – each peak higher than the upper threshold and lower under the threshold. The threshold is defined by a band, symmetrically separated around the mean line (result is expressed in peaks/cm).

3 FRACTALS

Geometrical irregularities in dimensions of naturally created subjects led to need of more specific way of dimension evaluation, which would guarantee more accurate results. First from researchers who came with idea of the application of fractal geometry was Benoit Mandelbrot, who introduced the idea on a simple example of imaginary measurement of the UK perimeter. He showed that with increasing precision of measuring, the dimensions are more and more accurate because more details are captured. The first measurement was done with one hundred kilometers long fractal units, and the length of coastline was approximately two thousand and eight hundred kilometers. The second attempt was done with fifty kilometers and the value obtained was apparently higher - three thousand and forty kilometers long coastline. [9]

Fig. 9 – Coastline paradox

The Mandelbrot´s idea was that fractals can describe irregular objects which cannot be expressed in common topological dimensions. These, in general, can be expressed by: smooth curve (1 – dimensional) and surface (2 – dimensional). *"The topological dimension of a set is always an integer and is 0 if it is totally disconnected, 1 if each point has arbitrarily small neighborhoods with boundary of dimension 0, and so on."*. [10]

An example of simple fractals can be the Cantor set. It is constructed from lines (interval from 0 to 1) with application of repeated removal of their middle third. In the end the result is infinite and uncountable set F. This set is self-similar, it is created from copies of itself

in different scales. The Cantor set contains details at small scales and although it is infinite, its size is not quantified by usual measures. [9, 10]
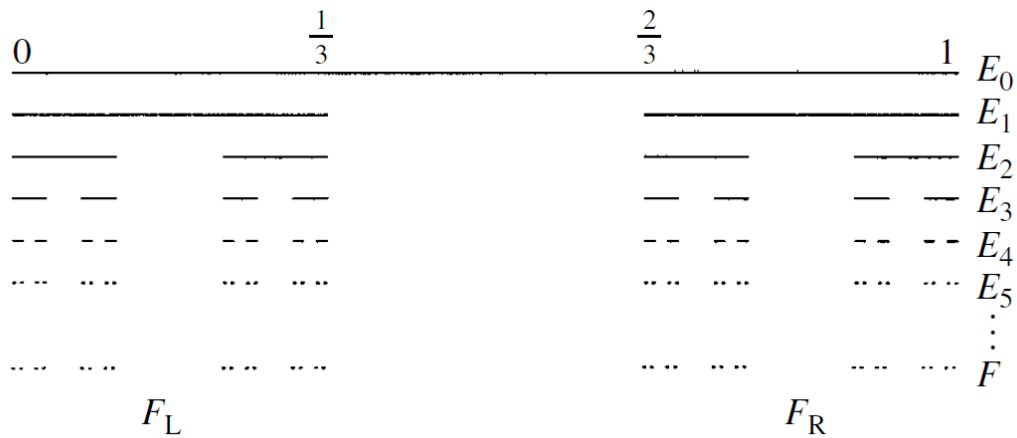

Fig. 10 – Cantor set

The properties of this set are considered to be common properties of the basic definition of fractals [9, 10, 15]:

- Details on small scales
- Irregularity, impossibility to be described by traditional geometrical language
- Often self-similarity (*Fig. 12*)
- The value of fractal dimension is greater than the topological dimension

3.1 Calculation of fractal dimension

The irregularity of the measured shape is described by Hausdorff – Besicovitch dimension F. For fractal-shaped objects dimension F is greater than the topological dimension. One of properties of non-fractal objects is that with an increasing magnitude of the measuring device, the measured dimension is approaching to the real value. On the other hand, in case of fractals, the measured dimension is ever-increasing. This is called the Richardson effect. [9]

Calculation of fractal dimension is based on division of the measured size and number of self-similar sections (description from source [9]). For example in case of line (1D object) divided into five parts (increase of magnitude), the length of one part will be:

$$r = \frac{1}{5} \implies r = \frac{1}{N} \text{ (in general form)}$$

In case of square (2D object) divided into twenty-five parts, the length of one part will be:

$$r = \frac{1}{5} \implies r = \frac{1}{N^{\frac{1}{2}}} \text{ (in general form)}$$

As similar situation also exists within 3D objects. The relation is:

$$r = \frac{1}{N^{\frac{1}{3}}}$$

The universal formula for calculation of the length of divided subjects then is:

$$r = \frac{1}{N^{\frac{1}{D}}}$$

where *D* (in case of refering to fractal dimension *F* mark is often used) is dimension of the solved object. *N* means the total number of distinct copies similar to the original object, and 1/r is the factor of change of scale.

With application of logarithms, dimension *D* can be expressed by this relation:

$$log r = -log N^{\frac{1}{D}}$$

From this:

$$D = \frac{log N}{log \left(\frac{1}{r}\right)}$$

Using this equation it is possible to express topological dimension within regular objects and also Hausdorff − Besicovitch dimension within fractal objects. In addition it serves for distinction between fractal objects and geometrically regular objects.

The basic idea of calculation of fractal dimension can be explained on von Koch curve (*Fig. 11*). With every transformation the length of every line is divided into thirds and the number of self-similar section *N* is four. The equation for this transformation will be:

$$F = \frac{log 4}{log 3} = 1.262$$

Fractal dimension for the Cantor set (*Fig. 10*) then is:

$$F = \frac{log 2}{log 3} = 0{,}631$$
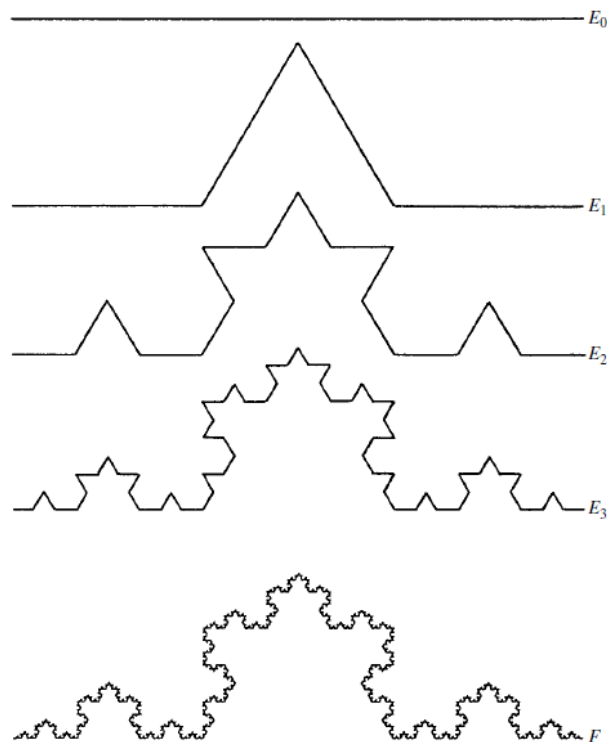
E_0

E_1

E_2

E_3

F

Fig. 11 – Construction of von Koch curve

3.2 Use of fractal geometry in surface roughness evaluation

Fractal dimension can be used for description of the surfaces in one value. For the assessment of surface or profile there are several types of calculations [4]:

- The method of including boxes
- The method of morphological envelopes.

Tab. 8 – Fractal values for different machining methods [1]

Machining process	D
Grinding	1.17
Turning	1.18
Bead-blasting	1.14
Spark erosion	1.39

3.2.1 The method of including boxes

The principle of this method is in enclosing each section of the profile by a box with a certain width (ε). The area Aε is then calculated from all the boxes that are included in the assessed profile. Measuring is repeated with the use of different widths of boxes and a graph ln(Aε)/ln(ε) is output result. In case of 3D measurement, the method can be extended to build a volume graph ln(Vε)/ln(ε). [4, 15]

3.2.2 The method of morphological envelopes

This method uses instead, of boxes, the upper and lower envelopes, *"calculated by morphological opening and closing using a structuring element which is a horizontal line segment of length ε."* From enclosing between elements is then calculated area Aε. Again, measuring is repeated with the use of structuring elements of different lengths to build a graph ln(Aε)/ln(ε). Volume graph ln(Vε)/ln(ε) for surfaces can be also built, as in previous case. [4]

3.2.3 Volume-scale graph

As a result of the methods described above a graph is plotted as a function of the scale (size of boxes or structuring elements) expressing calculated volume (in case of surfaces) or calculated area (in case of profiles). Axes are expressed in logarithmic scale, however, the values of graduations are in dimensional units. [4]

3.2.4 Calculated parameters

Tab. 9 – Calculated parameters for fractal analysis [4]

Slope	Slope of the regression line	Parameters calculated for two regression lines - one connecting the points to the left of the graph, the other connecting the points to the right. This enables to analyze multi-fractal curves with two different slopes depending on the scales in the analysis.
R^2	Correlation coefficient of the regression line	
D (F)	Fractal dimension	The fractal dimension is calculated from the slope of the first regression line.

3.2.5 Solving self-similarity

Self-similarity is significant for simple calculation of fractal dimension. Most of machined surfaces used to be produced by several processes. However to measuring instruments these surfaces appear as single-valued. Thus smaller features are considered to have steeper slopes than larger features. Hence, it is important with the change of observation scale also modify the scale of length dimension for restoration of the appearance of self-similarity appearance. [1]
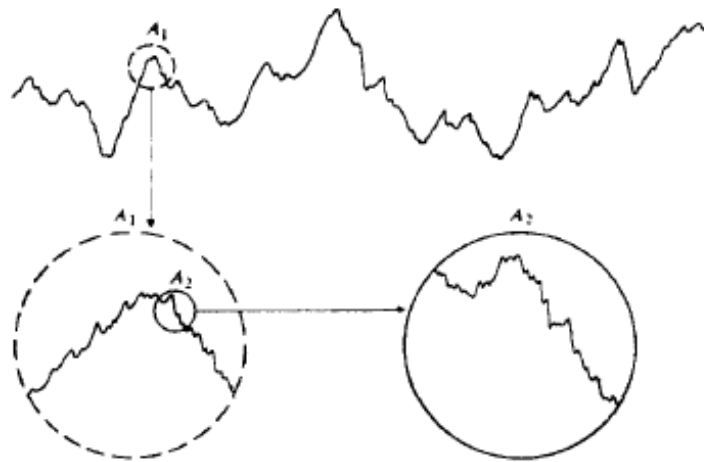
Fig. 12 – Self-similarity of surface profile [1]

4 MEASURING DEVICES

During the twentieth century there was great development in surface roughness measurement. Especially measuring devices used to scan the assessed surface were rapidly developing. The task of this chapter is to summarize the basic devices for surface roughness measuring and to explain methods of their evaluation.

4.1 Stylus devices

Stylus devices are the most used instruments in roughness measurement. These devices are working on the principle of phonograph or gramophone, where the sharp probe with a very small radius traces the paths on surface and transforms its irregularities into another form of energy. Stylus devices can be divided into mechanical and electrical types. [1, 2, 8]

Mechanical devices are based on a simple use of leverage mechanism enhanced by scale installation. Electrical devices use transformation of the acquired signal into analogue changes of voltage or induction. [8] The most important categories are described in the following.

4.1.1 Electromagnetic devices

Electromagnetic devices employ a magnetic circuit created by permanent magnet (1) and pole attachments (2). Change of voltage is generated by oscillation of stylus (4), mounted in the anchor (3) in a coil (5). Hence electrical voltage is inducted in the coil and is proportional to the change of movement speed of the measuring stylus. [8]
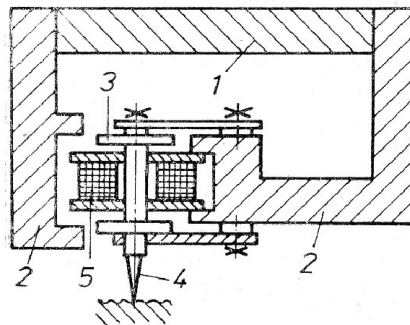
Fig. 13 – Scheme of electromagnetic device [8]

4.1.2 Piezoelectric devices

Piezoelectric measuring devices are based on deformation of plates made of quartz crystals, tourmaline or barium-titanate. When stressed by bending or pressed by measuring stylus (1) these plates (2) have opposite charges on opposite sites. The measured output is electrical voltage which is proportional to stress of the plates. [8]
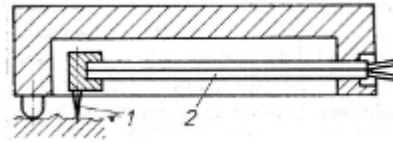

Fig. 14 – Scheme of piezoelectric
device [8]

4.1.3 Electro-inductive devices

In this case, the change of position of the measuring stylus causes a change of impedance of the electrical circuit – most often change of inductance. There are two basic construction types of this device [8]:

a) The measuring stylus (1), *Fig. 15*, changes the slope of two-arm lever (2) and this causes variation in size of the air gap between magnetic circuit (3, 4) and consequently inductance (5, 6). The rotary point (7) of the lever is chosen to ensure symmetrical change of the air gap on both sides of the device. [8]
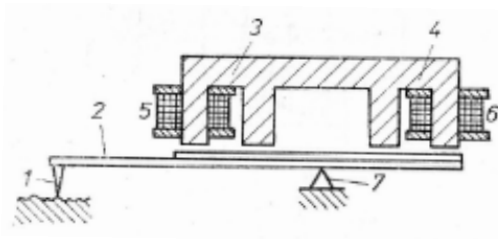
Fig. 15 – Scheme of electro inductive
device [8]

b) During the change of the position of stylus (1), *Fig. 16*, on the rotary point (6) there is a variation in inductance incurred by the movement of ferromagnetic core (3) inside the coil (4) (in some cases two coils arranged one above the other – part 5 in *Fig. 16*). [8]
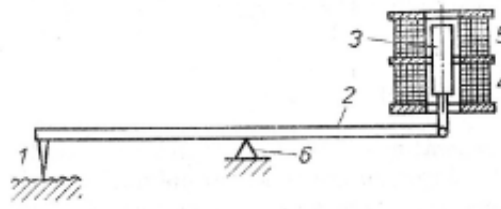
Fig. 16 – Scheme of electro inductive device with movable ferromagnetic core [8]

4.1.4 Capacitive devices

The basis for this type of measuring device are two isolated plates from electrical inductive material. They create a measuring capacitor (2) on which the change of capacity is measured. This change is caused by variation in the distance between isolated plates caused by moving stylus (1). [8]
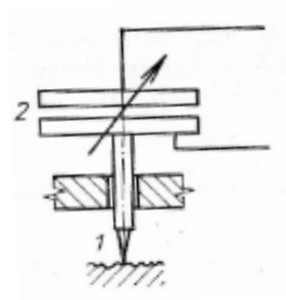

Fig. 17 – Scheme of electro capacitive device [8]

4.1.5 Possible measuring errors and problems

Advantages of stylus measuring in comparison with other methods are in fact that the stylus during scanning can push aside debris from machining and other particles which would affect the result. It can also penetrate residuary oil film which also depreciates the geometry of the measured surface. [2]

Besides these positive characteristics there are also some problems that should not be underestimated and had to be dealt with. They are [1]:

a) The effect of stylus size:
  – The measuring stylus has an angle of 60° or 90° and the tip radius of curvature of 2, 5 or 10 micrometers. In case of very accurate measurements in the order of micrometer units or profile with a lot of steep peaks and val-

leys, the dimension of the tip may be inappropriate and the result of measuring can be inaccurate. [1]

– The measuring can be also affected by losing the contact with profile steep slopes as a result of speed of the traverse. [1]
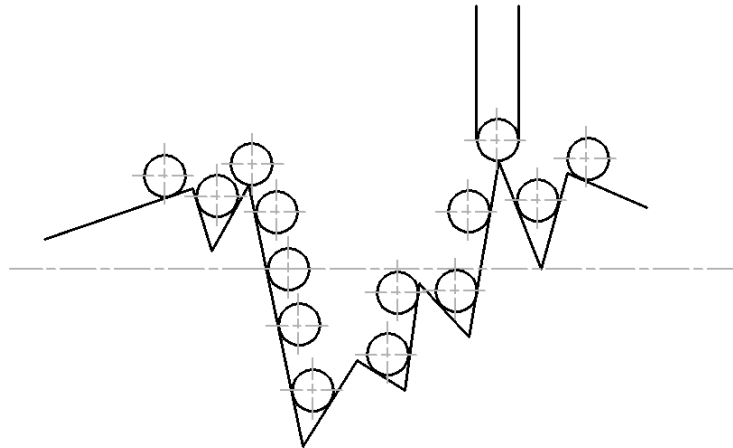

Fig. 18 – Illustrative example of the difference between the shape of surface and stylus trace [1]

b) Effect of stylus load

– In case of surface deformation during the measurement no elastic deformation was discovered within metal materials (Timoshenko and Goodyear, 1951). On the other hand, there have been some discoveries of plastic deformation of measured surfaces caused by the stylus tip. The result showed that stylus leaves a trace tens of nanometers deep. Simultaneously with this research some comparative experiments were done by Reason (1944) with different values of stylus load. The result was that the measured surface profiles were almost identical. [1]

– In case of plastic and soft materials, however, the situation is slightly different and use of stylus device for surface roughness measuring of polymer materials must be considered. The same applies for elastomeric (flexible) materials, where the deformation with standard stylus load can be about one hundred micrometers. [1]

4.2 Optical devices

Measuring the roughness of surfaces by optical methods is possible due to the reflection of optical rays on the measured surface. Radiation can be, in contact with the measured surface, reflected in two different ways and their combination – specularly or (and) diffusely. In case of specular reflection, optical beam follows Sneel´s law: "Angle of reflection is equal to angle of incidence". This applies to surfaces that are considered smooth. For diffuse reflection the Lambert´s law is obeyed: "Reflection is totally diffuse when the energy in the incident beam is distributed as the cosine of the angle of reflection". Reflections from real surfaces are in most cases combination of both phenomena and there is certain relationship between used wavelength of optical beam and the texture of measured surface. [1, 2, 12]

Combined reflection

Specular reflection

Diffuse reflection
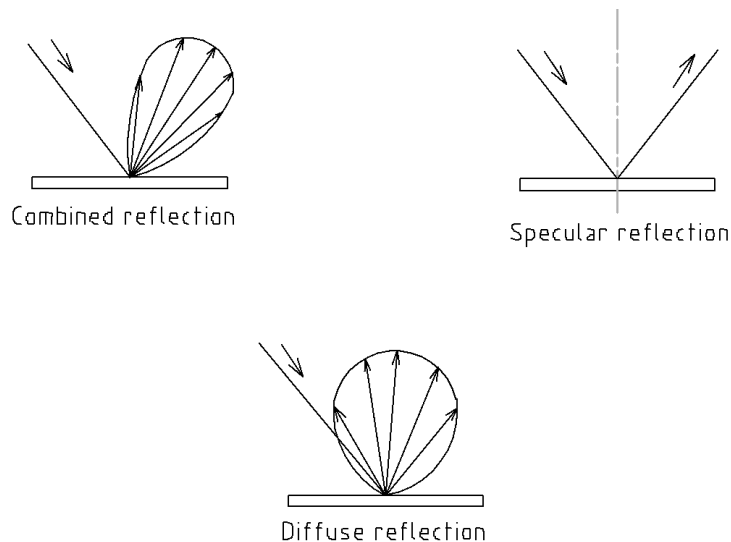
Fig. 19 – Possibilities of electromagnetic reflection from a measured surface [1]

4.2.1 Gloss meters

These devices are sometimes called scatterometers. The principle of gloss meter is the beam of light which is projected on the measured surface and scattered light is scanned by two detectors. One detector is set at the specular angle and the other against the first detector at a small angle (about 10°). In case of smooth surface the light enters only the first sensor. Both sensors are hit equally in case of very rough surface. This method can provide cheap comparison for surfaces made in a single machining operation. [2]
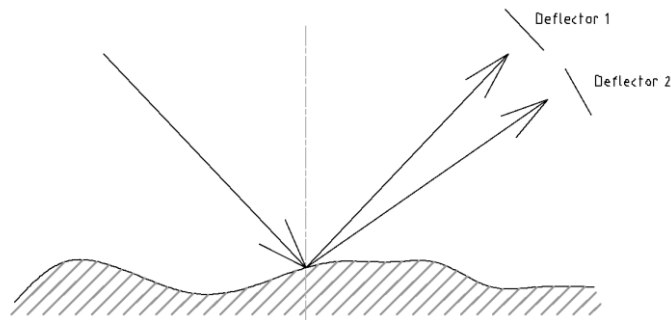
Fig. 20 – Principle of gloss meter comparison device [2]

4.2.2 Interferometers

As the name indicates, interferometers work on the principle of light interferometry, which compares the measured and reference surfaces (the latter can be part of measuring device). The measured surface should have the same shape as the reference surface or it should at least similar. With the use of multiple reflection between the measured surface and reference element, the signal can be enhanced and noise level can be reduced to zero. [1, 2]
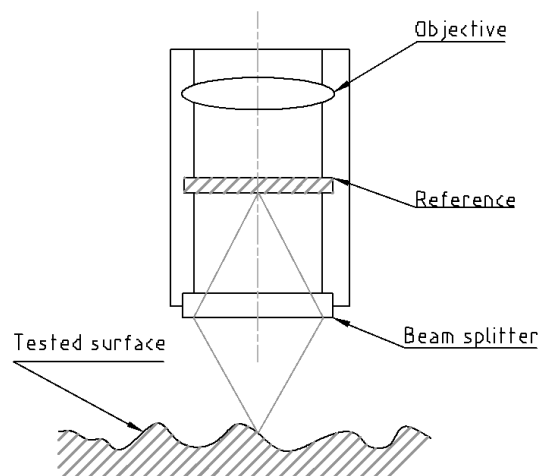

Fig. 21 – Basic Mireau interferometer [2]

4.2.3 Confocal devices

The confocal device uses a source of white light (polychromatic radiation), which is, during measuring, divided into two component in beam splitter – one ray goes to sensor and the second is led through lens with spectral aberration [12]. After contact with surface, the beam of light is scattered – every wavelength is focused on different peak and then reflected back and compared with original wavelength spectrum.

A great advantage of confocal measuring devices is that the stray and widely scattered light beams do not influence the measuring results. It is because of positioning a pin hole near

to the detector plane. This prevents the axial light to enter the detector except for the light in the focus – only the spot that is directly illuminated contributes to the signal. [2]
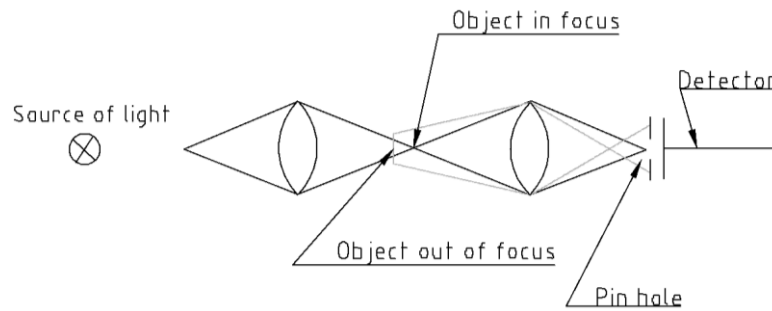
Fig. 22 – Principle of confocal microscope [2]

4.2.4 Comparison of optical devices with stylus devices

In case of use of optical devices the speed of measuring is very important. As illustrated in *Fig. 23*, measuring is cheaper with higher speed (time of measuring is substantially shorter), but on the other hand fidelity to the measured surface is lower. Choosing the right type of optical device can be in many cases crucial in term of accuracy and correct evaluation.

Another important thing is that devices with slower speed and better accuracy also have greater versatility. Using the higher speed of measuring, optical devices are much faster than stylus methods. On the other hand accuracy of this fast evaluation is not as good as the accuracy gained from stylus devices. However, with application of slower speeds, optical devices can achieve very satisfying results. [2, 12]
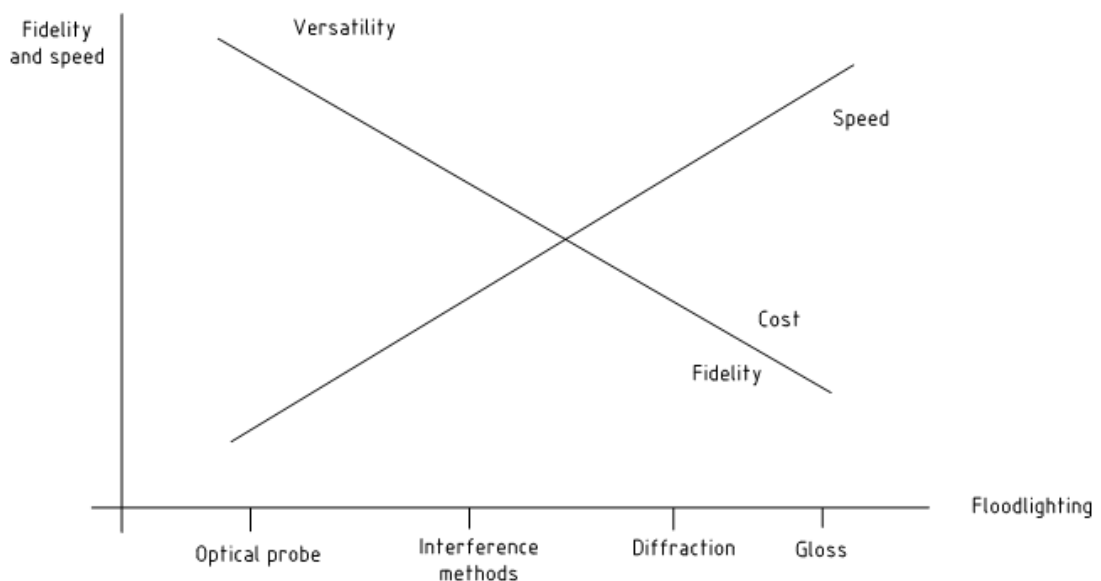
Fig. 23 – Comparison of optical methods [2]

Other issues of optical methods are (description from source [2]):

a) Optical path length

- If the measured surface is unclean from different types of fluid films with the same thickness but different refractive indices, there is a visible step in measurement results in the borderline of films.

b) Depth of penetration

- Optical rays can penetrate the measured surface during its assessment. Penetration value ranges in order of nanometers. And in case of nanometric surfaces it can affect the result.

- The depth of penetration is dependent on conductivity of the surface.

c) Diffraction effects

- Sharp edges or highly curved peeks included on the surface relief can be a source of optical rays diffraction.

- Also surface edges and grain boundaries can cause scattering of optical rays, this result is distortion in roughness profile, which must be further treated.
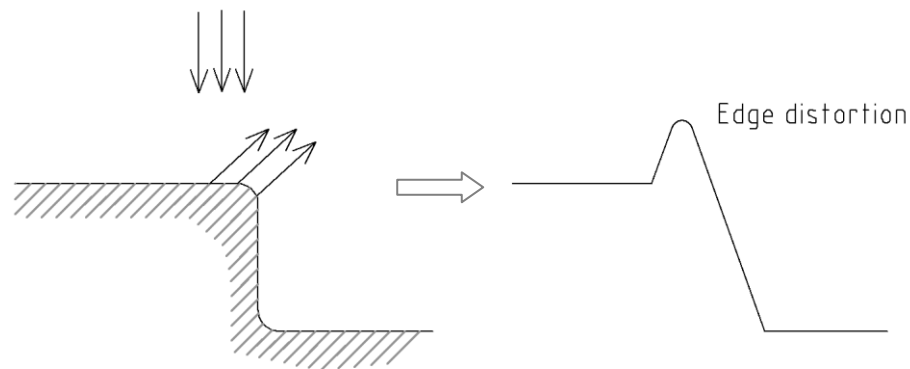
Fig. 24 – Diffraction effect from edge distortion [2]

There are many advantages and also disadvantages in optical devices area. Hence it is important which methodology to chose and which parameters to apply. Optical devices are more appropriate for fine surface and, thanks to absence of stylus, can be used for measuring of surfaces with steep peaks and valleys.

Tab. 10 – Comparison between stylus and optical methods [2]

Stylus	Optical
Possible surface damage **-**	No damage **+**
Measures geometry **+**	Measures optical path **-**
Tip dimension and angle independent **+**	Tip resolution and angle dependent **-**
Stylus can be damaged **-**	Probe cannot be broken **+**
Insensitive to tilt of workpiece **+**	Limited tilt only allowed **-**
Relatively slow speed **-**	Can do very fast scan **+**
Removes unwanted debris and coolant **+**	Measured surface must be perfectly clean **-**
Can be used to measure physical parameters as well as geometry (hardness, friction) **+**	Only optical path **-**

4.3   Scanning microscopes

The need to achieve better differentiability and high sensitivity has led to use of devices with stiff microscope structures and isolation from mechanical noise. Scanning microscopes are equipped with a precise nanometer – scale probes or beam of electrons. Where wavelength of electrons is about 10^{-5} times the wavelength of light used in optical devices. [1, 2]

4.3.1   Scanning probe microscope (SPM)

As already mentioned, SPMs serve for measuring surface topography on a scale that is much smaller than the scale of conventional stylus and optical instruments. SPM has nanometer – scale probes to trace the surface of the sample. For scanning probe it uses a predefined pattern and the signal of interaction is recorded during the measuring to be used as control of the distance between the probe and the surface of measured sample. [12]

One of the most widely used SPMs is the atomic force microscope (AFM), which is suitable for studying of topography of non-conductive material surfaces. A sharp diamond tip

is moved by piezoelectric elements towards the measured sample until interatomic forces between the tip and the sample deflect the cantilever. This deflection is monitored by [12]:

- Optical interferometry
- Optical beam deflection (laser beam)
- Tunneling methods

4.3.2 Scanning electron microscopes (SEM)

SEM uses a beam of electrons, which are reflected – backscattered after hitting the surface or generated by interaction of the primary electrons with the sample (secondary electrons). The number of secondary electrons emitted by the surface is relative to the surface topography and nature. Emitted electrons are collected, amplified and analyzed before modulating the beam of a cathode ray tube scanned synchronously with the scanning beam. [12]

Scanning electron microscopes are used for measuring surface topography on a smaller spatial wavelength scale compared to other instruments (stylus, optical). SEM can be also used on relatively large ranges but lacks the ability of three dimensional measuring techniques. [12]

5   SPECIFIC TYPES OF SURFACE ROUGHNESS MEASUREMENT

Surface roughness measuring has made a great progress during last few years and techniques that were originally only for scientific purposes are extending nowadays among manufacturing companies.

One of the most important improvements in surface evaluation is application of optical devices in 3D measurement, which enables to examine the surfaces in far more details than before. Another very helpful application, in connection with previous, is replication of the surfaces. This enables to measure even inaccessible surface (for example cavity of an injection mold).

5.1   3D Measurement

In principle, 3D devices are profiling instruments. Measuring in three dimensions enables determination of surface relief over the assessed area and construction of a topography map. The footprint of the probe or sensor used for measuring must be as small as possible to get the best result of surface approximation. For graphical representation of the surface or for extraction of quantitative information about relief, scan should be functional in Cartesian coordinates. Polar or spiral scans have also been developed, but non-Cartesian spacing was not so convenient for subsequent analysis. [1, 2, 12]
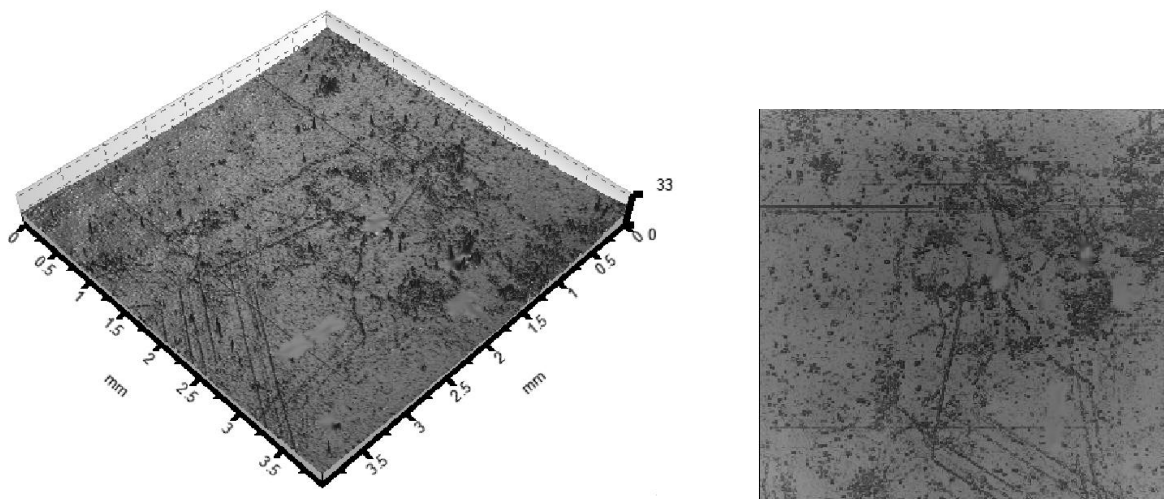
Fig. 25 – Projection of 3D surface measurement results

Measuring in three dimensions is realized with a stationary probe and movable translation tables with a clamped workpiece. This has proved to be most convenient due to ready availability of precision x-y translation tables that were already developed for optical engi-

neering applications. Construction of these tables is very difficult, as they must have certain properties [1, 12]:

- − Precisely controlled movement in very small increments
- − Gain of accurate positional information
- − Provision of an absolute reference datum of height

5.1.1 Application of chromatic confocal microscopy for 3D measurement (CHCM)

For measuring chromatic confocal microscopy uses single point optical sensors (chromatic confocal probes) built around a confocal coaxial setting. The surface distance is obtained by decoding chromatic dispersion. CHCM is insensitive to ambient light and stray reflection from surface. The chromatic confocal probe monitors every point of measured surface and extracts its height and light intensity. It is possible to measure a line or, an areal surface. [12, 13]

The principle of CHCM is demonstrated in *Fig. 26*. The basic condition for correct function is that the optical path from the light source to the measured surface must have the same length as the path from the object surface to the spectrometer. The measuring signal is received when the focal point lies exactly on the measured surface. In this case reflected light passes through the pinhole which generates an intensity peak on the photo-detector. When the confocal probe is focused above or below the surface, the reflected light does not pass through the detector pinhole. [12, 13]

Main physical phenomenon which provides received data is axial chromatic dispersion. For each wavelength of the applied chromatic light a different focal point is generated. This serves as a space-coding method when a different wavelength is associated to each point of the optical axis within the vertical range. A mathematical relationship between the surface height and wavelength focused on the surface can be found within spectral encoding of the measurement space. The vertical range of chromatic probe is defined by the distance between focal points of extreme wavelengths. [12]

As mentioned above, when the reflected light passes through the pinhole, an intensity peak is recorded on the photo-detector. This peak belongs to just one wavelength, other wavelengths are out of focus and therefore blocked by the detector pinhole. This implies that only a single wavelength is in focus on the surface at a time (see *Fig. 26*). For detection of wavelength with maximum intensity the confocal microscope uses spectrometer.

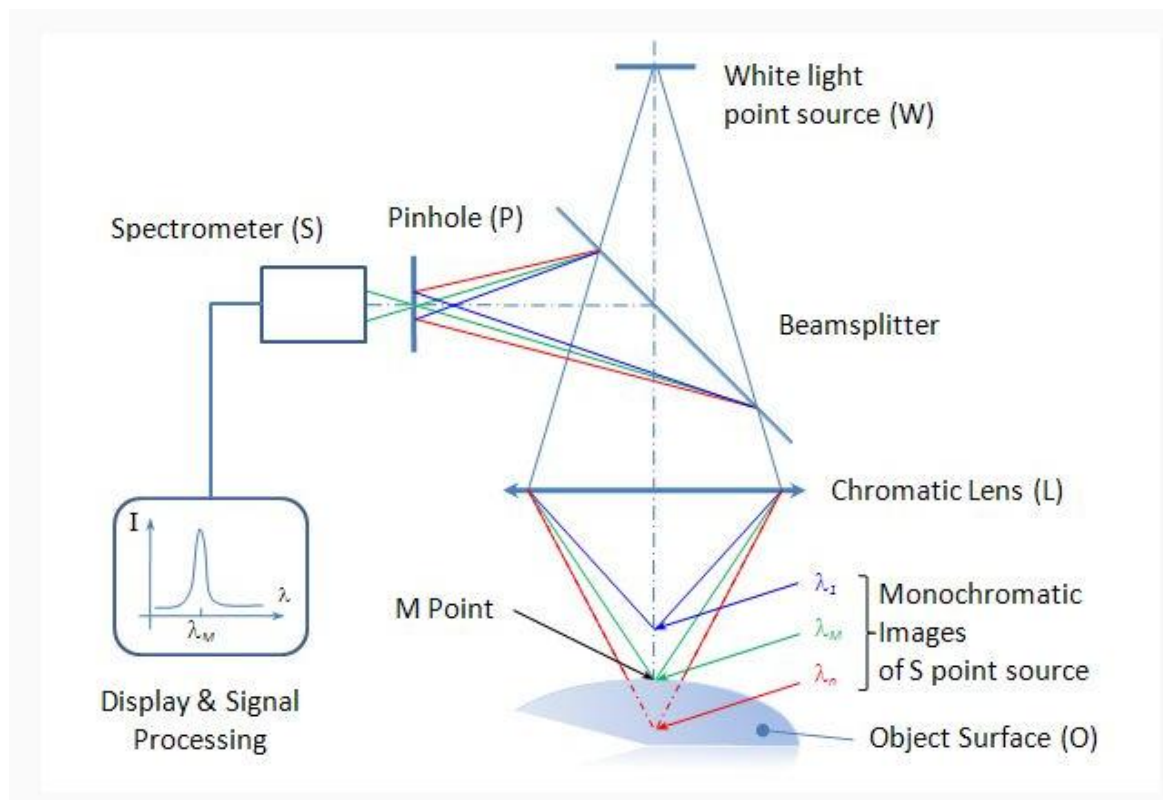The wavelength of maximum intensity is, through calibration, associated with surface height. [12]

Fig. 26 – Classical confocal setting [13]

To obtain satisfying results of measurement, it is important to define the spot size (dimension of the measuring ray of light). It has a direct influence on the lateral resolution of the measurement and depends on [12]:

- *"Numerical aperture of the objective*
- *Magnification used in the optical head*
- *Size of the pinhole*
- *The mean focal distance of the objective"*

Function of optoelectronic controller (description from source [12])

- Optoelectronic controller contains a source of light and a spectrometer. These two elements are connected to a beam splitter (or optical coupler in some cases) and from the beam splitter to an optical head. The connection of these units is ensured by optical fiber with a diameter of about fifty micrometers which provides a good pinhole.

‒ Optoelectronic controller must be separated from the measuring part of the instrument. It is because this device generates quite high temperatures, therefore it must be cooled by fans, which, unfortunately, generates vibrations.
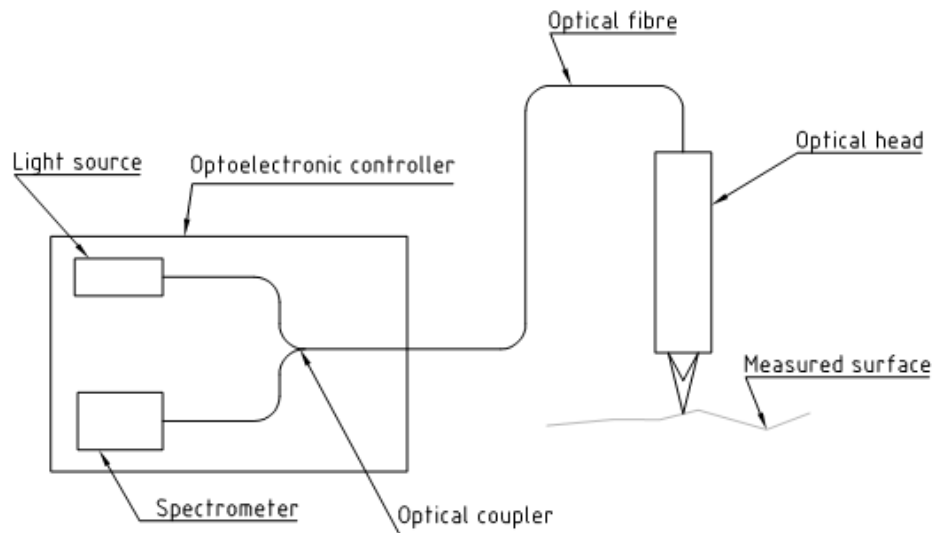
Fig. 27 – Communication between optoelectronic controller and optical head

5.1.2 Limitations of chromatic confocal microscopy (description from source [12])

‒ Local slopes

As explained above, the light focused on the surface is reflected toward the detector for analysis. Flat and smooth surfaces act as a mirror – they create reflection of light outside of the reach of objective lens. This causes generation of non-measured points by detection algorithm – the detector does not receive enough light and so the algorithm cannot detect the peak.

Rough surfaces generate diffuse reflection, which means that part of light is reflected back to the detector and another part is reflected beyond its reach. When measuring on diffuse materials (metal, plastics, rubber), it is possible to measure slopes up to eighty degrees. The maximum measureable slope is influenced by several factors:

‒ Power of light source

‒ Color

‒ Reflectivity of the measured surface

‒ Acquisition frequency

‒ Scanning speed

Limitation from scanning speed is caused by acquisition frequency which determines the exposure time. Exposure time is the period for which the detector accumulates light coming back from the measured sample

- Light intensity

With insufficient light the detector is not able to detect any peak. This leads to receiving non-measured points. In these cases surface height cannot be detected and received data must be repaired by post-processing.

When, on the other hand, the applied light is too bright, it causes saturation of the detector with consequent outliers. These are understood as points that are significantly above or below the surface. They are created by distortion of the peak shape by light reflection (as mentioned above), when semi-transparent material is measured or when the local slope is close to the limit.

- Interference

Interference can be present when thin transparent material films are measured. It is created between upper and lower interfaces and affects the result of detection – causes errors in determination of vertical axis position.

- Ghost foci

This problem occurs when the surface of the sample is locally spherical. Then the focal point is detected not on the surface but in the centre of the sphere.

5.2 Replication

Method of replication is important for measuring by some optical methods that requires a transparent specimen. It is also important for electron microscopy in case of need of conducting material – to make conductive specimen from non-conducting workpiece. Another area of use of replication method are parts which are not accessible or measurable [1]:

- Internal surfaces
- Surfaces situated under water
- Parts that cannot be embedded on the measuring instrument because of their dimension, weight or because it is impracticable in some other way
- Fine surfaces where direct measuring with a stylus would damage or spoil the surface

A replica of the demanded surface is usually made by contact of the surface with replication material in liquid form. When applied, replication material transforms into solid and creates a negative of the original surface. Most common materials used for replication are: plaster, dental cement and polymerizing liquid. [1]

The main problem of replication is how close the replica is to the original surface and its features. Lack of fidelity to the original is inflicted by the following problems [1]:

− The liquid used for replication may not wet the whole surface. To secure complete bunk–up of the replication material it is important to the degrease replicated surface.

− Wet surfaces and surfaces with biological specimens have problems with diffusion and in some instances a chemical reaction can appear during setting.

− During parting from the original surface, the replica may adhere to it. It is then considerable to use some release agent to secure safe parting.

− When using a stylus measuring device, a further replica must be made (negative of negative). This is because the stylus does not responds to valley bottoms in exactly same way as to peaks.

− Optical measuring devices are dependent on detecting an optical path difference which is a function of the refractive index. Since transparent replicas are used for some optical methods, there can be misinterpretation due to in homogeneity of the replica or because of changes in the refractive index due to temperature.

− If rigid a replica is used, short wavelengths are not reproduced precisely. On the contrary, when a flexible replica is used, long wavelengths are not produced accurately.

Surface replication can be used also for visualization of measured specimen in an enlarged scale. This type of replication differs in use of optical scanning machine with proper 3D evaluation program instead of replication material. Scanned surface data are transferred and adjusted for rapid prototyping machine or imported into CAM program, where the milling operations are programmed. The size of replicated specimen is then limited only by proportions of rapid prototyping unit or by milling machine [21].
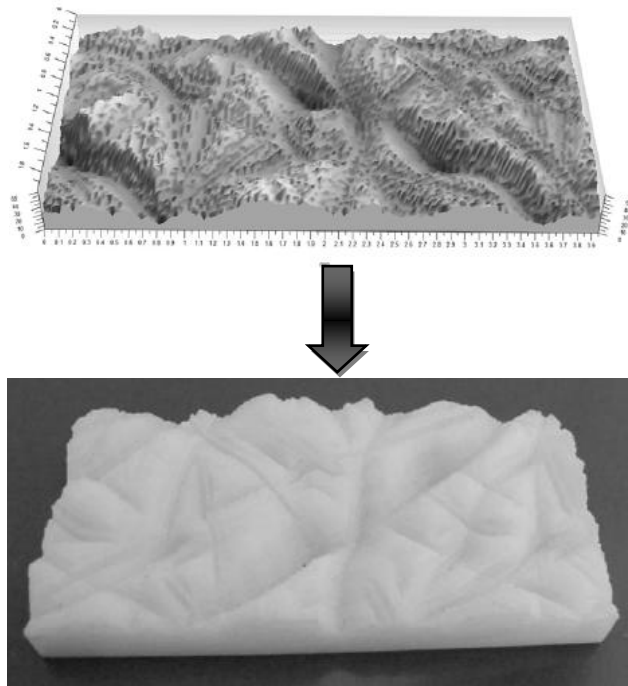
Fig. 28 – Enlarging replication by rapid prototyping
for surface properties assessment [21]

This type of replication can be used in many different ways. Mainly it can serve for visualization of assessed surface and its properties like scratches, cracks, fissures and similar. It can very helpful in forensic engineering and it found its utilization in tribological assessment [21].

Important role it can also play in measuring of micro hardness of polymer materials. It is because polymer materials are subject to relaxation and immediately after the test of micro hardness material has a tendency to return back into its former form. With replication following after the test, the stable specimen is gained for further measurement (*Fig. 29*). And also with application of enlarging scale, its dimensions can be examined by less precise measuring devices [21].
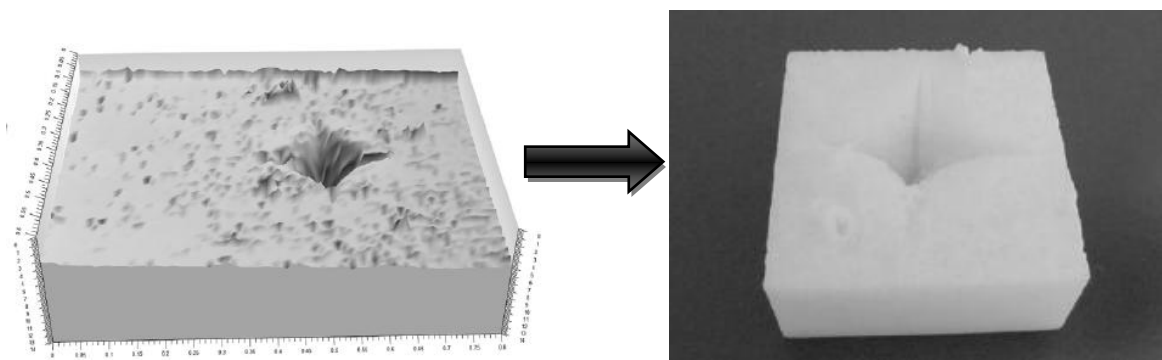
Fig. 29 – Enlarging replication by rapid prototyping for micro hardness assessment [21]

6 STATISTICAL EVALUATION OF DATA SET

Measured data alone do not tell anything without proper statistical evaluation in most cases. Only by assessing obtained set of values by various statistical operations, there can be acquired some meaningful results. Basic solution for comparison of various data sets will be described by following sections.

6.1 Outliers check

As outlier can be described numerical value that is significantly distant from the rest of the data. It deviates from the rest of data set of the measured sample. Outliers can be evaluated in two different ways. First says that outlier indicates a measurement error. In this case distant value used to be discarded or statistical methods robust to outliers are used to deal with it. Second way indicates that deviated data are sign of heavy-tailed distribution = distribution has high kurtosis. [22, 23]
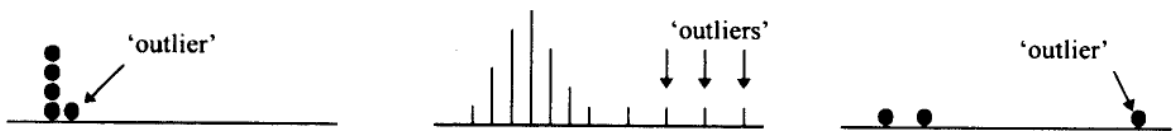
Fig. 30 – Some cases of outlier images [24]

Outliers mostly indicates faulty data, erroneous procedures or areas where a certain theory might not be valid. Though there is a strong possibility that in every large set of measured values will be present a small number of outliers. One of robust methods for statistical evaluation of data sets with deviated values is box – plot diagram (*Fig. 31*). [22, 23]
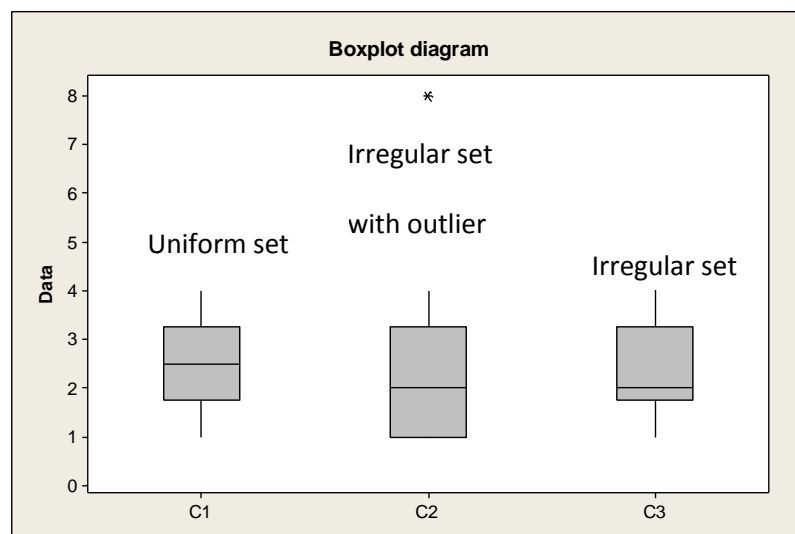
Fig. 31 – Box-plot diagrams

This method uses as basic output quantity median instead of mean. It is because median is not so susceptible and presence of distant values cannot affect its value significantly. [22, 23]
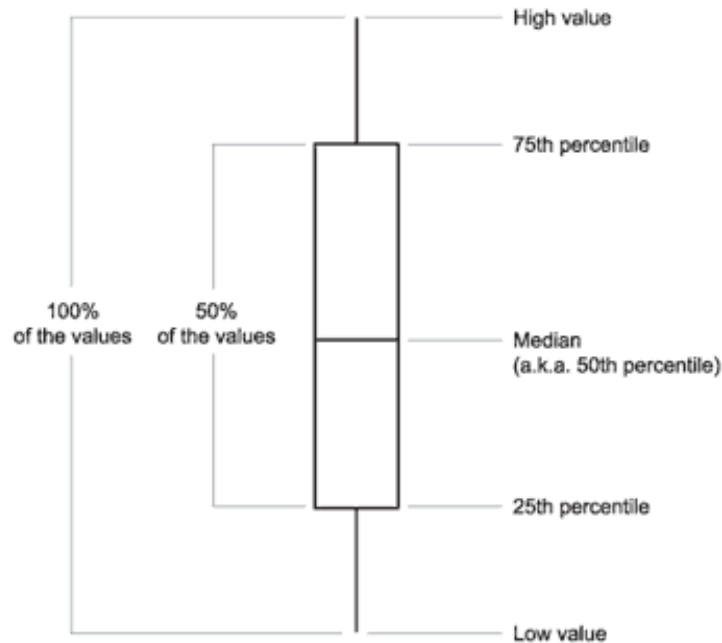
Fig. 32 – Box-plot description

6.2 Basic statistical parameters

One of main outputs from statistical operations are following parameters:

- **Mean**

For data set assessment mean is sum of measured values divided by the number of values.

- **Standard deviation**

Provides a measure of the spread of data. Standard deviation shows how much variation exists from the average (mean).

- **Standard error of the mean**

It is calculated as standard deviation divided by the square root of number of non-missing observations.

- **Minimum and maximum values**
- **First quartile**

Indicates lowest 25% of data set

- **Third quartile**

Marks highest 25% of data set

- **Median** (second quartile)

It is the middle (50%) of data set

- **Interquartile range**

Difference between the first (upper) and third (lower) quartiles.

- **Skewness**

Skewness is a measure of the asymmetry of the probability distribution of a real-valued random variable. It can be positive, negative or undefined.
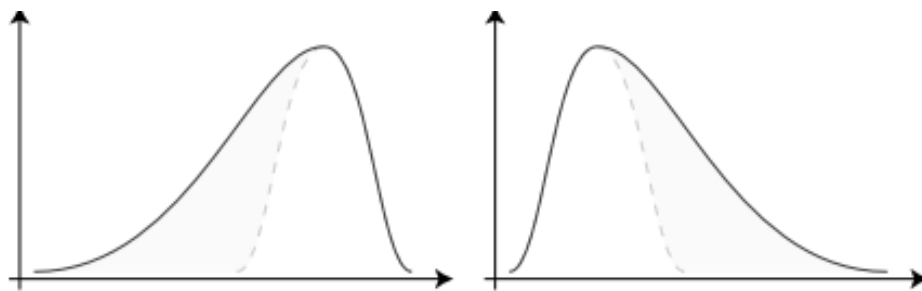
Fig. 33 – Negative and positive skewness

- **Kurtosis**

Kurtosis also describes the shape of the probability distribution of a real-valued random variable. There three basic shapes described by kurtosis:

Mesokurtic Curve   Leptokurtic Curve   Platykurtic Curve
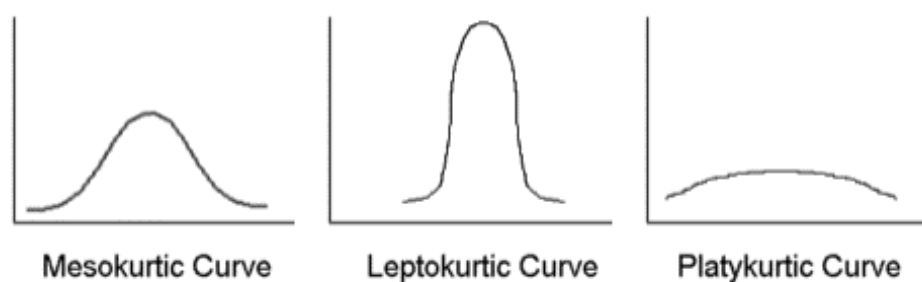
Fig. 34 – Basic shapes of kurtosis

6.3 Hypothesis theory

Hypothesis theory consists from several statistical tests which helps to compare two or more data sets and tell how much they are similar or different (how and if they are comparable). Each test consists of the null and the alternative hypothesis, which indicate the properties of evaluated data, and has its own level of significance. In following sections are described statistical elements which were used further in the Analysis part.

6.3.1 Level of significance

The significance level determines if something has occurred by chance – result is statically significant only if it was not random. Values of the significance level are: 10%, 5%, 1%, 0,5% and 0,1%. Chosen value is during the testing compared with p-value which is output value from the tests and means the probability of obtaining a test statistic at least as extreme as the one that was actually observed. The null hypothesis is not rejected when the p-value is higher or equal to level of significance. Otherwise the alternative hypothesis is accepted [25].

The selection of the significance level value involves a compromise between significance and power. When the significance level is small, there is a risk of not rejecting a false null hypothesis. On the other hand, when the significance level is large, there is a probability that a null hypothesis will not be accepted even if it is true [25, 26, 27].

6.3.2 Normality test

Normality test examines the distribution of data, whether the data set has a normal distribution or not. As a test result is chosen either alternative hypothesis or a null hypothesis is not rejected [28]:

- − Null hypothesis (H_0): Measured data have a normal distribution
- − Alternative hypothesis (H_A): Measured data do not have a normal distribution

6.3.3 F – test

F – test examines ratio of two or more variances to determine their equality. Normal distribution of data sets is basic condition for a performing this test. A null and an alternative hypothesis are following [28]:

- − Null hypothesis (H_0): Compared sets have equal variances

– Alternative hypothesis (H_A): Compared sets do not have equal variances

6.3.4 ANOVA

Analysis of variances (ANOVA) can compare the means of two or more data sets, which were subjected to different experimental interventions, between themselves. The preconditions for implementation of ANOVA are an independent selection, normal data distribution (tested by normality test) and homogenous dispersion inside of data sets (secured by outliers check). Results of ANOVA [24, 29]:

– Null hypothesis (H_0): Compared sets have equal means
– Alternative hypothesis (H_A): Compared sets do not have equal means

6.3.5 Kruskal – Wallis test

Kruskal – Wallis test is a non-parametric method and serves as an equivalence to ANOVA. It is applied when assessed data groups do not have normal distribution. Data comparison is based on the medians of tested data sets and results in [30]:

– Null hypothesis (H_0): Compared sets have equal medians
– Alternative hypothesis (H_A): Compared sets do not have equal medians

II. ANALYSIS

7 INTRODUCTION OF THE MEASUREMENT

To provide a detailed description of polymeric part surface measuring the Analysis part was divided into following sections:

− Sample preparation

− Measuring (description of the measuring software)

− Evaluation of the results

− Discussion about the behavior of polymeric material during the injection molding
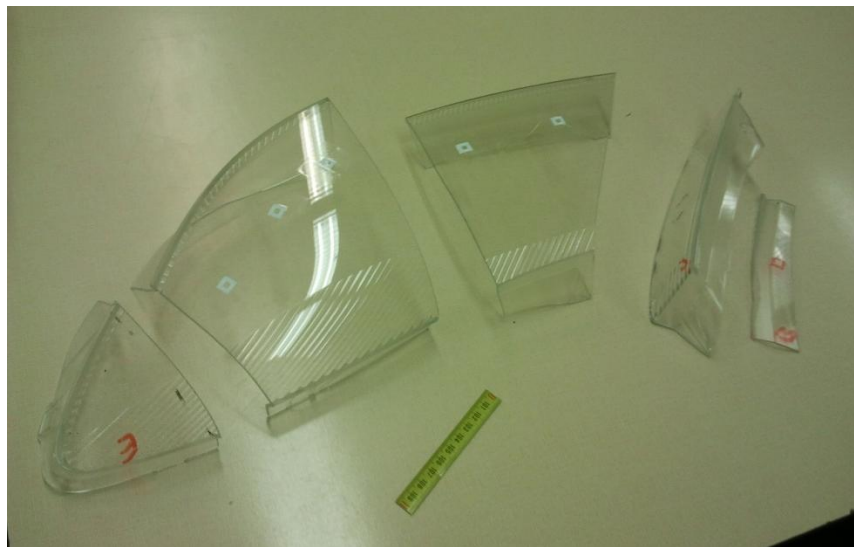
Fig. 35 – Measured product

For surface assessment was chosen the polymeric glass (polycarbonate) from passenger car headlamp. This product appeared to be suitable because of well known entrance to the cavity (gate) and predictable flow behavior (generally meant). Benefits of these two features will be discussed in the sample preparation section together with detailed description of measuring places selection.

Measuring was done by 3D scanner Talysurf 300 which is based on chromatic confocal microscopy. There were two options how to measure the specimen. First one was to measure just on one line (similar to 2D measurement). Other possibility was to scan the specified plane – 3D measurement. Since the flow of the melt can be only predicted and was not known, the plane scanning was chosen. To secure the ever-changing behavior of the polymeric melt, two ways of evaluating were chosen according to sample preparation: from north to south and from west to east, and two filters were used – Gaussian filter and Robust Gaussian filter.

The expected result of the measuring is to gain an image about the changing properties of the polymeric melt during its injecting into the mold. Presumption is that the polymeric melt is during its way to the opposite end of the mold cooled and also there must be some pressure drop with an increasing distance from the cavity entrance. As a result, all of these features should be reflected in the ability to copy the surface of the mold and consequently its roughness.

7.1 Sample preparation

After choosing suitable polymer product for the measurement, it was important to specify places on it where the surface will be scanned. *Fig. 36* shows places selected for the measurement realization. Selection of locations were totally random, however, they were made with regard to expected melt flow behavior, which is based on fountain flow characteristic.
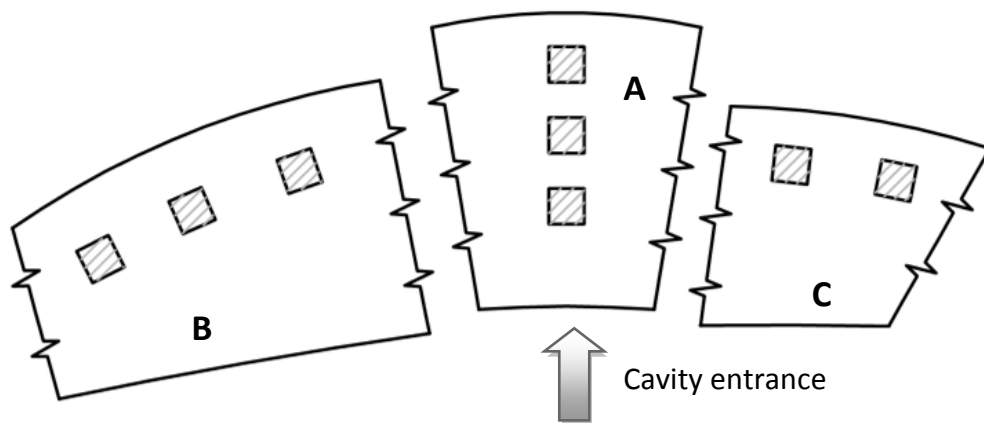
Fig. 36 – Measuring places scheme

Picked places were marked by small paper squares with square shaped holes inside them – these indicated the measuring planes with dimensions 4x4 millimeters. For better manipulation and mainly due to inability to place the whole product on the measuring machine, the assessed sample was cut into eight independent squares.
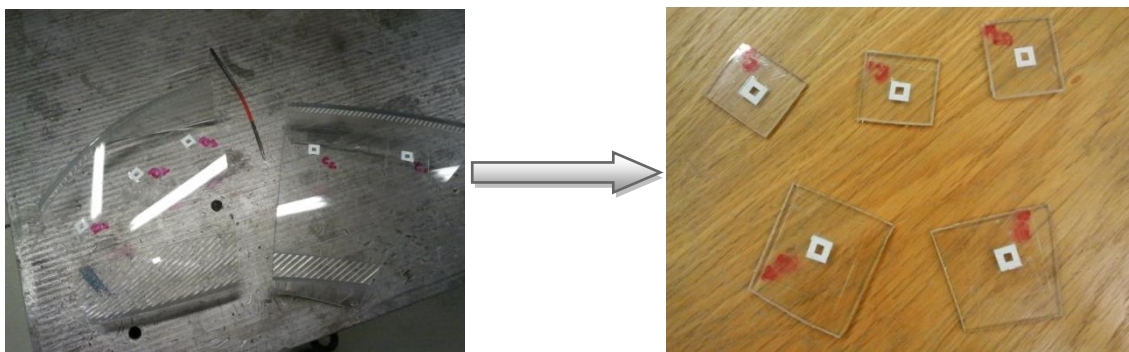
Fig. 37 – Adaptation of the sample

Fig. 37 shows only five samples from B and C sections because other three from A section were measured earlier than the others and were not available for taking the photos because of their another use for different research.

Every single sample was then checked by Carl − Zeiss microscope for possible scratches and dirt which would occur during the preparation of samples.

Fig. 38 – Samples control

7.2 Description of the measurement evaluation

All the samples were measured on the 3D scanner Talysurf 300 and results were collected and evaluated by software specially designed for this measuring equipment − Talymap 5. To obtain required data from this software following steps were taken:

− Scanned plane acquired from scanning operation was firstly leveled to eliminate the possibility of crooked surface of the samples.
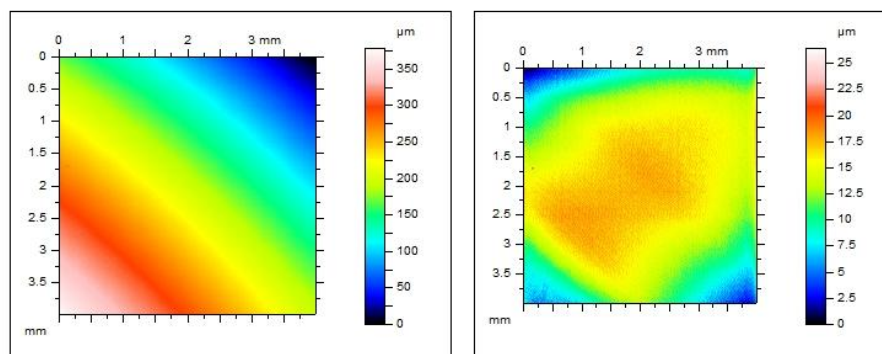
Fig. 39 – Difference between original and leveled plane

For leveling operation were left default conditions with rectangular contour marking for included (excluded) area:
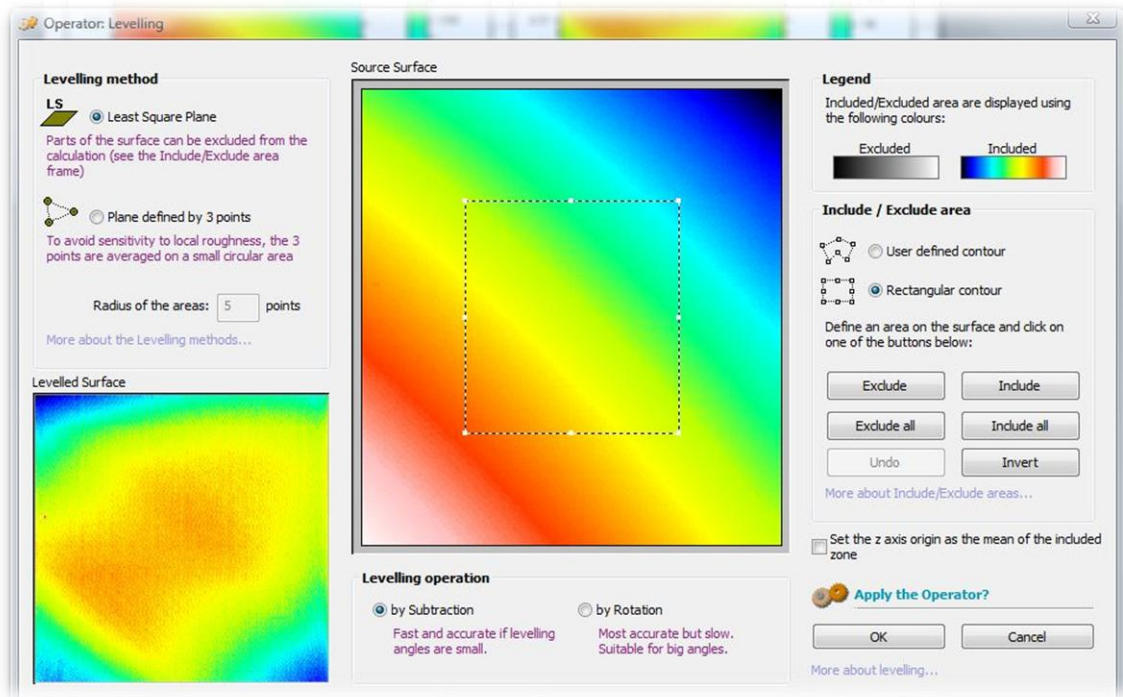
Fig. 40 – Settings of leveling

− In case of some extremities which would occur during the scanning, the retouching operation had to be used. These extremities could have originated primary from edge distortion and nature of the sample surface.
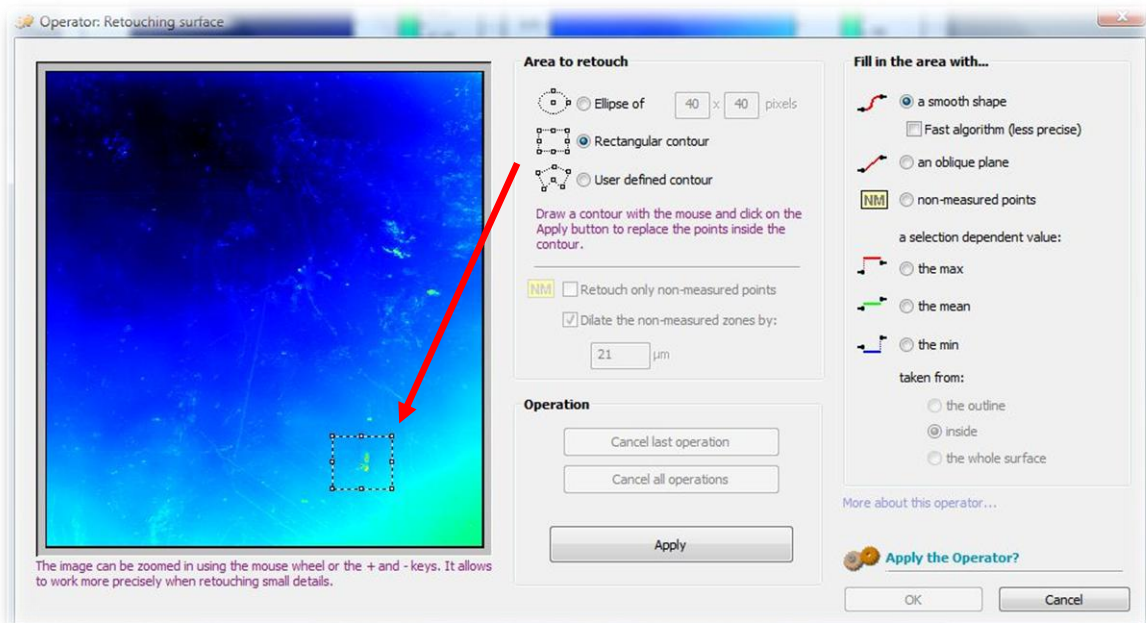
Fig. 41 – Retouching operation

Purpose of retouching operation is to find problematic extremes and circumscribe them by selected contour as illustrated on *Fig. 41*. It was important to designate an area as small as possible that the measurement outcome would be the least affected. Scanned plane had to be again leveled after retouching operation.

− From leveled surface were created 3D models which visually represent an appearance of the scanned sample.
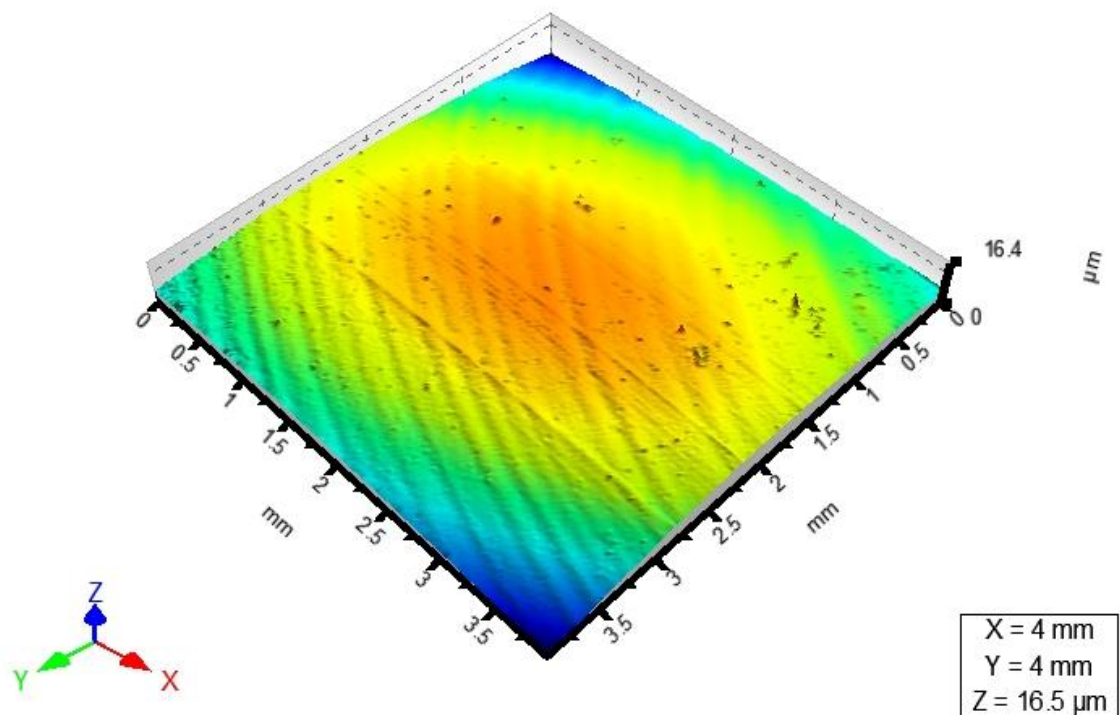
Fig. 42 – 3D representation of the scanned surface

− After the retouching and leveling operations, scanned planes were converted into the series of profiles for following evaluation (*Fig. 43*). Conversions were realized in two different directions to secure the ever-changing behavior of the polymeric melt. Firstly it was west – east direction (axis Y) and secondly the north – south direction (axis X). Number of profiles was left default, which means that it was converted the maximum of available profiles for the statistical evaluation of scanned surface roughness.
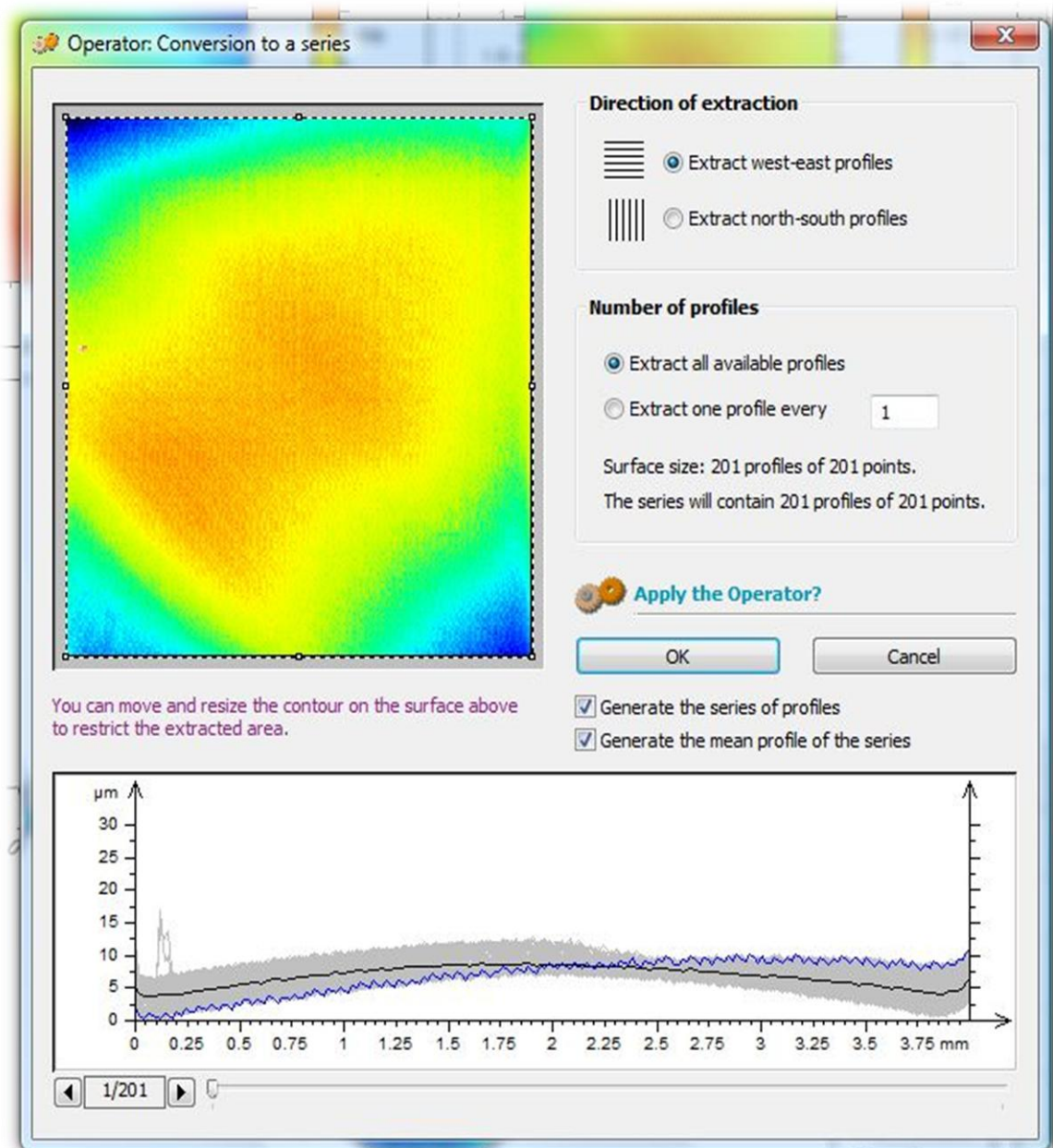
Fig. 43 – Conversion to series of profiles

- From each series of profiles were created two tables with statistical results, containing basic statistical values for common amplitude parameters and material ratio parameters. Difference between them was in use of filter – Gaussian or Robust Gaussian filter. Filter size was in every case set on 0.8 millimeters and option "Manage end – effects" was on (*Fig. 44*).
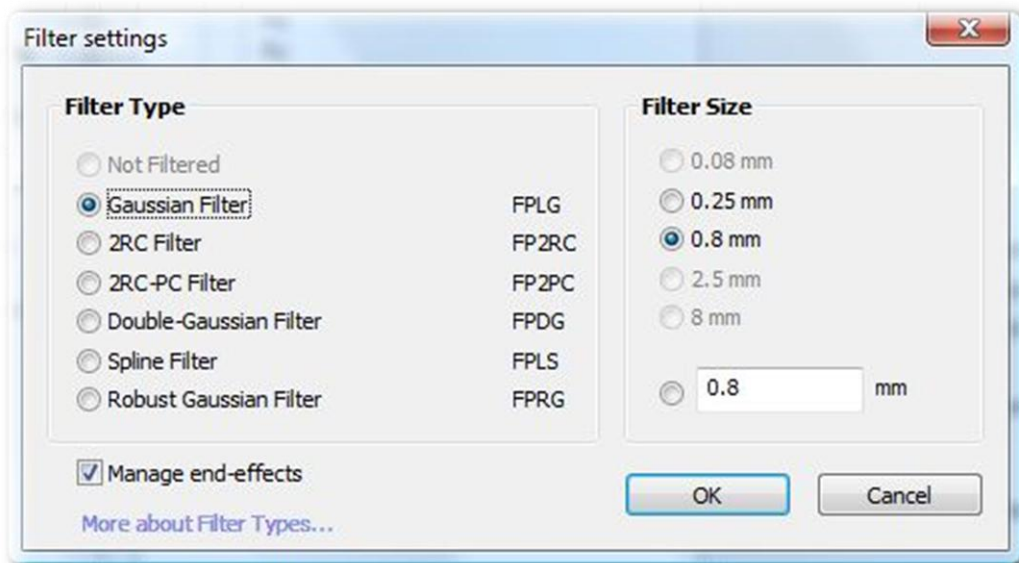
Fig. 44 – Filter settings

- − Last performed operation was creation of the fractal analysis from leveled plane of the measured surface. Where the most important result was the fractal dimension, located at the bottom edge. Purpose of the fractal analysis results will be discussed in "Results description" section below.
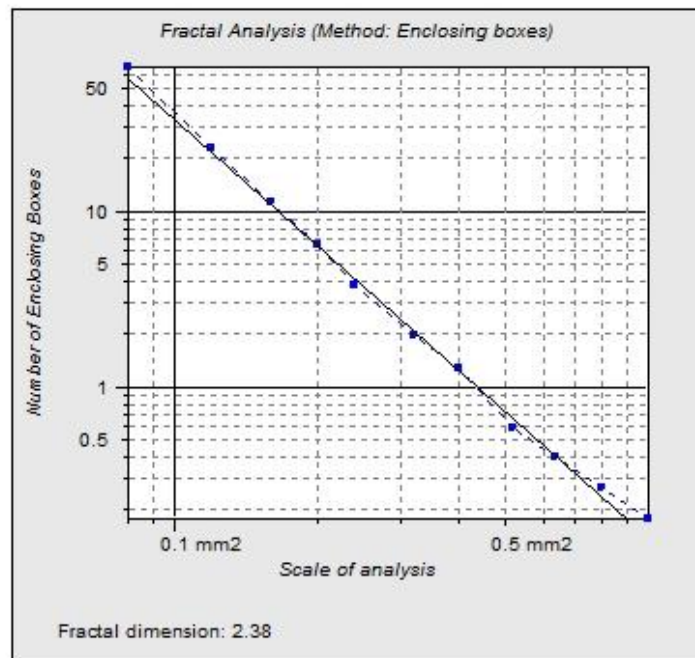
Fig. 45 – Fractal analysis

8 DATA COMMENTARY

In this chapter, only one of the six results of the surface roughness scanning (B_1) will be described in detail. The rest of results are contained in the annexes for further insight.

As was mentioned at the beginning of the Analysis part, there were eight places suitable for measuring marked on the measured product. During the sample preparations and especially during the evaluation procedure, there was an idea to adjust samples in one row and assess only those for reasons of better interpretation and visualization of measured results. This means that some of measured planes were excluded from final evaluation (specifically, planes A_1 and A_3 – see *Fig. 46*).
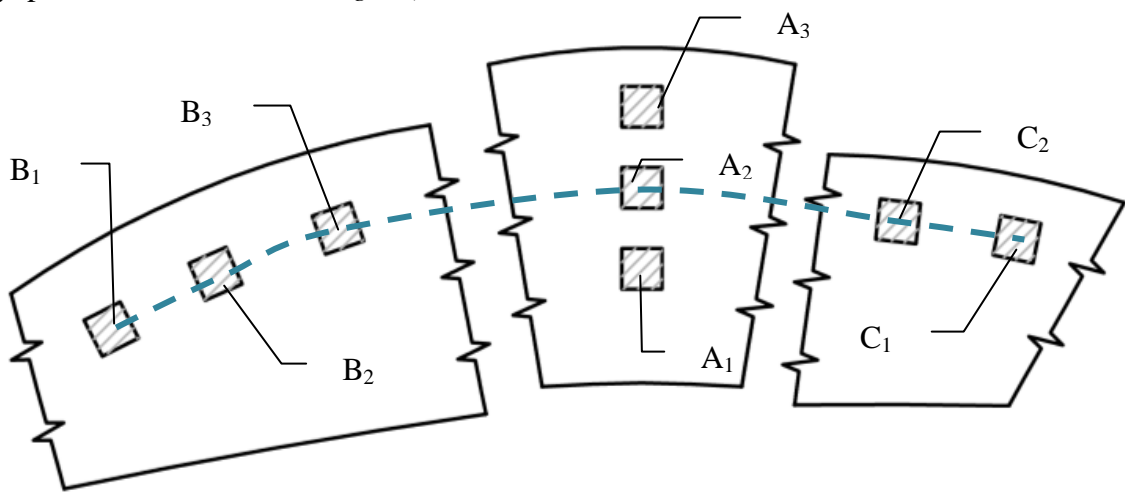
Fig. 46 – Measuring places scheme – marking

Previous chapter illustrated every step of the measurement evaluation to show the procedure of the data preparation. In the text below, obtained results and their meaning for the final global treatment will be discussed.
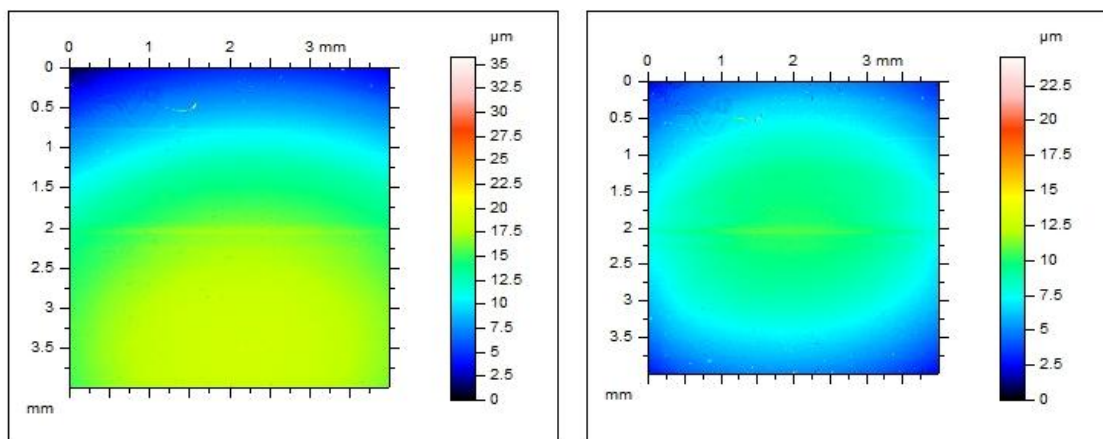
Fig. 47 – Original and leveled plane of the sample B1

After the scanning process, data were evaluated in Talymap 5 and projected as it is displayed in *Fig. 47* on the left. It can be seen on the scale that the highest value of the surface roughness is about 35µm. However, looking at the colored square which illustrates scanned surface, there is no red color present. Same situation occurred on the right side of the *Fig. 47*, where leveled data of the same sample are shown. Nevertheless, both of these squares illustrate the distribution of roughness on the sample and its uniformity.
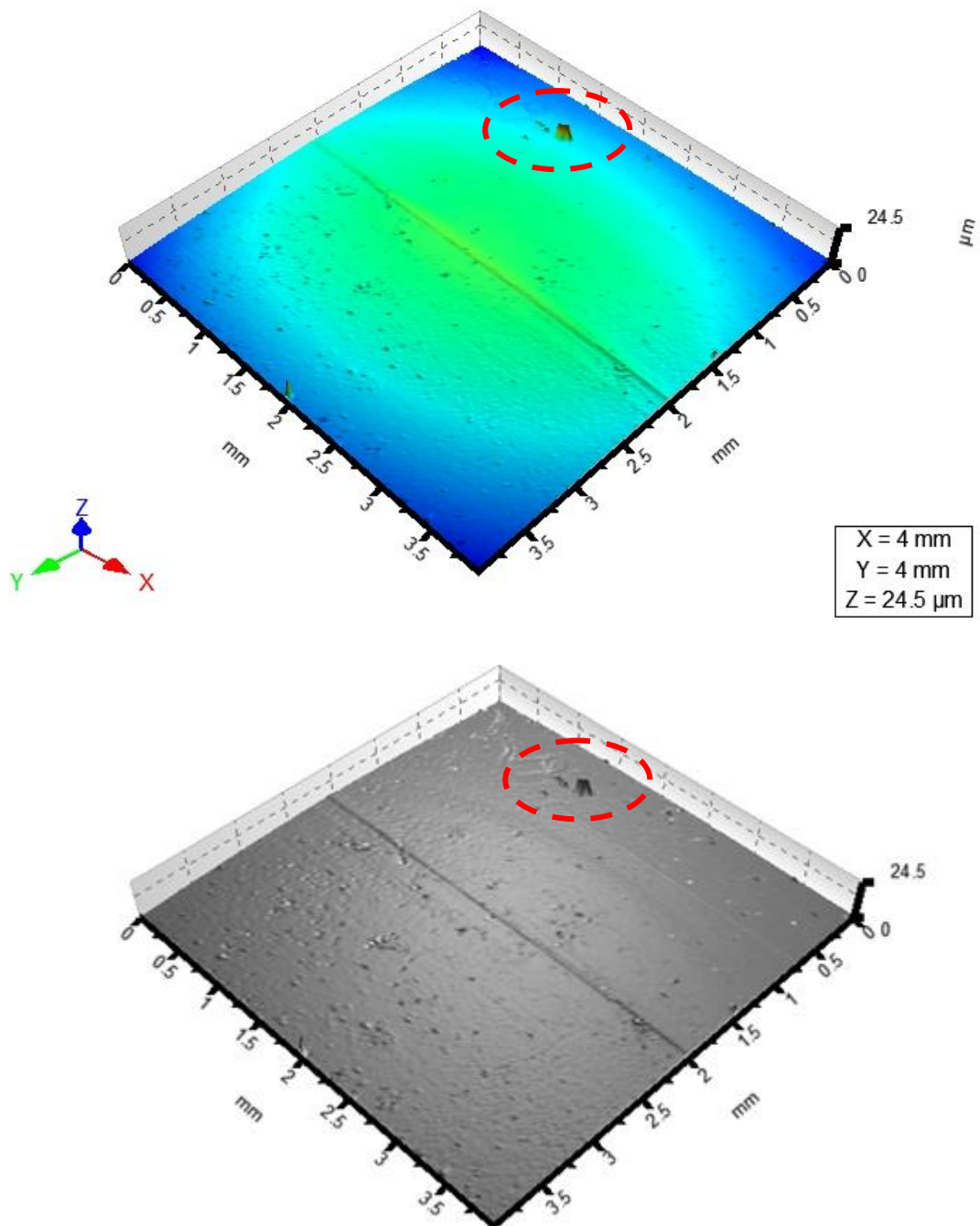
Fig. 48 – 3D projection of the sample B1

For a better view of the surface serves the 3D projection (visualized in *Fig. 48*). Colored projection is the spatial illustration of the sample with coloring according to previously visualized scale. Projection in the gray shows surface of scanned sample with its scratches, cavities and also the direction of the melt flow is slightly visible.

As can be seen, there is one big peak on the sample. However, it cannot be removed because it is likely the part of the sample B1 surface's structure. Cause of this peak is unknown. It could probably arise from some scratch either on the measured product or even on the injection mold's cavity.
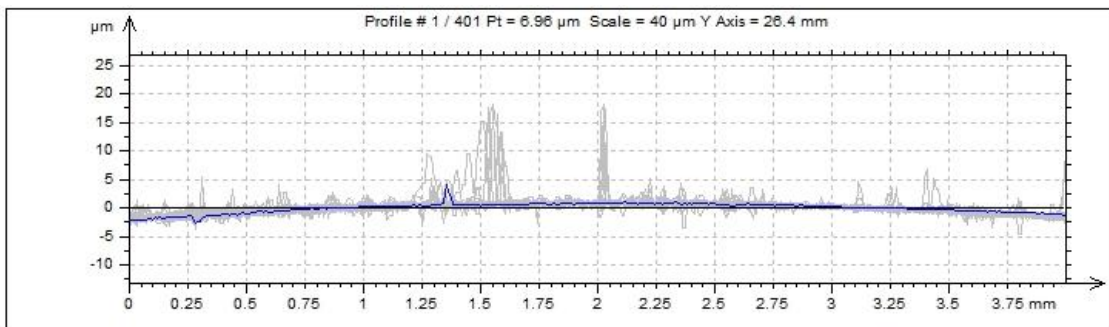
Graph 1 – Series of profiles of the sample B1, west – east direction (Y axis)

Graph 1 shows every roughness profile that is available on scanned surface in a fixed direction. Thick blue curve then represents the average of these profiles. It is obvious, that final data has not been too affected by the present peak.

The same applies to *Graph 2*, which describes series of roughness profiles in north – south direction, where extreme peak is also visible but does not influence the average of all profiles:
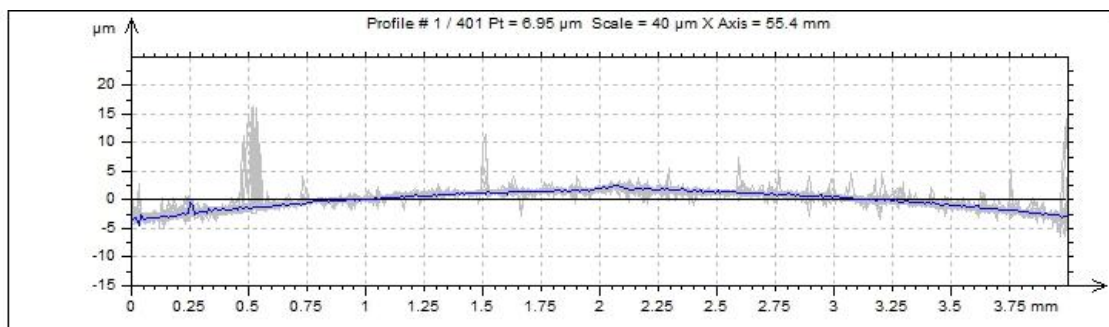
Graph 2 - Series of profiles of the sample B1, north – south direction (X axis)

From prepared *Graph 1* were created *Tab. 11* and *Tab. 12* and from *Graph 2* were created

Tab. 13 and *Tab. 14*. Data in tables are means from all gathered data, created by evaluation software. Difference between *Tab. 11*, *Tab. 12* and *Tab. 13*, *Tab. 14* is in use of a filter. In the first case (*Tab. 11* and *Tab. 13*), the Gauss filter was used for the evaluation. Second tables were calculated using the Robust Gauss filter. As it can be seen when comparing data of these two, there is slight difference between values of amplitude parameters (average and extreme – value parameters). It is mainly because of different calculations between those two (for more precise info see page 16).

For further data processing were from created tables selected following amplitude parameters:

- Ra (Arithmetic mean deviation of the assessed profile)
- Rz (Maximum height of the profile within sampling length)
- Rt (Total height of the profile on the evaluation length)

Tab. 11 – Statistical results of the sample B1 – Gauss filter, Y axis

ISO 4287		Mean	Std dev	Min	Max	Lower Quartile	Upper Quartile	Median
Amplitude parameters - Roughness profile								
Rp	µm	0.414	0.503	0.118	3.83	0.193	0.398	0.276
Rv	µm	0.339	0.157	0.124	1.18	0.229	0.392	0.303
Rz	µm	0.752	0.594	0.306	4.98	0.483	0.805	0.605
Rc	µm	0.306	0.411	0.118	4.14	0.175	0.288	0.215
Rt	µm	1.76	2.06	0.471	15	0.853	1.78	1.18
Ra	µm	0.0703	0.0407	0.0405	0.45	0.0536	0.074	0.0626
Rq	µm	0.117	0.0923	0.0581	0.817	0.0796	0.119	0.0956
Rsk		1.37	8.43	-24	42	-2.2	2.34	-0.844
Rku		66.2	124	5.5	918	13	55.6	23.4
Material Ratio parameters - Roughness profile								
Rmr	%	75.2	40.9	0.249	100	59.6	99.8	99.3
Rdc	µm	0.104	0.0275	0.0652	0.272	0.0881	0.111	0.0979

Tab. 12 - Statistical results of the sample B1 – Robust Gauss filter, Y axis

ISO 4287		Mean	Std dev	Min	Max	Lower Quartile	Upper Quartile	Median
Amplitude parameters - Roughness profile								
Rp	µm	0.57	0.69	0.14	4.98	0.279	0.531	0.379
Rv	µm	0.437	0.196	0.169	1.45	0.294	0.524	0.401
Rz	µm	1.01	0.762	0.403	6.04	0.664	1.04	0.811
Rc	µm	0.494	0.489	0.185	5	0.307	0.494	0.378
Rt	µm	2.46	2.76	0.614	19.5	1.27	2.44	1.71
Ra	µm	0.126	0.0386	0.0669	0.439	0.103	0.141	0.122
Rq	µm	0.187	0.112	0.0849	1	0.139	0.195	0.166
Rsk		0.878	9.49	-24.6	67.7	-2.49	0.335	-1.26
Rku		62.6	185	3.11	1888	8.88	31.2	14.4
Material Ratio parameters - Roughness profile								
Rmr	%	63.4	43	0.249	100	1.6	98.9	89.6
Rdc	µm	0.238	0.0496	0.132	0.414	0.203	0.269	0.23

Tab. 13 - Statistical results of the sample B1 – Gauss filter, X axis

ISO 4287		Mean	Std dev	Min	Max	Lower Quartile	Upper Quartile	Median
Amplitude parameters - Roughness profile								
Rp	µm	0.6	0.589	0.272	4.05	0.334	0.547	0.399
Rv	µm	0.363	0.139	0.163	1.14	0.262	0.432	0.326
Rz	µm	0.963	0.625	0.486	4.5	0.626	0.986	0.78
Rc	µm	0.388	0.351	0.142	2.42	0.235	0.378	0.289
Rt	µm	2.39	2.49	0.989	16.4	1.22	2.18	1.54
Ra	µm	0.0977	0.0237	0.0728	0.299	0.0849	0.102	0.0922
Rq	µm	0.155	0.0736	0.101	0.681	0.12	0.153	0.135
Rsk		4.19	11.8	-12.9	80.8	0.209	2.24	1.03
Rku		93.7	287	6.35	2401	10.9	28.9	14.1
Material Ratio parameters - Roughness profile								
Rmr	%	65.6	43.1	0.249	100	2.71	97.7	95.3
Rdc	µm	0.149	0.0248	0.103	0.254	0.13	0.159	0.144

Tab. 14 - Statistical results of the sample B1 – Robust Gauss filter, X axis

ISO 4287		Mean	Std dev	Min	Max	Lower Quartile	Upper Quartile	Median
Amplitude parameters - Roughness profile								
Rp	µm	0.802	0.693	0.308	4.8	0.473	0.798	0.574
Rv	µm	0.475	0.2	0.148	1.39	0.327	0.557	0.439
Rz	µm	1.28	0.747	0.602	5.3	0.849	1.37	1.06
Rc	µm	0.604	0.399	0.222	2.74	0.378	0.67	0.482
Rt	µm	3.27	2.96	1.32	18.6	1.83	3.12	2.22
Ra	µm	0.162	0.0376	0.0864	0.305	0.134	0.185	0.158
Rq	µm	0.234	0.0868	0.12	0.815	0.183	0.254	0.216
Rsk		3.54	10.8	-9.84	71.5	-0.656	2.52	0.676
Rku		80.2	252	3.95	2037	8.03	21.7	11.4
Material Ratio parameters - Roughness profile								
Rmr	%	42.8	34.4	0.249	91	1.02	73.8	61.3
Rdc	µm	0.354	0.0733	0.195	0.567	0.295	0.405	0.347

Last element that was investigated was fractal analysis – mainly its result, fractal dimension. It serves as support for other gained data and incorporates all the assumptions about the behavior of polymer material during the injection molding. At the beginning, it was mentioned that assumption for this work is that the polymeric material changes its behavior during its progress through the mold. Change of behavior is caused by temperature and pressure loss during the filling of the remote areas of cavity. Result of all of these is that the polymeric melt loses its ability to copy mold cavity surface, which is subsequently passed on surface roughness of injected product. Polymeric melt does not fill precisely all the valleys and peaks on the surface and its own roughness is lower with increasing distance from the cavity entrance.

Fractal dimension describes this change in behavior. Since the fractal analysis was applied on plane, its dimension cannot be lower than two and higher than three, as was explained in the Theoretical part of this work. So, for further inspection the numbers after the deci-

mal point are important. For a simple explanation may be said that the larger the fractal dimension, the more is the surface ragged. *Graph 3* shows fractal dimension for the sample B1. Its value is really low (2.09) which means that sample's surface is almost equal to simple plane. As can be seen in *Fig. 46*, the sample B1 is together with C1 the most remote sample. Therefore it can be assumed that in this place was fluidity of polymeric melt relatively low.
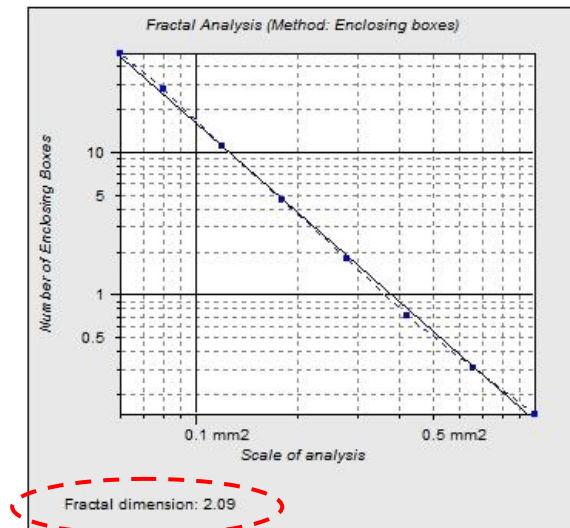
Graph 3 – Fractal dimension of the sample B1

9 PROCESSING OF THE RESULTS

Last part of data evaluation included creation of time series plot graphs for Ra, Rz and Rt parameters. These graphs serve as the proof for the assumption about fluidity of the polymeric melt that was explained in previous pages.

Data for the time series plot graphs were obtained from the "statistical results" tables, which were described in the previous chapter. For every parameter were created four graphs:

- – West – east direction + Gauss filter
- – West – east direction + Robust Gauss filter
- – North – south direction + Gauss filter
- – North – south direction + Robust Gauss filter

9.1 Ra (Arithmetic mean deviation of the assessed profile)

The Ra parameter was evaluated as first. It was because of its universality and its simple interpretation.
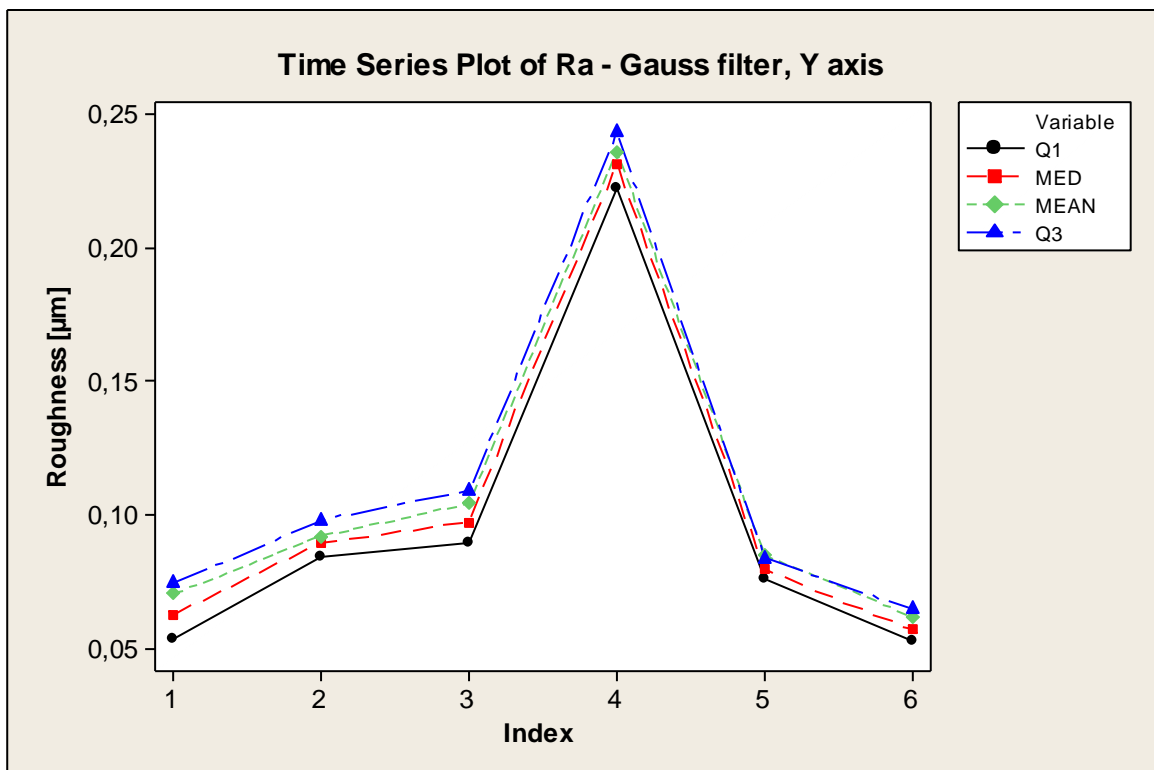
Graph 4 – Time series plot – Ra, Gauss filter, Y axis

As can be seen on the *Graph 4*, the change of roughness perfectly corresponds to the mentioned assumptions. Index numbers describes each measurement places in relation to *Fig. 46*. Large increase of roughness in the middle of the graph is caused by greater distance of sample A2 from the others. However, even in case of relatively close samples C1, C2 or B1, B2 and B3, there can be seen difference in roughness values – roughness of measured product surface increases, the closer is the center of the cavity and entrance into mold (see *Fig. 36*).

Same situation occurred when using the Robust Gauss filter:
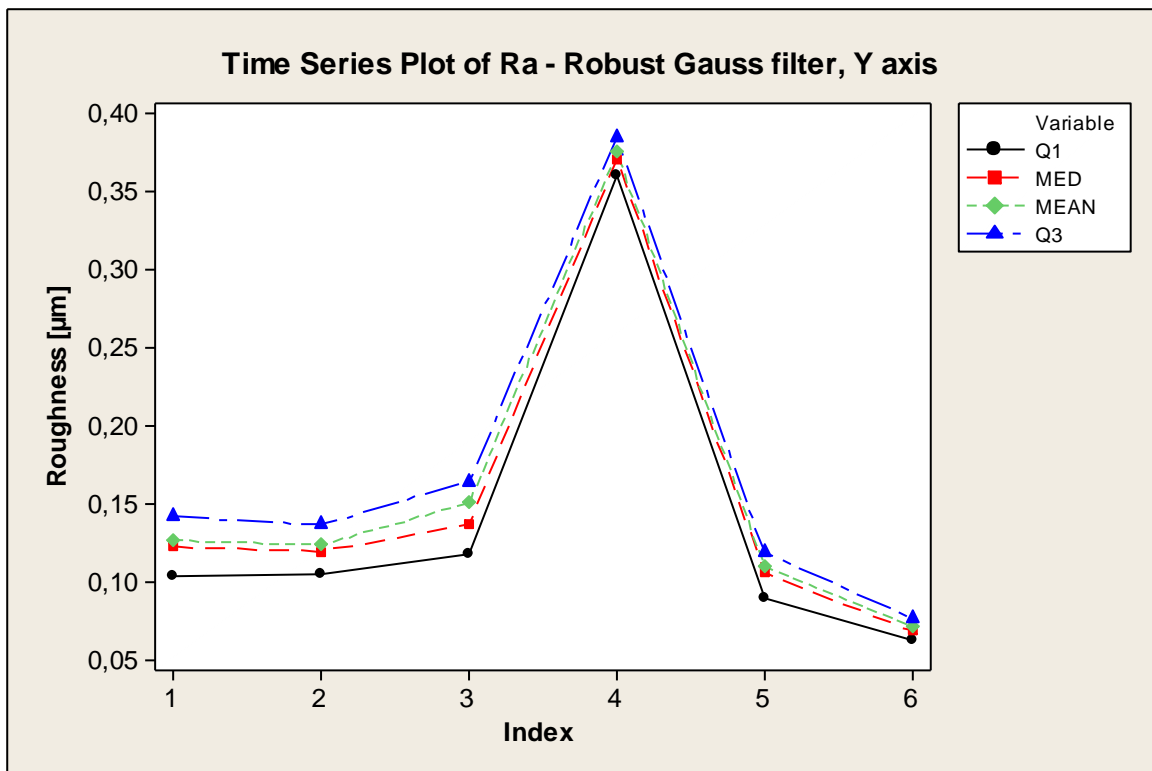
Graph 5 - Time series plot – Ra, Robust Gauss filter, Y axis

Data obtained by Robust Gauss filter achieve higher values, but have very similar course. Only in case of sample B1, there is difference which could be caused probably by present peak, which was discussed in previous chapter (*Fig. 48*). Presence of the outlier is certain also because of greater Interquartile range illustrated in *Graph 5*. While first quartile behaves according the assumptions.

In case of evaluation in X axis, the situation is more complicated. *Graph 6* shows considerable drop in case of B3 sample. While *Graph 7* behaves again exactly according the assumptions, though with big IQRs in case of samples B2 and B3. Reasons of this behavior

can be justified by what filter was used and by detailed analysis of surface roughness re-
sults in the appendix.
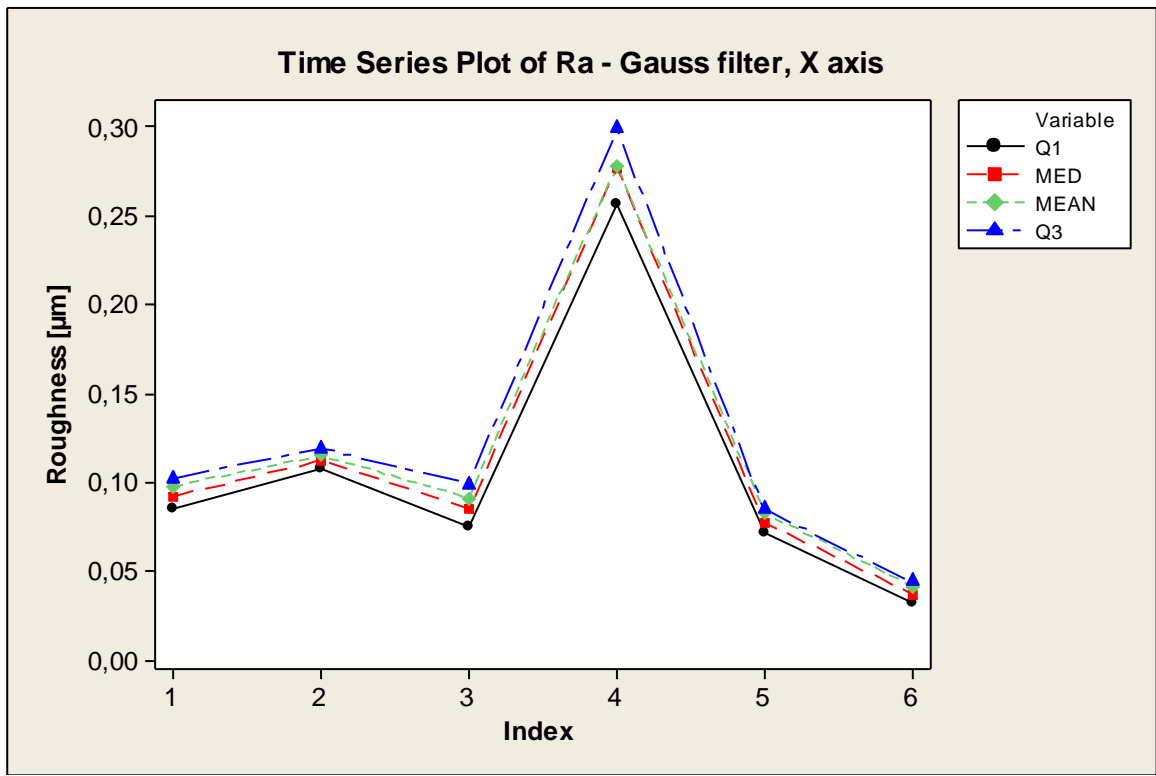
Graph 6 - Time series plot – Ra, Gauss filter, X axis
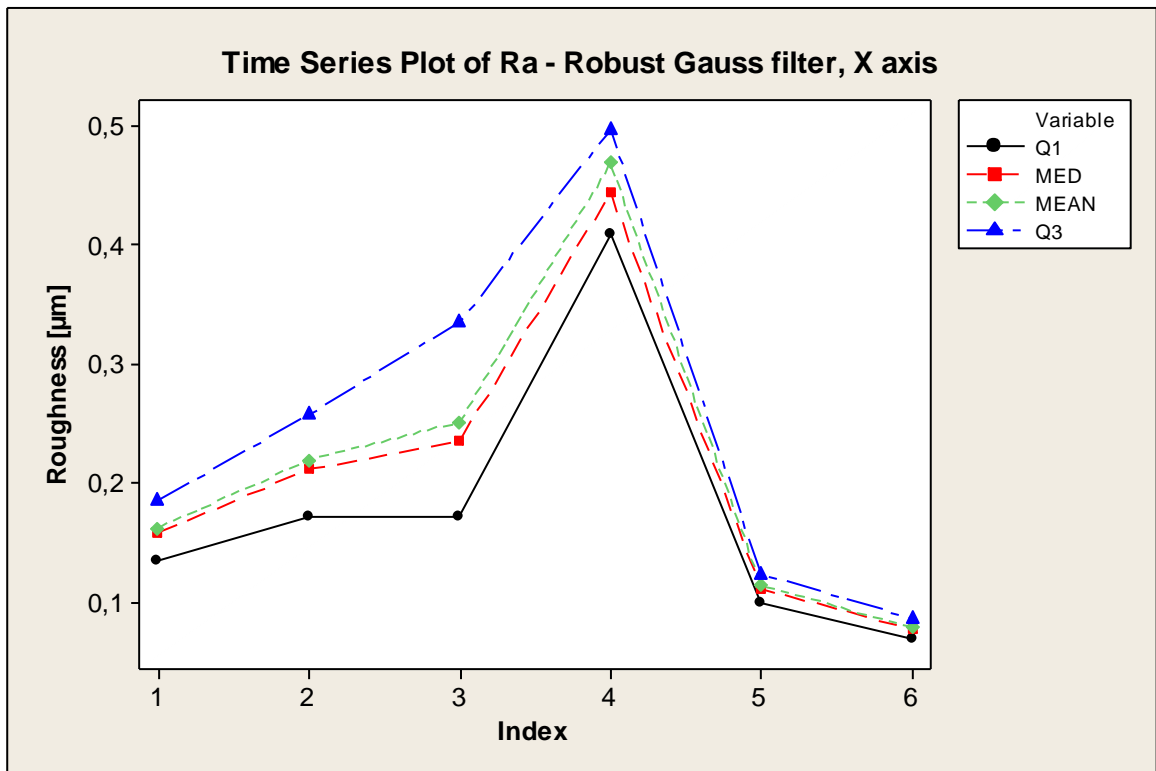
Graph 7 - Time series plot – Ra, Robust Gauss filter, X axis

## 9.2 Rz (Maximum height of the profile within sampling length)

Evaluation of parameters Rz and Rt is little complicated due to their origin. As can be seen in graphs below, individual variables are behaving almost as expected. As the most important indicators can be identified Mean (green line) and mainly Median (red line), because it cannot be influenced by outliers so much as mean variable. It is obvious that IQRs of Rz value are far more greater than it was in case of Ra. For an explanation why this is so can serve *Tab. 3*. Since the measured surfaces contain large peaks and valleys, there are also large IQRs.

Graph 8 - Time series plot – Rz, Gauss filter, Y axis

Graph 8 and *Graph 9* are very similar and there is again only difference in larger values in case of Robust filter. Bigger values in case of sample B1 were probably caused by larger peak, which was mentioned in previous chapter. However, the difference between the values of B1, C1 and A2 is more than double, and also the close places like B1, B2, B3 or C1 and C2 vary. This can be seen as in the case of west – east evaluation (*Graph 8* and *Graph 9*), as well as in the case of north – south evaluation (*Graph 10* and *Graph 11*), where data differs even more and apart from sample B1 (mainly because of Q_3 and mean variables, which are strongly influenced by outliers), they follow supposed trend.
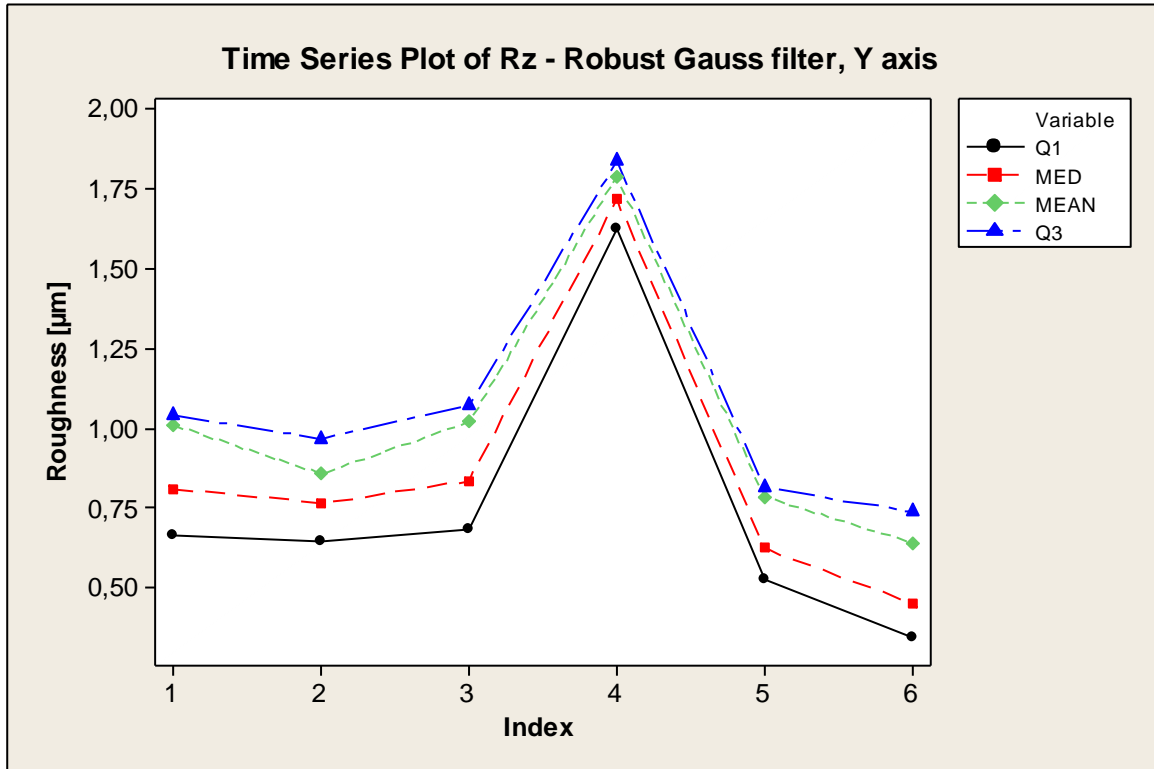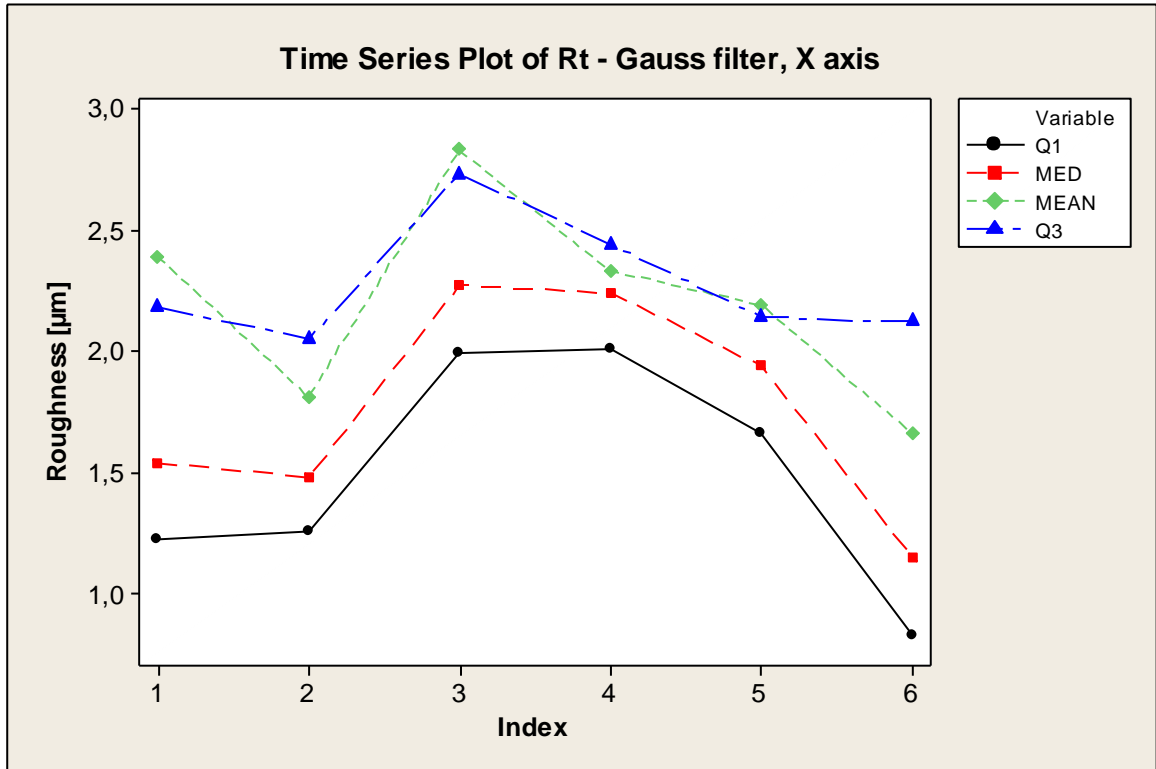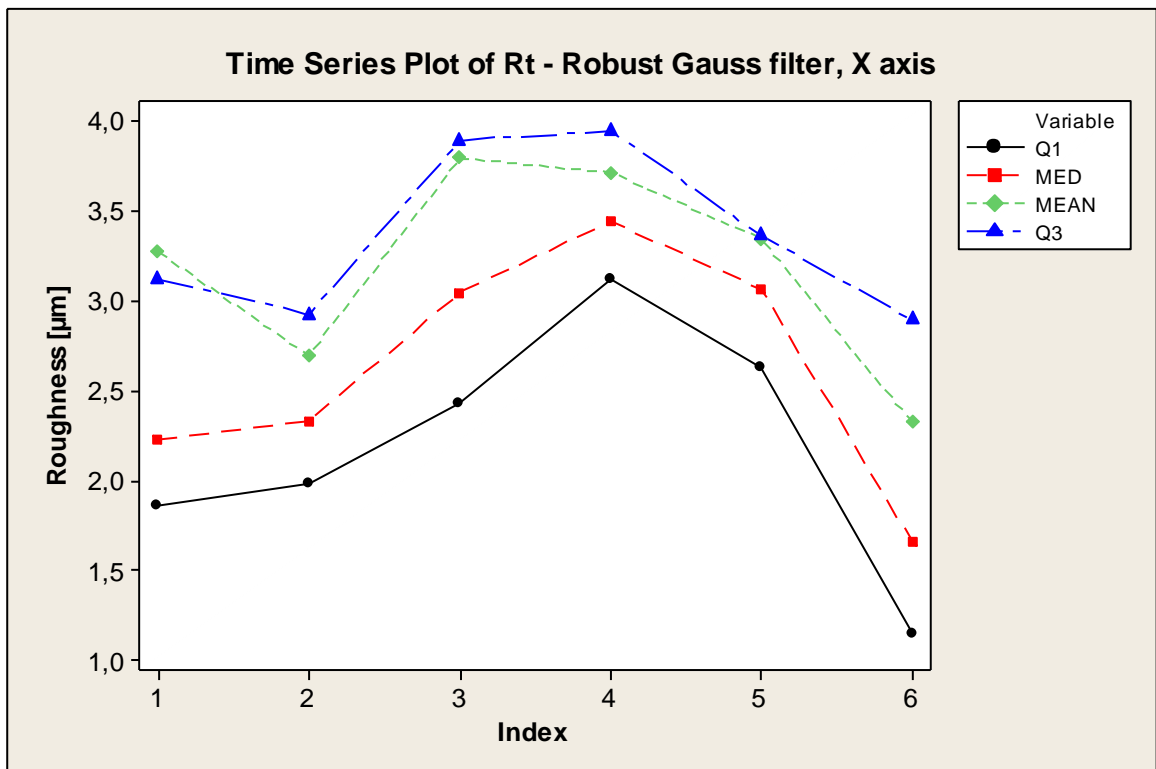
Graph 9 - Time series plot – Rz, Robust Gauss filter, Y axis
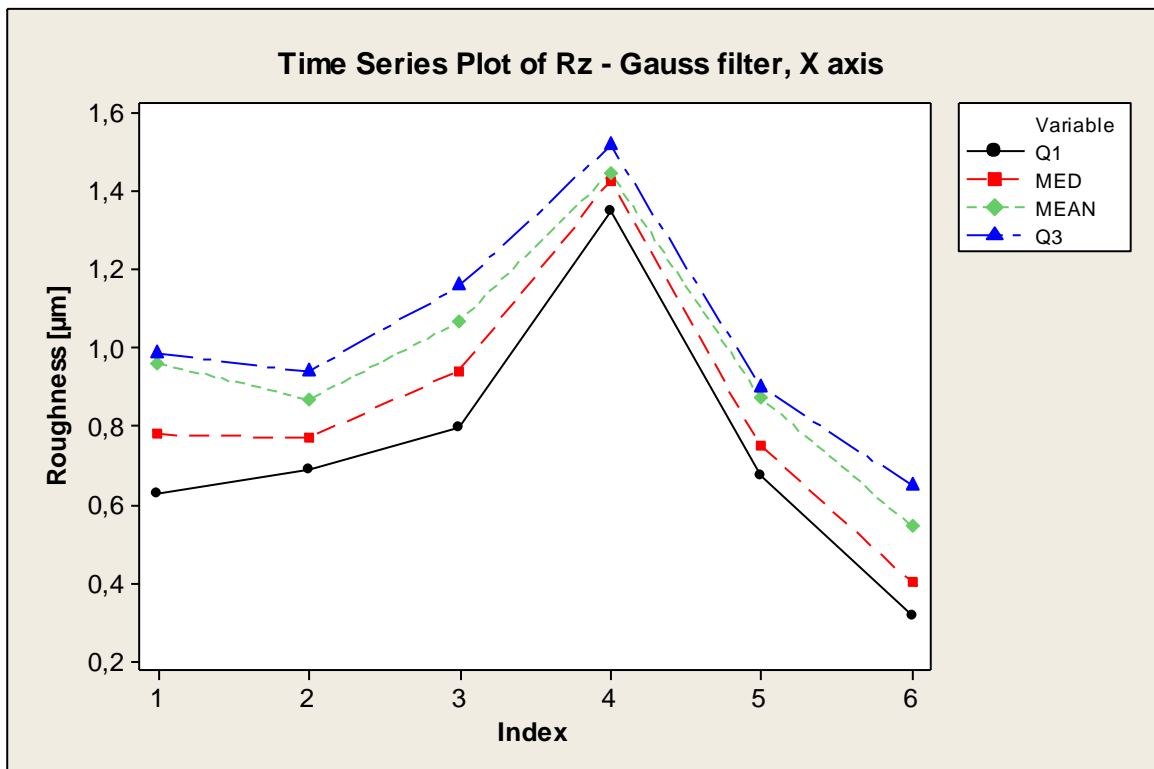
Graph 10 - Time series plot – Rz, Gauss filter, X axis
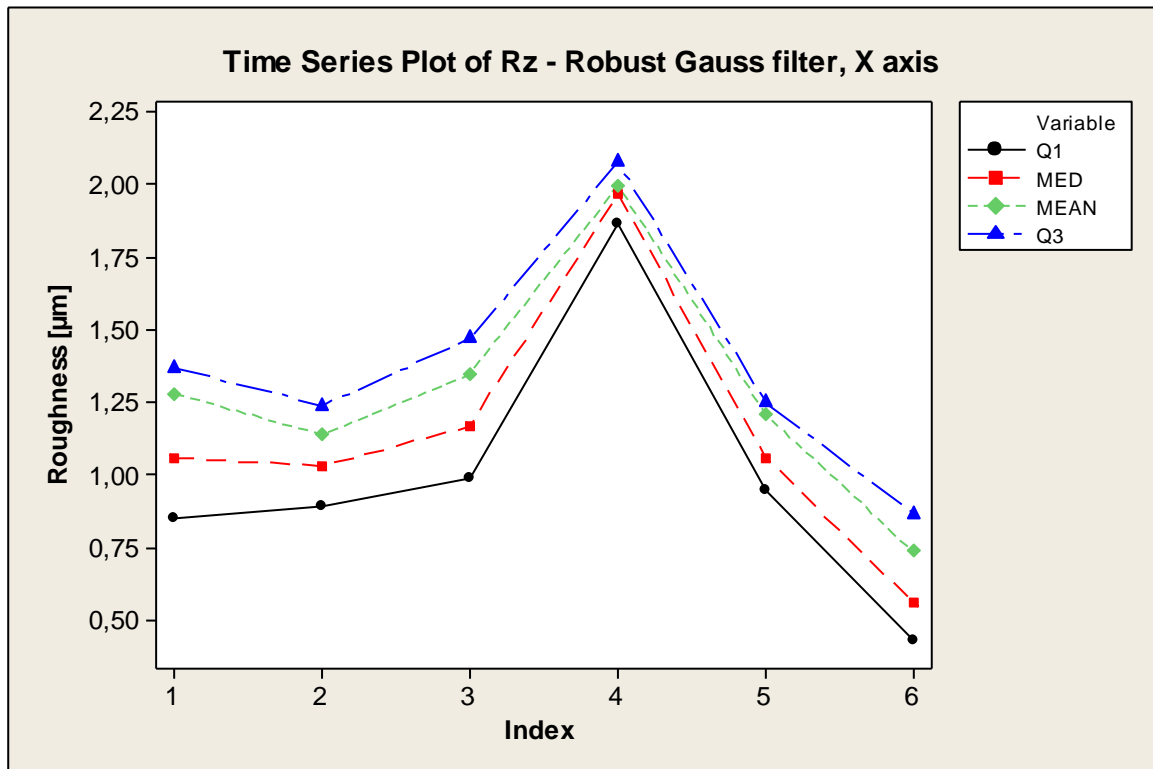
*Graph 11 - Time series plot – Rz, Robust Gauss filter, X axis*

9.3 Rt (Total height of the profile on the evaluation length)

Same situation, as in the case of Rz, only again even a little more complicate occurred in the case of Rt parameter. IQRs of individual samples are even greater than Rz's IQRs (for explanation see *Tab. 3* again). However, *Graph 12* and *Graph 13* show expected trend quite well. At least in case of median variable, which is the most suitable for evaluating of data sets with possible outliers and too differing values, is the trend very convincing.

Far more troublesome situations occurred in *Graph 14* and *Graph 15*, where rendered time series plots were absolutely different from all the others. Most of all, the *Graph 14* is different than anything else and even the median does not behave according to the expected trend. This complicated results originate most probably from existence of outliers (mean is sometimes greater than third quartile) in measured data which could not be excluded. Mainly because only the results of individual variables (their means) were available for processing and the data sets were not accessible in evaluation program. Moreover, the scanned surfaces of the samples could not be simply retouched (if it was not extreme peaks from measurement errors), because it could affect larger area than needed of the sample and thus also the entire evaluating. Hence these results are behaving in such way. Never-

theless, the data trends in *Graph 14* and *Graph 15* at least partially approximates to the assumptions.
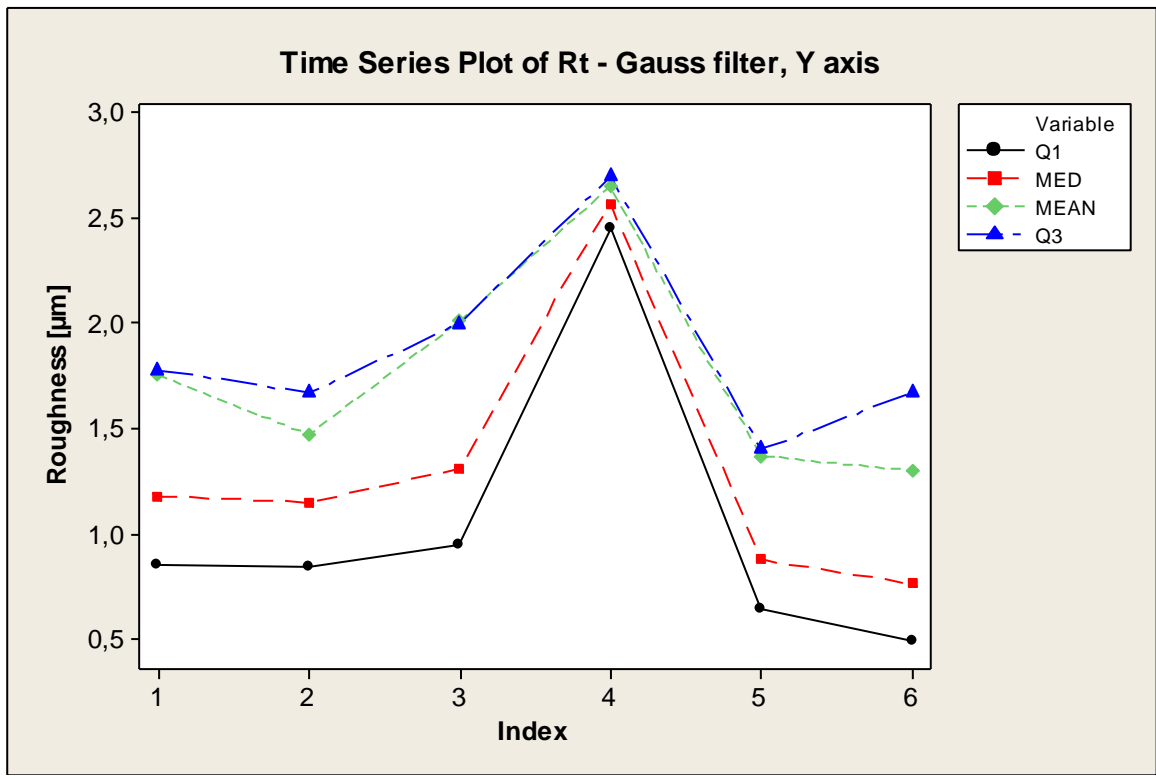
Graph 12 - Time series plot – Rt, Gauss filter, Y axis
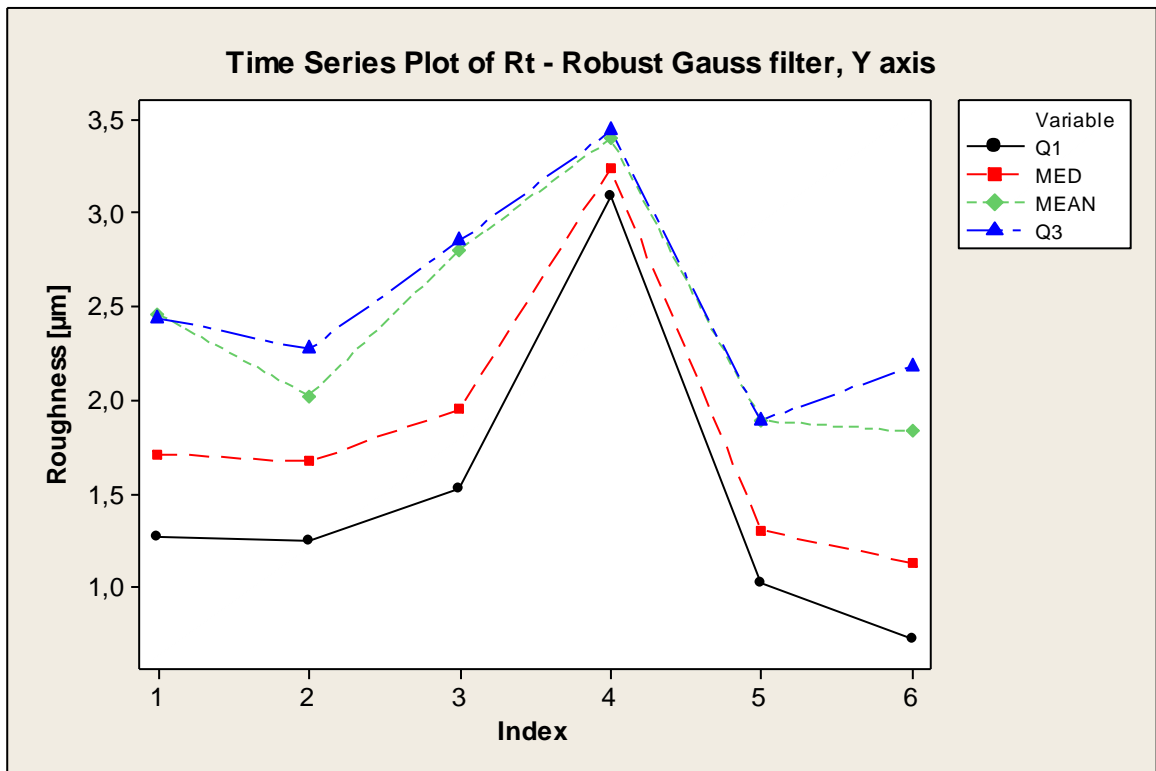
Graph 13 - Time series plot – Rt, Robust Gauss filter, Y axis

Graph 14 - Time series plot – Rt, Gauss filter, X axis

Graph 15 - Time series plot – Rt, Robust Gauss filter, X axis

9.4 Fractal dimension

Fractal dimension of some measured surfaces could not be calculated. The most probably reason is that computation was set on certain accuracy and within its terms was overloaded. This could be resolved by use of different type of fractal dimension, but this action would be incorrect in this case because of deliberate searching for ideal solution. Another possible cause of calculation failure could be in too ragged surface, which could not be evaluated by computation system of used software.

However, in *Graph 16* can be seen that value, which were computed exactly follow the expected trend.
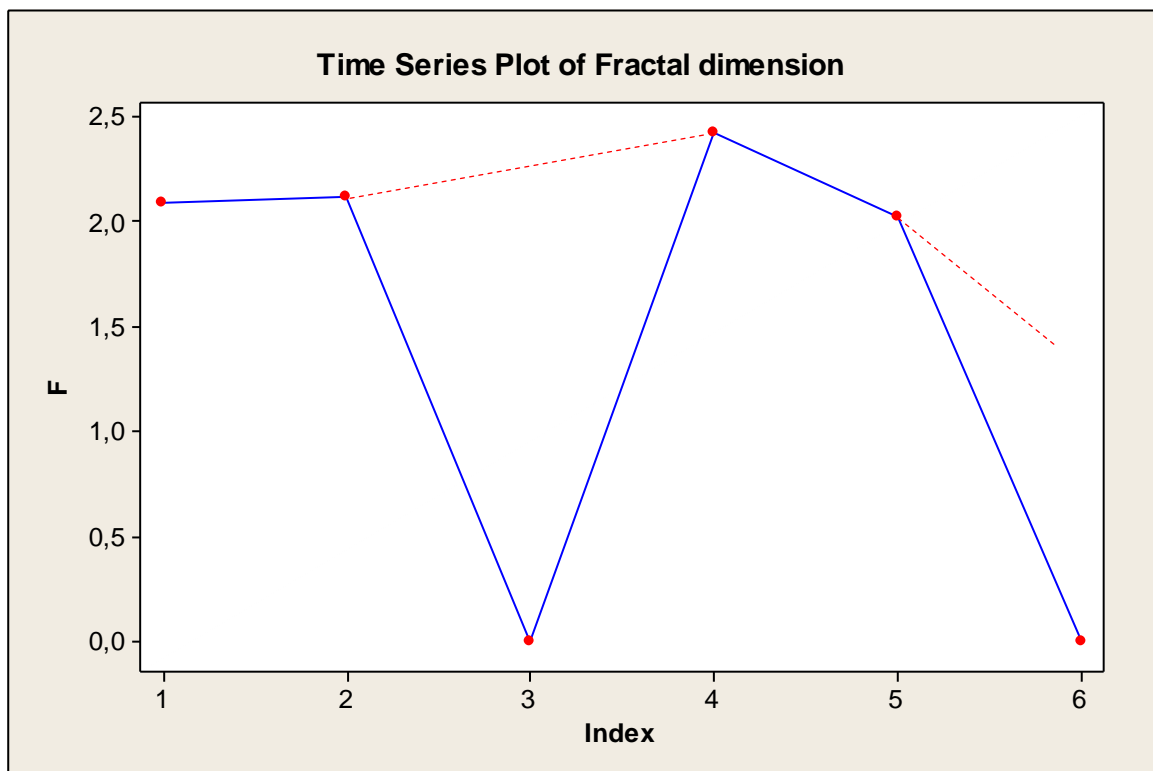
Graph 16 – Time series plot - Fractal dimension

CONCLUSION

The results from the Analysis part confirm the assumptions made at the beginning of the study. Time series plots, created in Minitab 14, show that surface roughness of polymeric part is strongly dependent on the distance of the measured area from the entrance into the cavity. Created graphs shows considerable difference in roughness between remote areas of mold and its centre area, which is directly opposite from the mold entrance. This is really important for further surface evaluation of the polymeric parts which were molded. As was shown, the most suitable places for roughness measurement are close to the entry (injection molding, transfer molding), or, in case of simple pressure molding, close to the warmest place in the mold. In these places the melt has the highest pressure and temperature, which are the two most important factors for polymeric melt fluidity. It follows that the area close to the mentioned places will show the greatest roughness and therefore it should be finished with the greatest precision.

During the analysis also some problems, which can influence other measurements and should be mentioned, occurred. First of all, the evaluation in this work was made only from data obtained from the Talymap software. These data were unfortunately only the means of all sections made by the program from the studied surface and could not be properly inspected. For further assessment and inspection of surface quality should be used either different evaluation system or the approach to the data acquisition must vary. In that case, the Hypothesis theory, which is described in the Theoretical part, could be used for further statistical treatment. Second problem is that polymeric materials are far more vulnerable against the scratches and defects arising during the production, which can affect results from measurement. Another issue is that in case of polycarbonate or other transparent or glossy materials, there can be problem with an optical surface scanning (possible errors were mentioned in the Theoretical part). The last encountered issue was that in many cases it can be very problematic to allocate the best places for the measurement on the assessed sample, mainly because of complexity of polymeric parts.

Anyway, despite these problems it can be seen that surface roughness of the injected polymeric parts is ever-changing and strongly depends on the distance from the cavity entrance. That is why these places should be mainly measured and used as comparatives for individual products.

BIBLIOGRAPHY

[1]   THOMAS, R. Tom. Rough Surfaces. 2nd edition. Imperial College (London) : Imperial College Press, 1999. 278 s. ISBN 1-86094-100-1.

[2]   WHITEHOUSE, David. Surfaces and their measurement. 1st edition. Hermes Penton Science (London) : Hermes Penton Science, 2002. 425 s. ISBN 1-9039-9601-5.

[3]   RAJA, J; MURALIKRISHNAN, B; FU, Shengyu. Recent advances in separation of roughness, waviness and form. Journal of the International Societies for Precision Engineering and Nanotechnology [online]. 2002, [cit. 2011-11-25]. Available from WWW: <www.sciencedirect.com>.

[4]   Talymap 5 : Surface texture analysis software. France : Digital Surf, 2008.

[5]   ISO 11562. Geometrical Product Specifications (GPS) -- Surface texture: Profile method - Metrological characteristics of phase correct filters. Germany : ISO, 1996.

[6]   TOMOV, M; KUZINOVSKI, M. Function on Gaussian and 2RC filters to determine the roughness profile in real non-periodic and periodic surfaces. 14th International Research/Expert Conference "Trends in the Development of Machinery and Associated Technology" [online]. 2010, [cit. 2011-11-25]. Avaiable from: WWW: <www.tmt.unze.ba>.

[7]   Robustní Gaussův filtr – nový způsob filtrace . In Taylor Hobson - Precision [online]. 2007 [cit. 2011-11-25]. Available from WWW: <http://imeco-th.cz>.

[8]   BUMBÁLEK, B.; ODVODY, V.; OŠŤÁDAL, B. Drnost povrchu. Praha : Nakladatelství technické literatury, 1989. 340 s. ISBN 04-252-89.

[9]   Martin.hinner.info [online]. 1999 [cit. 2011-11-25]. Jemný úvod do fraktálů. Available from WWW: <http://martin.hinner.info/math/Fraktaly/>.

[10]   WILEY, John. Fractal Geometry : Mahematical foundations and Applications. 2nd edition. Cornwall (Great Britain) : John Wiley & Sons, 2003. 337 s. ISBN 0-470-84862-6.

[11]   SCOTT, P. J. The case of surface texture parameter RSm. [online]. 2006. Available from: iopscience.iop.org

[12]   LEACH, Richard. Optical Measurement of Surface Topography. Teddington, UK: Springer-Verlag, 2011. ISBN 978-3-642-12011-4.

[13]   STIL. Chromatic confocal imaging. In: Optical principles. Pierre Berthier – Domaine St Hilaire, France.

[14]   HARA, S, T TSUKADA and K SASAJIMA. An in-line digital filtering algorithm for surface roughness profiles. [online]. 1998[cit. 2011-12-27]. Available from: www.sciencedirect.com

[15]   BUCZKOWSKI, S, P HILDGEN and L CARTILIER. Measurements of fractal dimension by box-counting: a critical analysis of data scatter. [online]. 1997. Available from: www.sciencedirect.com

[16]   KRYSTEK, M. P. ISO Filters in Precision Engineering and Production Measurement. [online]. 2010[cit. 2011-12-27]. Available from: http://arxiv.org

[17]   JANG, X. Robust solution for the evaluation of stratified functional surfaces. Manufacturing Technology [online]. [cit. 2011-12-27]. Available from: www.sciencedirect.com

[18]   GADELMAWLA, E. S., M. M. KOURA, T. M. A. MAKSOUD, I. M. ELEWA and H. H. SOLIMAN. Roughness parameters. Materials processing technology [online]. 2002[cit. 2011-12-27]. Available from: www.sciencedirect.com

[19]   PAWLUS, P. Simulation of stratified surface topographies. Wear [online]. 2007[cit. 2011-12-27]. Available from: www.sciencedirect.com

[20]   ŠPERKA, P. Struktura povrchů a vybraných strojních součástí. Brno: Vysoké učení technické učení v Brně, 2009.

[21]   PATA, V., MAŇAS, M., MAŇAS, D. a STANĚK, M. 3D replication of surface structures by rapid prototyping technique. Chemické listy. 2011(105), pp. 733-734. Available from: http://www.chemicke-listy.cz

[22]   BARNETT, V. a T. LEWIS. Outliers in statistical data. John Wiley & Sons, 1994. 3rd edition.

[23]   GRUBBS, F. E. Procedures for detecting outlying observations in samples. Technometrics 11 (1969), pp. 1–21.

[24]   GAŠKO, R. A KOLEKTIV. Štatistické metódy pre klinickủ epidemiológiu a laboratórnu prax. Košice: Aprilla, 2008. ISBN 978-80-89346-00-4.

[25]   FISHER, R. A. Statistical methods for research workers. University of Michigan Library, 1944.

[26]   HUBBARD, R. a M. J. BAYARRI. P Values are not Error Probabilities. 2003.

[27]   TIGLER, S. Fisher and the 5% level. CHANCE. 2009 (Volume 21 / 2008 - Volume 24 / 2011). DOI: 10.1007/s00144-008-0033-3.

[28]   Help. Minitab: Statistical software.

[29]   ANOVA (Analýza rozptylu, Analysis of Variance). In: Investice do rozvoje a vzdělávání.

[30]   KRUSKAL, W. H. a W. A. WALLIS. Use of Ranks in One-Criterion Variance Analysis. Journal of the American Statistical Association. 1952, 47, pp 558 - 621.

LIST OF ABBREVIATIONS

Ra   Arithmetic mean deviation of the assessed profile

Rt   Total height of the profile on the evaluation length

Rz   Maximum height of the profile within sampling length

Rsk   Skewness (asymmetry) of the assessed profile

Rku   Kurtosis of the assessed profile

RMR   Relative material ratio

ISO   International standard organization

ASME American society of mechanical engineers

SPM   Scanning probe microscope

AFM   Atomic force microscope

SEM   Scanning electron microscope

CHCM Chromatic confocal microscope

ANOVA Analysis of variances

LIST OF FIGURES

LIST OF TABLES

LIST OF GRAPHS

APPENDICES

APPENDIX P I: RESULTS OF SAMPLE B2

Fig. 49 – Measuring places scheme – marking B2

Fig. 50 - Original and leveled plane of the sample B2
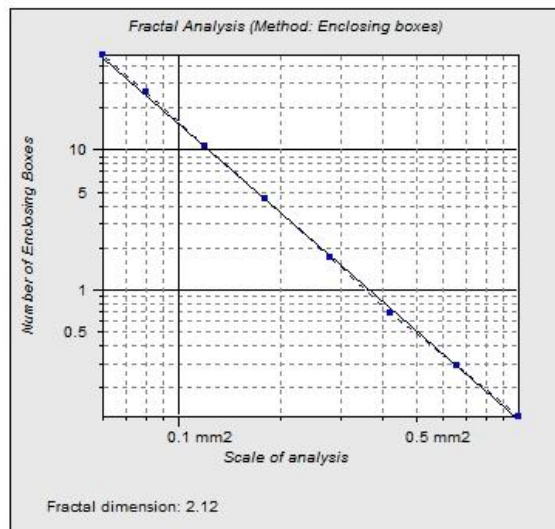
Graph 17 - Fractal dimension of the sample B2

X = 4 mm
Y = 4 mm
Z = 16.5 µm

X = 4 mm
Y = 4 mm
Z = 16.5 µm

Fig. 51 – 3D projection of the sample B2
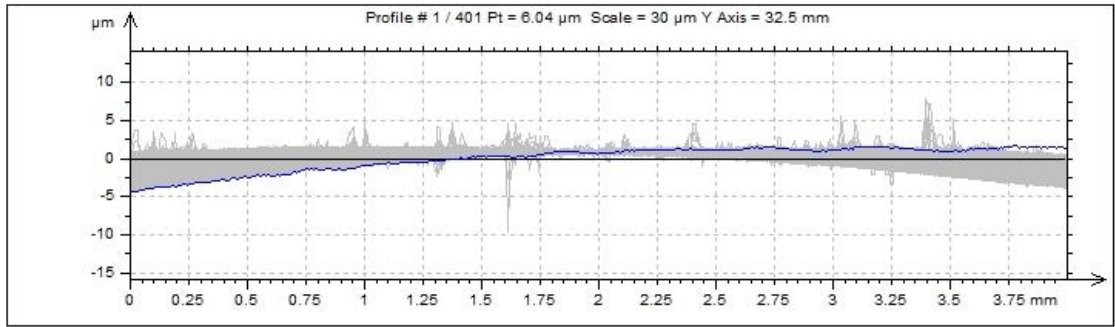
Graph 18 - Series of profiles of the sample B2, west – east direction (Y axis)

Tab. 15 – Statistical results of the sample B2 – Gauss filter, Y axis

ISO 4287		Mean	Std dev	Min	Max	Lower Quartile	Upper Quartile	Median
Amplitude parameters - Roughness profile								
Rp	µm	0.363	0.191	0.166	1.37	0.236	0.416	0.287
Rv	µm	0.308	0.154	0.176	2.41	0.236	0.33	0.272
Rz	µm	0.671	0.284	0.383	3.39	0.499	0.756	0.577
Rc	µm	0.327	0.121	0.169	1.01	0.248	0.362	0.295
Rt	µm	1.47	1.03	0.508	10.6	0.844	1.67	1.15
Ra	µm	0.0919	0.0118	0.0702	0.153	0.0838	0.0979	0.0895
Rq	µm	0.125	0.0324	0.0888	0.41	0.107	0.134	0.116
Rsk		0.95	4.1	-29.7	25.1	-0.482	1.13	-0.0162
Rku		26.1	61.9	2.63	652	4.07	18.4	6.93
Material Ratio parameters - Roughness profile								
Rmr	%	74.3	40.4	0.249	100	47.7	99.8	99.2
Rdc	µm	0.184	0.019	0.149	0.258	0.171	0.193	0.18

Tab. 16 - Statistical results of the sample B2 – Robust Gauss filter, Y axis

ISO 4287		Mean	Std dev	Min	Max	Lower Quartile	Upper Quartile	Median
Amplitude parameters - Roughness profile								
Rp	µm	0.471	0.237	0.209	1.62	0.308	0.553	0.391
Rv	µm	0.386	0.193	0.18	2.99	0.293	0.429	0.348
Rz	µm	0.857	0.344	0.436	4.03	0.642	0.966	0.765
Rc	µm	0.366	0.127	0.173	1.24	0.276	0.415	0.332
Rt	µm	2.02	1.23	0.713	12.2	1.25	2.27	1.67
Ra	µm	0.123	0.0234	0.0785	0.196	0.104	0.136	0.119
Rq	µm	0.17	0.0438	0.1	0.485	0.139	0.192	0.161
Rsk		0.345	4.16	-29.2	26.2	-1.65	1.22	-0.461
Rku		27	58.8	2.77	638	6.58	19.8	9.83
Material Ratio parameters - Roughness profile								
Rmr	%	61.3	42.6	0.249	100	1.81	97.7	88.1
Rdc	µm	0.227	0.0232	0.173	0.309	0.212	0.24	0.223
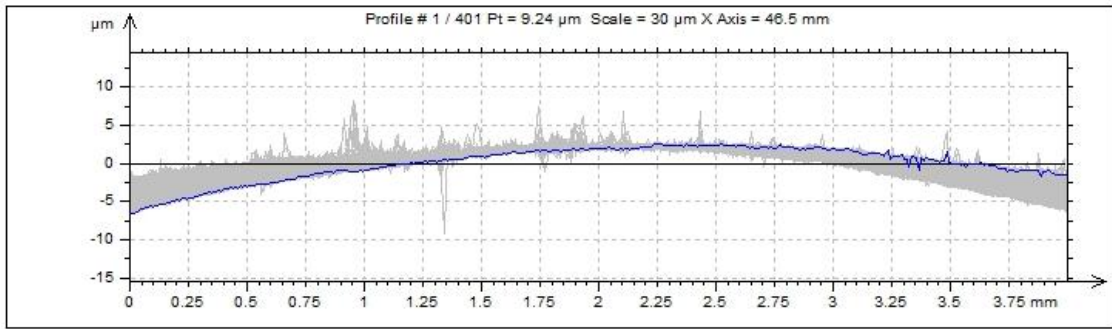
Graph 19 - Series of profiles of the sample B2, north - south direction (X axis)

Tab. 17 - Statistical results of the sample B2 – Gauss filter, X axis

ISO 4287		Mean	Std dev	Min	Max	Lower Quartile	Upper Quartile	Median
Amplitude parameters - Roughness profile								
Rp	µm	0.472	0.219	0.262	1.78	0.332	0.538	0.384
Rv	µm	0.397	0.144	0.223	2.35	0.325	0.431	0.376
Rz	µm	0.868	0.302	0.541	3.52	0.687	0.941	0.77
Rc	µm	0.406	0.118	0.22	1.24	0.333	0.441	0.378
Rt	µm	1.81	0.976	0.862	11.4	1.26	2.05	1.48
Ra	µm	0.115	0.013	0.0936	0.2	0.107	0.119	0.112
Rq	µm	0.163	0.0324	0.125	0.416	0.143	0.17	0.154
Rsk		0.142	3.03	-17.2	21.8	-1.33	0.574	-0.324
Rku		20	39	3.18	426	6.84	15.7	11
Material Ratio parameters - Roughness profile								
Rmr	%	70.5	40.6	0.249	100	26.3	98.4	96.6
Rdc	µm	0.217	0.0197	0.163	0.288	0.203	0.231	0.215

Tab. 18 - Statistical results of the sample B2 – Robust Gauss filter, X axis

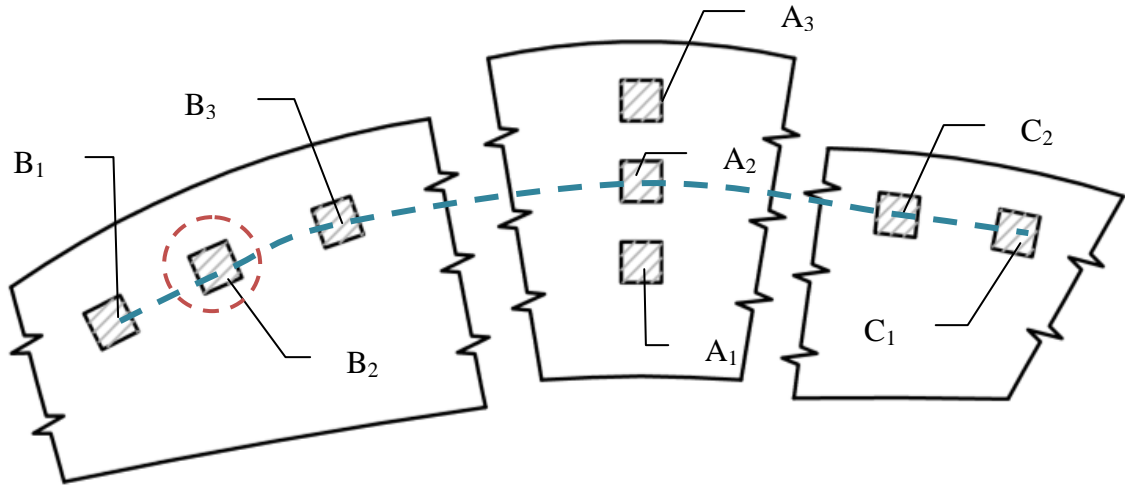| ISO 4287		Mean	Std dev	Min	Max	Lower Quartile	Upper Quartile	Median
Amplitude parameters - Roughness profile								
Rp	µm	0.666	0.302	0.275	2.44	0.477	0.761	0.568
Rv	µm	0.475	0.199	0.206	3.17	0.373	0.537	0.452
Rz	µm	1.14	0.404	0.653	4.53	0.892	1.24	1.03
Rc	µm	0.728	0.361	0.276	4.32	0.532	0.835	0.654
Rt	µm	2.69	1.23	1.29	14.1	1.98	2.92	2.33
Ra	µm	0.219	0.0564	0.105	0.365	0.172	0.257	0.211
Rq	µm	0.282	0.0711	0.144	0.631	0.228	0.324	0.276
Rsk		-0.459	2.86	-12.1	18.1	-2.16	0.816	-0.872
Rku		14.9	29.4	2.11	253	5.57	13.1	9.09
Material Ratio parameters - Roughness profile								
Rmr	%	49	36.2	0.249	99	1.53	81.3	68.7
Rdc	µm	0.444	0.0997	0.247	0.815	0.373	0.502	0.427

APPENDIX P I: RESULTS OF SAMPLE B3

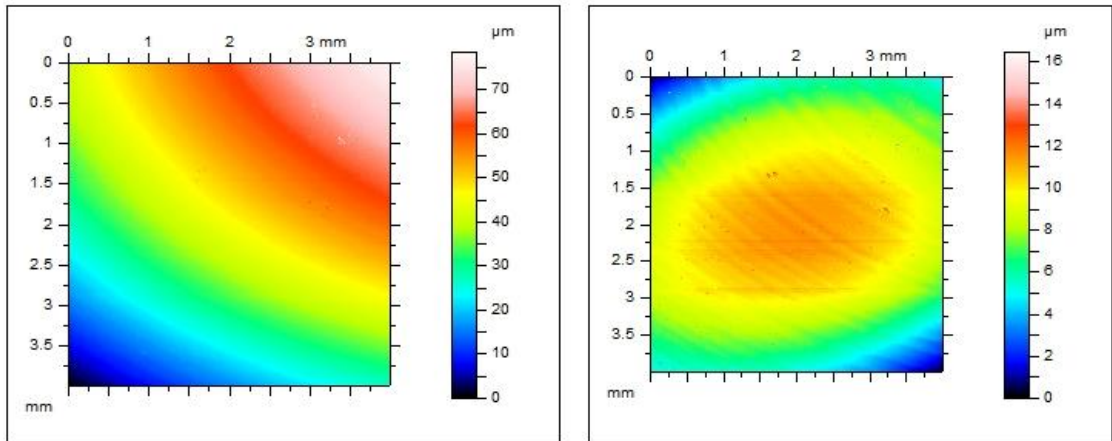
Fig. 52 – Measuring places scheme – marking B3
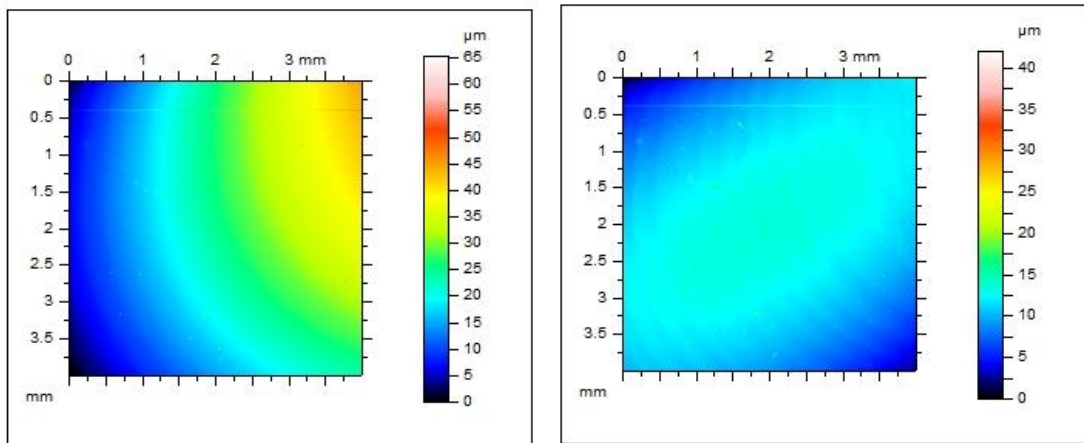
Fig. 53 - Original and leveled plane of the sample B3

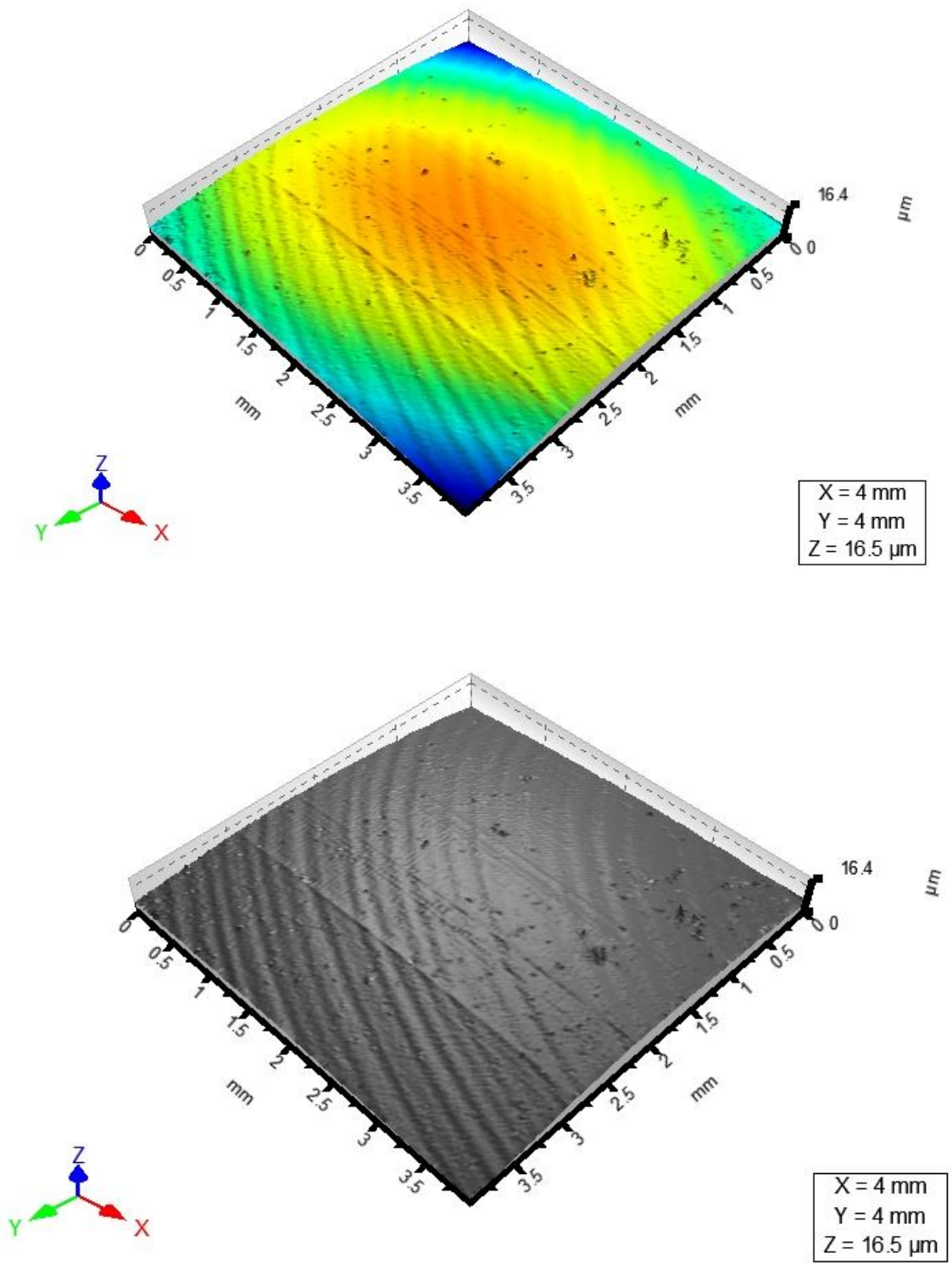*Graph 20 - Fractal dimension of the sample B2*

*Fig. 54 – 3D projection of the sample B3*
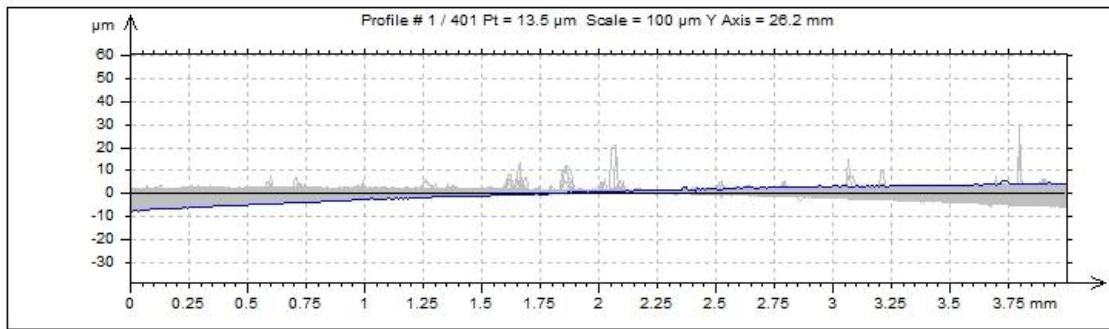
Graph 21 - Series of profiles of the sample B3, west – east direction (Y axis)

Tab. 19 – Statistical results of the sample B3 – Gauss filter, Y axis

ISO 4287		Mean	Std dev	Min	Max	Lower Quartile	Upper Quartile	Median
Amplitude parameters - Roughness profile								
Rp	µm	0.508	0.494	0.179	4.9	0.267	0.529	0.35
Rv	µm	0.297	0.0914	0.162	0.679	0.229	0.338	0.277
Rz	µm	0.804	0.543	0.341	5.53	0.53	0.838	0.647
Rc	µm	0.392	0.287	0.2	3.57	0.27	0.393	0.318
Rt	µm	2.01	2.66	0.563	32.4	0.944	2	1.31
Ra	µm	0.104	0.0293	0.0761	0.383	0.0894	0.109	0.097
Rq	µm	0.148	0.0774	0.0897	0.915	0.112	0.148	0.128
Rsk		3.23	8.36	-3.97	75.6	-0.228	2.85	0.271
Rku		54.7	165	2.23	2187	4	26	8.09
Material Ratio parameters - Roughness profile								
Rmr	%	63.4	45.8	0.249	100	1.22	99.8	98.2
Rdc	µm	0.195	0.0195	0.147	0.29	0.183	0.206	0.194

Tab. 20 - Statistical results of the sample B3 – Robust Gauss filter, Y axis

ISO 4287		Mean	Std dev	Min	Max	Lower Quartile	Upper Quartile	Median
Amplitude parameters - Roughness profile								
Rp	µm	0.676	0.614	0.207	5.5	0.366	0.699	0.473
Rv	µm	0.349	0.125	0.0758	0.699	0.257	0.421	0.342
Rz	µm	1.02	0.647	0.427	5.92	0.685	1.07	0.835
Rc	µm	0.49	0.377	0.221	4.12	0.316	0.507	0.382
Rt	µm	2.8	3.01	0.756	33.4	1.52	2.85	1.95
Ra	µm	0.15	0.053	0.0903	0.376	0.117	0.164	0.136
Rq	µm	0.215	0.101	0.109	1.07	0.157	0.234	0.185
Rsk		2.88	9.26	-3.71	84.5	-1.79	2.65	0.343
Rku		61	187	1.7	2548	7.06	25	10.6
Material Ratio parameters - Roughness profile								
Rmr	%	51.7	44.2	0.249	100	0.568	94.2	78.1
Rdc	µm	0.247	0.0346	0.188	0.409	0.224	0.262	0.238
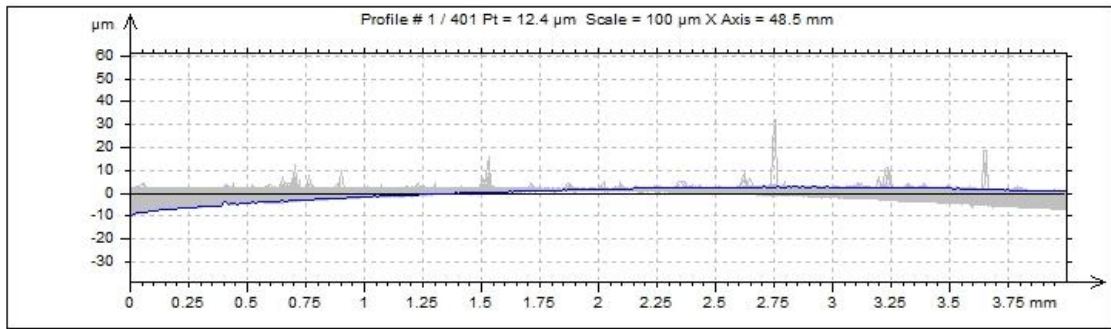
Graph 22 - Series of profiles of the sample B3, north - south direction (X axis)

Tab. 21 - Statistical results of the sample B3 – Gauss filter, X axis

ISO 4287		Mean	Std dev	Min	Max	Lower Quartile	Upper Quartile	Median
Amplitude parameters - Roughness profile								
Rp	µm	0.731	0.478	0.385	6.28	0.495	0.766	0.581
Rv	µm	0.339	0.124	0.139	0.684	0.234	0.427	0.325
Rz	µm	1.07	0.513	0.549	6.77	0.796	1.16	0.943
Rc	µm	0.461	0.577	0.171	9.76	0.287	0.436	0.339
Rt	µm	2.83	2.18	1.49	24.8	1.99	2.73	2.27
Ra	µm	0.091	0.0272	0.0603	0.352	0.0752	0.0987	0.0849
Rq	µm	0.16	0.0735	0.0925	0.963	0.12	0.172	0.143
Rsk		5.17	8.74	-8.97	70	0.578	6.78	4.33
Rku		101	147	23.3	1586	46.7	88.9	62.1
Material Ratio parameters - Roughness profile								
Rmr	%	7.51	17.6	0.249	91.8	0.611	3.11	1.32
Rdc	µm	0.142	0.0247	0.0948	0.288	0.125	0.155	0.14

Tab. 22 - Statistical results of the sample B3 – Robust Gauss filter, X axis

ISO 4287		Mean	Std dev	Min	Max	Lower Quartile	Upper Quartile	Median
Amplitude parameters - Roughness profile								
Rp	µm	0.933	0.686	0.241	8.81	0.586	1.02	0.751
Rv	µm	0.416	0.177	0.021	1.12	0.287	0.528	0.408
Rz	µm	1.35	0.683	0.723	9.03	0.988	1.47	1.17
Rc	µm	1	0.603	0.228	6.49	0.595	1.21	0.896
Rt	µm	3.79	2.88	1.47	34.5	2.43	3.89	3.04
Ra	µm	0.251	0.108	0.0828	0.497	0.171	0.335	0.235
Rq	µm	0.322	0.127	0.123	1.23	0.224	0.413	0.298
Rsk		1.72	8.41	-5.18	79	-2.82	2.88	-0.319
Rku		55.2	160	4.49	1938	10.3	31.5	14.5
Material Ratio parameters - Roughness profile								
Rmr	%	19.8	31.2	0.249	87	0.392	25.5	1.56
Rdc	µm	0.434	0.152	0.184	0.899	0.319	0.529	0.413

APPENDIX P I: RESULTS OF SAMPLE A2

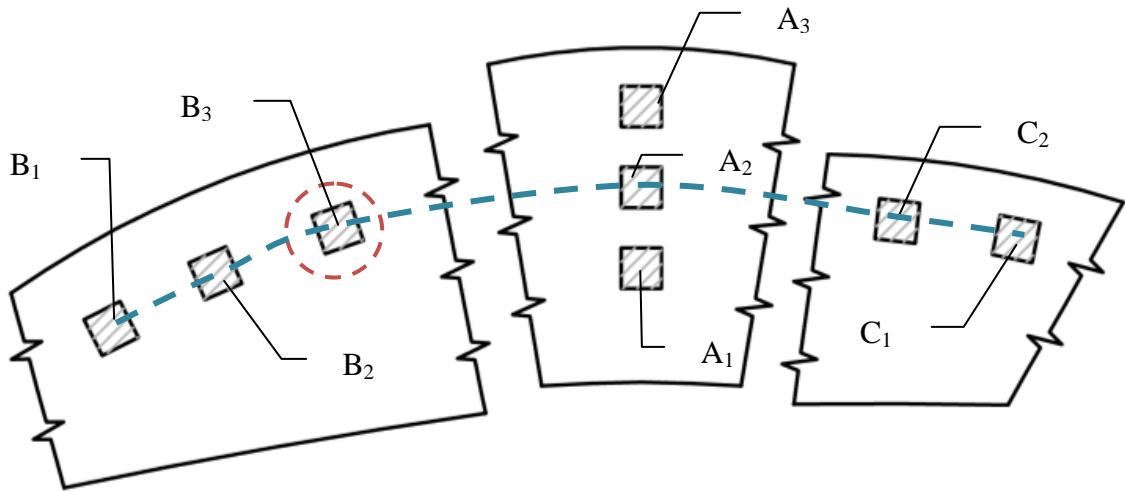*Fig. 55 – Measuring places scheme – marking A2*
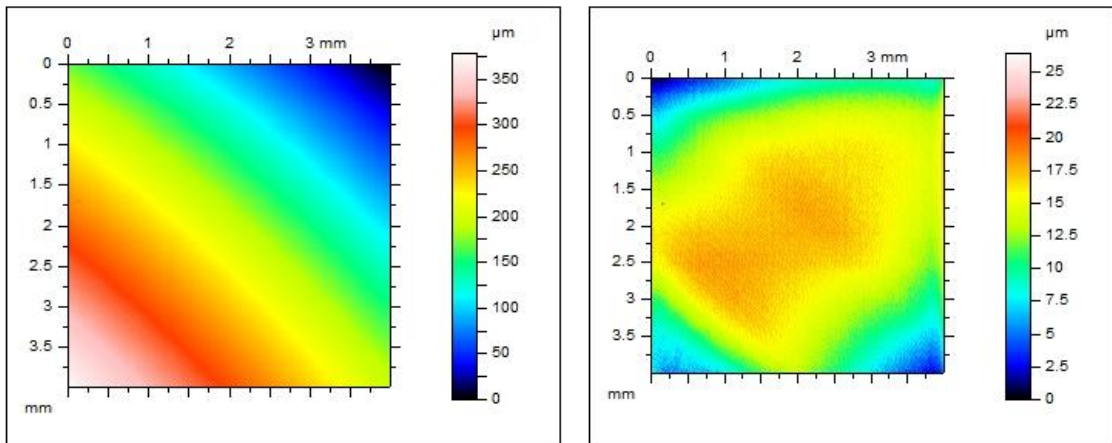
Fig. 56 - Original and leveled plane of the sample A2
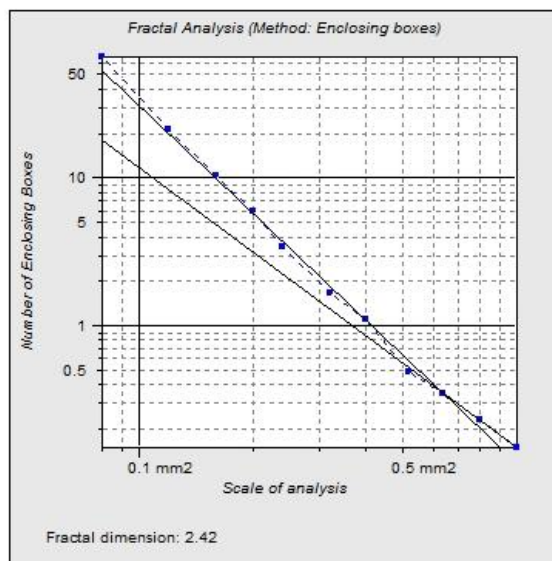
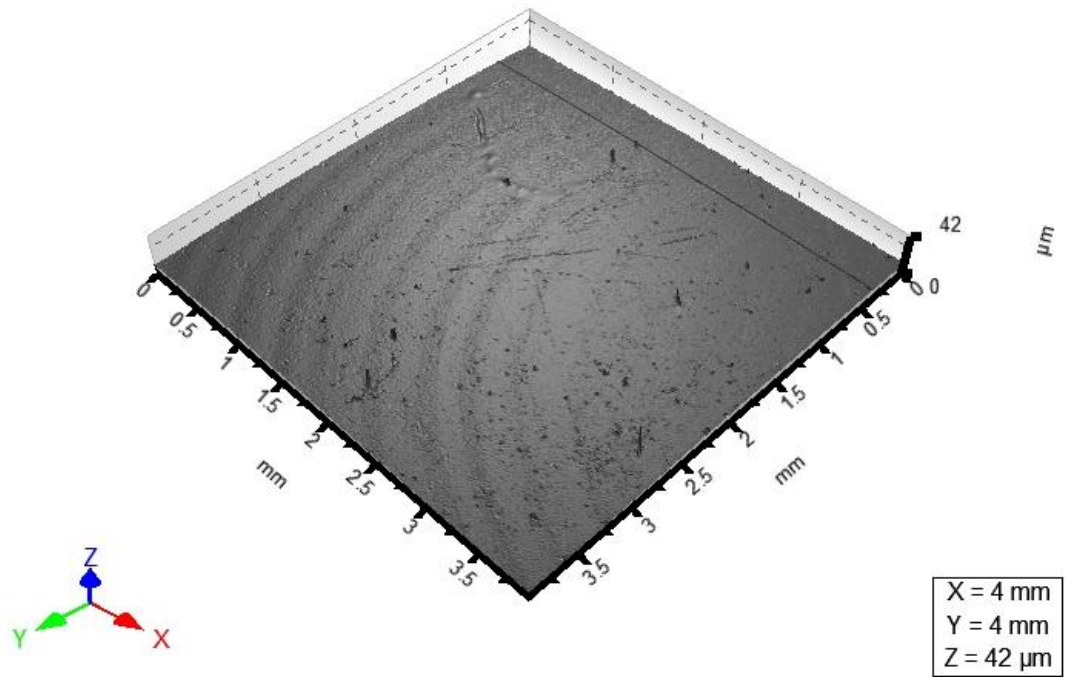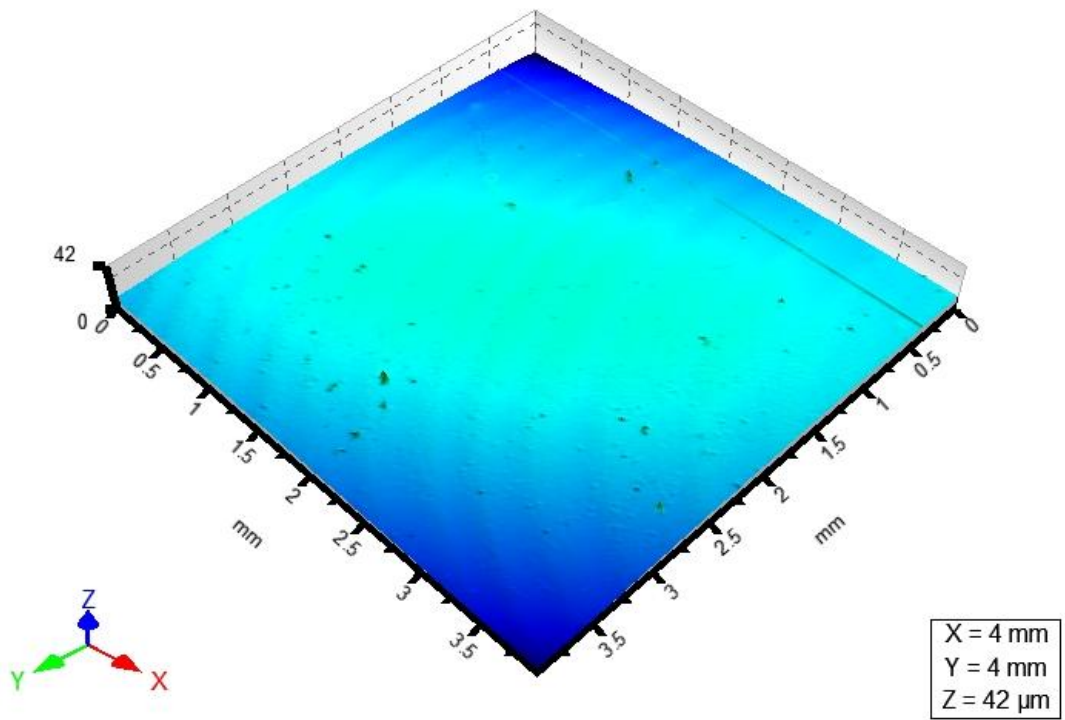*Graph 23 - Fractal dimension of the sample A2*
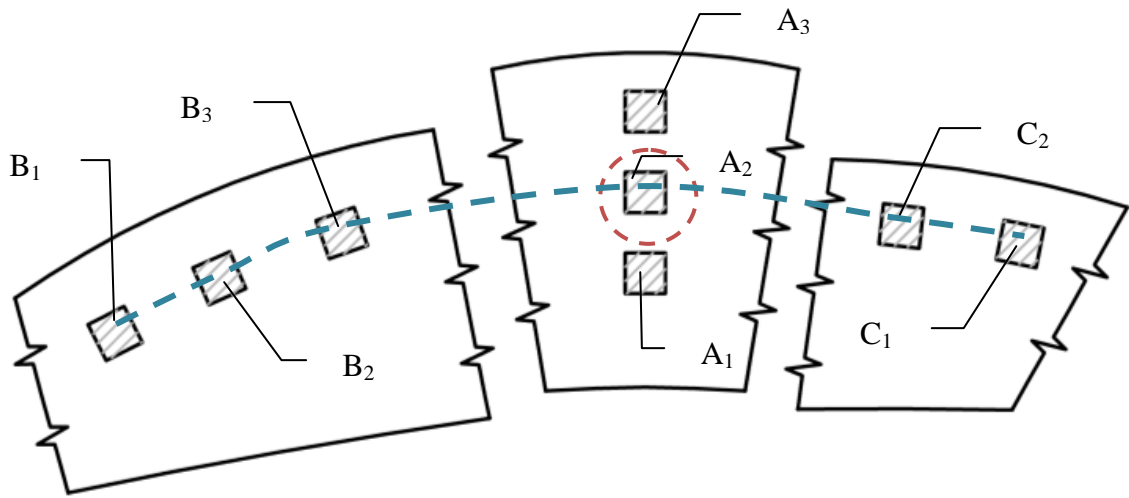
Fig. 57 – 3D projection of the sample A2
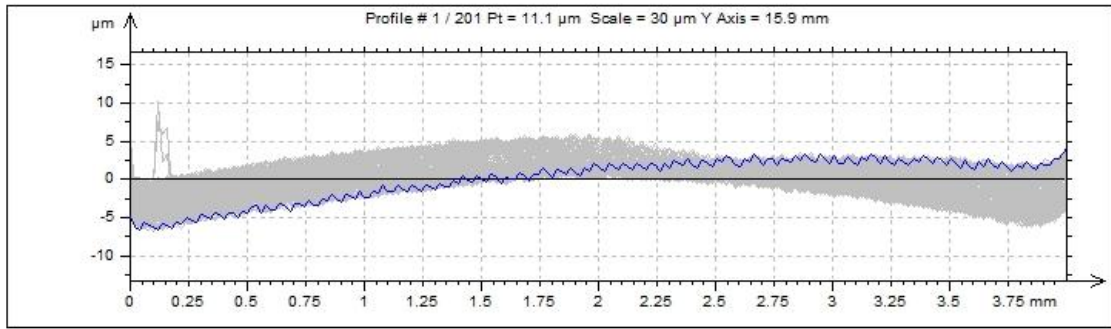
Graph 24 - Series of profiles of the sample A2, west – east direction (Y axis)

Tab. 23 – Statistical results of the sample A2 – Gauss filter, Y axis

ISO 4287		Mean	Std dev	Min	Max	Lower Quartile	Upper Quartile	Median
Amplitude parameters - Roughness profile								
Rp	μm	0.708	0.187	0.509	2.07	0.606	0.745	0.66
Rv	μm	0.616	0.0633	0.498	0.97	0.574	0.649	0.611
Rz	μm	1.32	0.226	1.08	3.04	1.2	1.36	1.27
Rc	μm	0.687	0.0693	0.568	1.06	0.634	0.725	0.674
Rt	μm	2.65	0.61	1.81	8.3	2.45	2.7	2.57
Ra	μm	0.236	0.0229	0.202	0.41	0.222	0.243	0.231
Rq	μm	0.299	0.0385	0.259	0.638	0.28	0.306	0.29
Rsk		0.325	1.18	-0.342	10.8	-0.0171	0.265	0.108
Rku		5.02	11.5	2.42	115	2.84	3.57	3.07
Material Ratio parameters - Roughness profile								
Rmr	%	4.16	5.07	0.498	44.3	1.19	4.77	2.23
Rdc	μm	0.512	0.039	0.422	0.641	0.484	0.538	0.507

Tab. 24 - Statistical results of the sample A2 – Robust Gauss filter, Y axis

ISO 4287		Mean	Std dev	Min	Max	Lower Quartile	Upper Quartile	Median
Amplitude parameters - Roughness profile								
Rp	μm	0.955	0.282	0.692	3.31	0.807	0.992	0.879
Rv	μm	0.837	0.0716	0.698	1.13	0.785	0.88	0.83
Rz	μm	1.79	0.308	1.46	4.23	1.63	1.84	1.72
Rc	μm	0.97	0.0545	0.891	1.33	0.941	0.991	0.963
Rt	μm	3.4	0.924	2.51	12.6	3.09	3.44	3.24
Ra	μm	0.375	0.0248	0.342	0.581	0.36	0.384	0.371
Rq	μm	0.452	0.055	0.406	0.973	0.427	0.46	0.439
Rsk		0.295	1.53	-0.453	15.8	-0.0847	0.198	0.0334
Rku		4.84	16.7	1.87	201	2.17	2.84	2.32
Material Ratio parameters - Roughness profile								
Rmr	%	1.99	2.41	0.498	22.7	0.87	1.47	1.05
Rdc	μm	0.864	0.0347	0.775	0.968	0.838	0.886	0.858
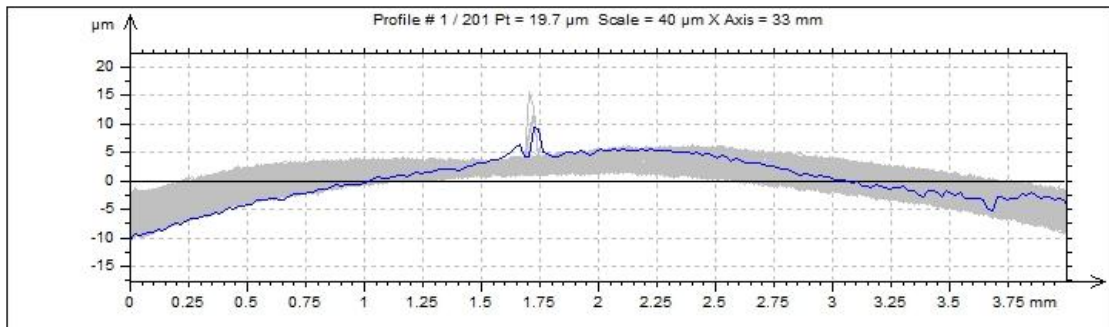
Graph 25 - Series of profiles of the sample A2, north - south direction (X axis)

Tab. 25 - Statistical results of the sample A2 – Gauss filter, X axis

ISO 4287		Mean	Std dev	Min	Max	Lower Quartile	Upper Quartile	Median
Amplitude parameters - Roughness profile								
Rp	µm	0.685	0.178	0.33	2.22	0.62	0.719	0.667
Rv	µm	0.76	0.108	0.364	1.21	0.7	0.826	0.757
Rz	µm	1.45	0.253	0.723	3.43	1.35	1.52	1.43
Rc	µm	0.747	0.0983	0.494	1.35	0.684	0.797	0.74
Rt	µm	2.33	0.744	1.67	9.29	2.01	2.44	2.24
Ra	µm	0.278	0.0355	0.138	0.433	0.256	0.299	0.277
Rq	µm	0.349	0.0508	0.177	0.732	0.321	0.371	0.348
Rsk		-0.419	1.17	-1.83	11	-0.832	-0.251	-0.499
Rku		5.99	9.4	2.54	110	3.62	5.61	4.4
Material Ratio parameters - Roughness profile								
Rmr	%	69.6	16.4	0.498	97.5	60.9	80.6	73
Rdc	µm	0.578	0.0774	0.234	0.762	0.532	0.627	0.579

Tab. 26 - Statistical results of the sample A2 – Robust Gauss filter, X axis

ISO 4287		Mean	Std dev	Min	Max	Lower Quartile	Upper Quartile	Median
Amplitude parameters - Roughness profile								
Rp	µm	0.949	0.293	0.551	3.65	0.845	0.993	0.913
Rv	µm	1.05	0.164	0.485	1.48	0.937	1.17	1.05
Rz	µm	2	0.347	1.12	5.01	1.87	2.08	1.97
Rc	µm	1.06	0.149	0.801	1.89	0.963	1.12	1.05
Rt	µm	3.71	1.35	2.44	16.1	3.12	3.94	3.44
Ra	µm	0.469	0.0873	0.315	0.767	0.408	0.496	0.444
Rq	µm	0.582	0.123	0.387	1.29	0.505	0.624	0.539
Rsk		-1.29	1.24	-4.05	6.58	-2.02	-0.544	-1.12
Rku		7.18	6.04	2.26	68.7	4.09	8.45	5.83
Material Ratio parameters - Roughness profile								
Rmr	%	46	12.5	0.498	79.1	39.4	54.1	47
Rdc	µm	0.902	0.0908	0.654	1.18	0.836	0.962	0.908

APPENDIX P I: RESULTS OF SAMPLE C2

*Fig. 58 – Measuring places scheme – marking C2*

Fig. 59 - Original and leveled plane of the sample C2
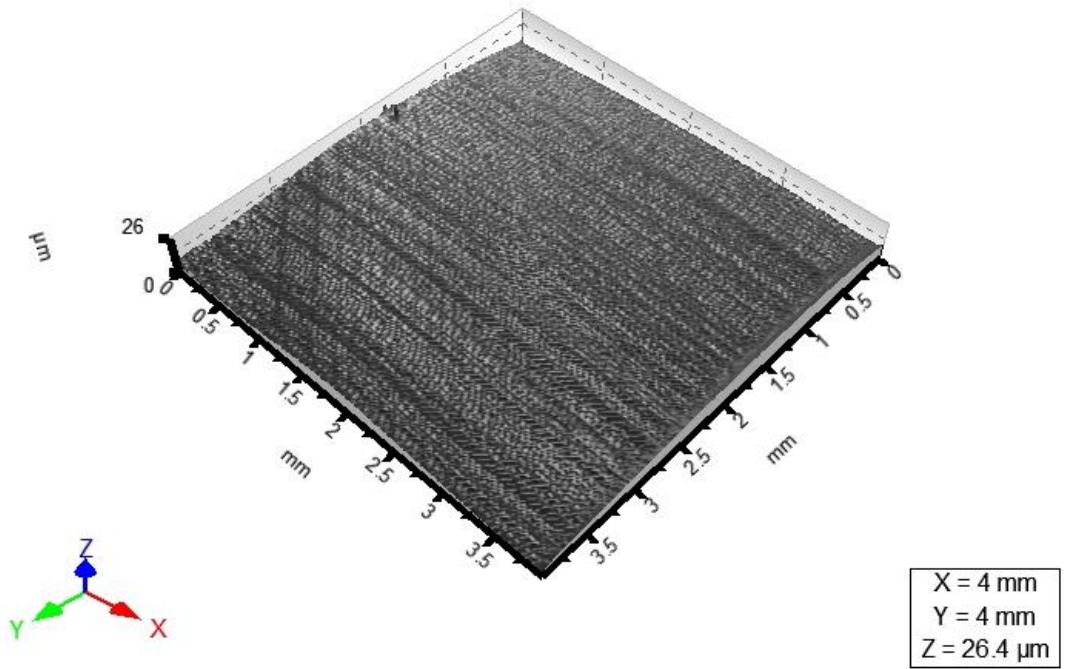

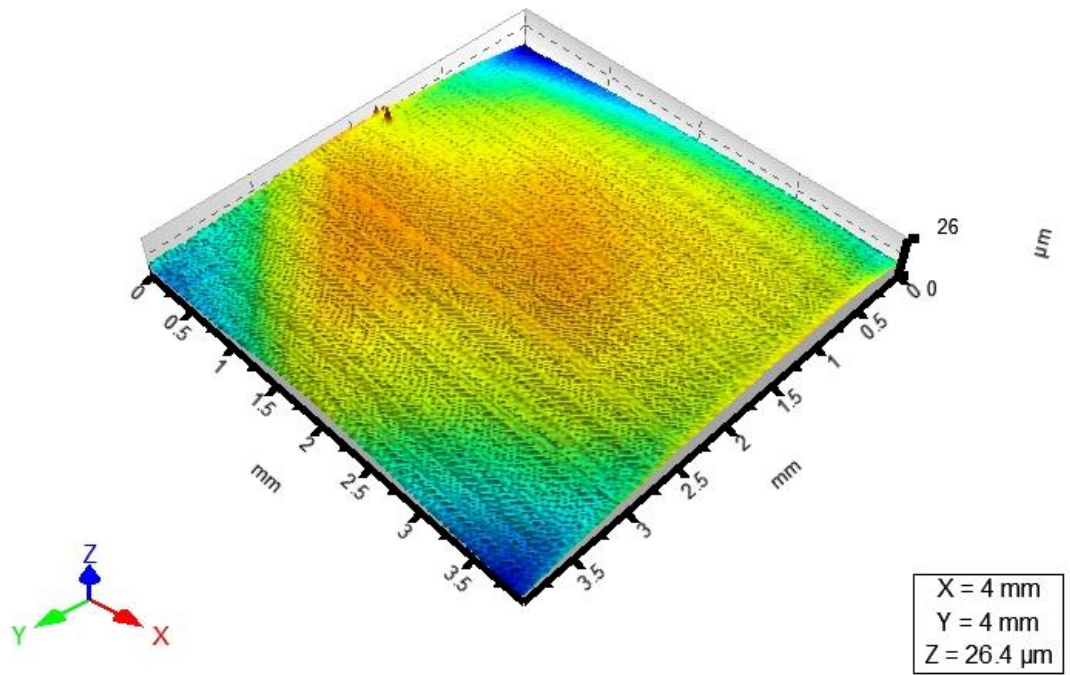*Graph 26 - Fractal dimension of the sample C2*

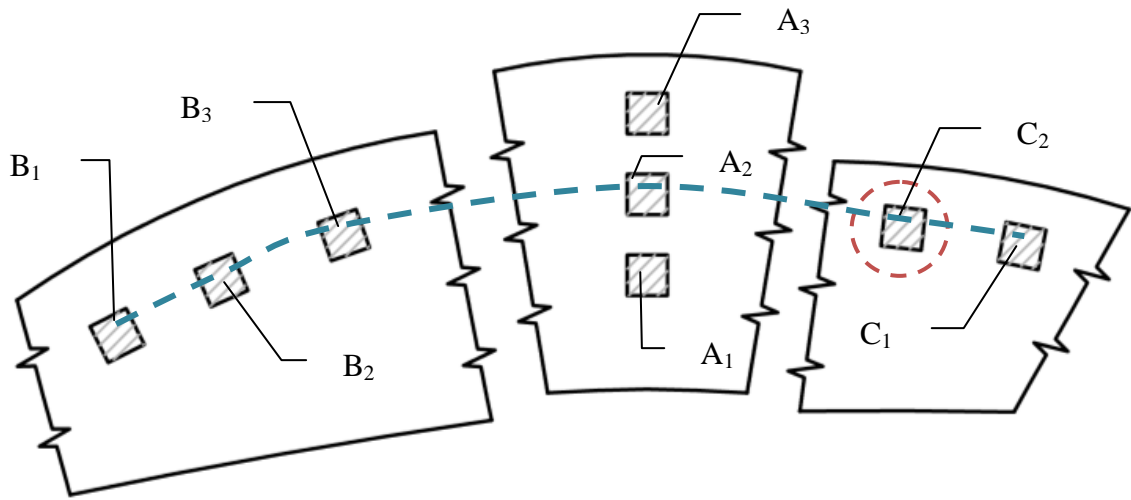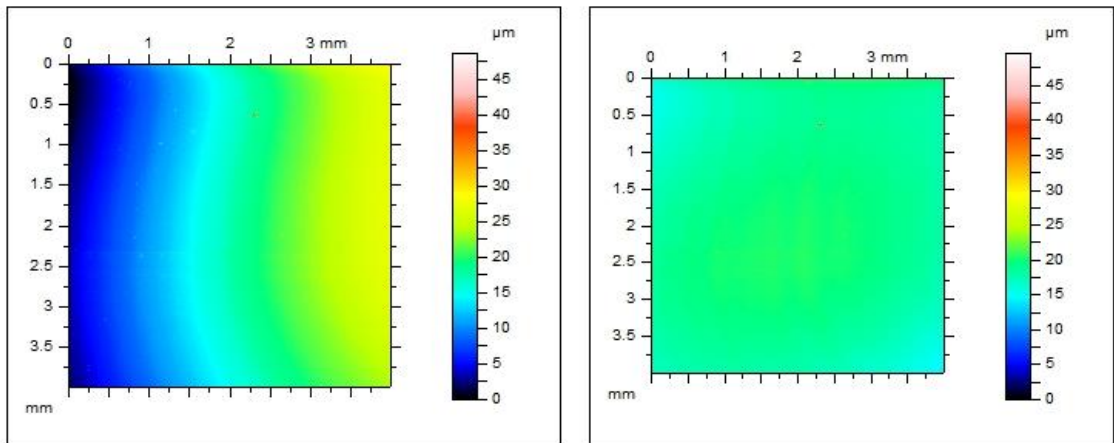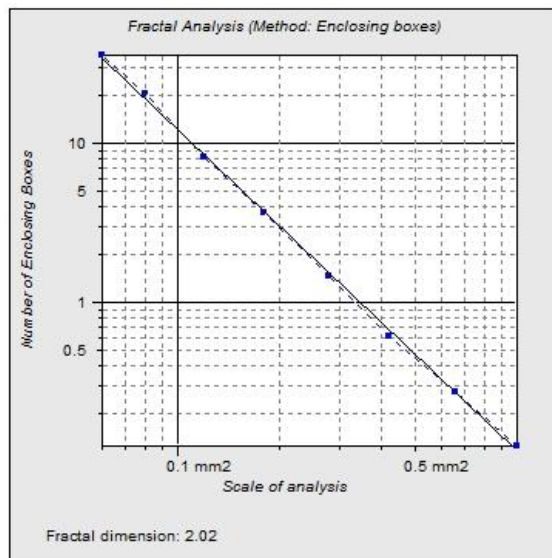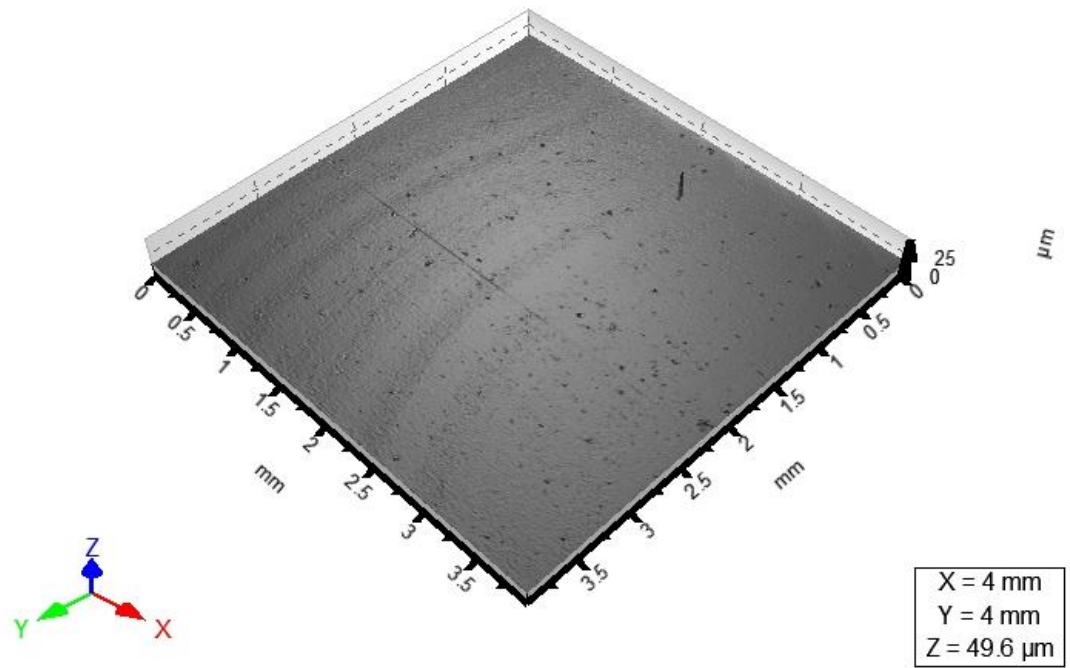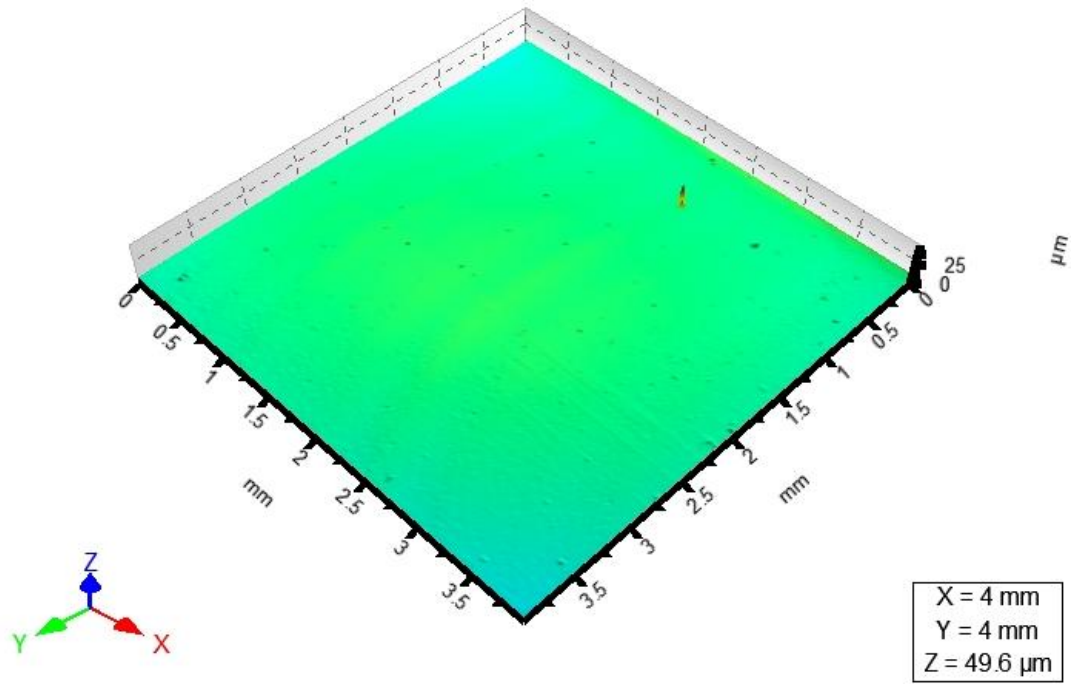*Fig. 60 – 3D projection of the sample C2*
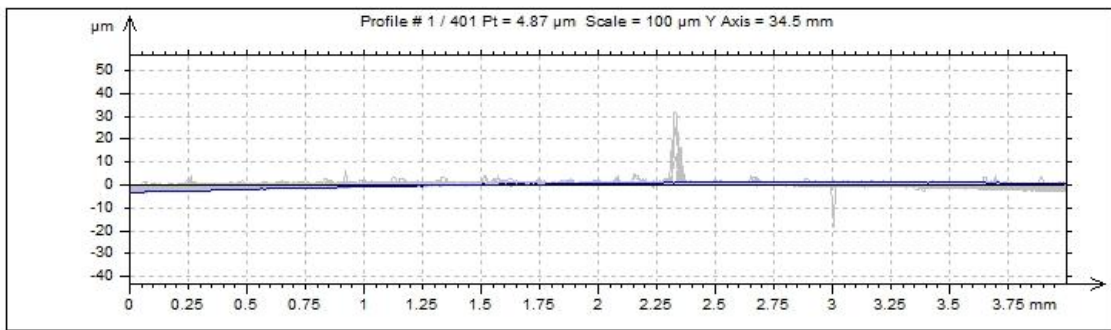
Graph 27 - Series of profiles of the sample C2, west – east direction (Y axis)

Tab. 27 – Statistical results of the sample C2 – Gauss filter, Y axis

ISO 4287		Mean	Std dev	Min	Max	Lower Quartile	Upper Quartile	Median
Amplitude parameters - Roughness profile								
Rp	µm	0.379	0.505	0.159	6.4	0.208	0.388	0.253
Rv	µm	0.239	0.202	0.134	3.92	0.19	0.248	0.213
Rz	µm	0.618	0.611	0.329	7.42	0.412	0.621	0.486
Rc	µm	0.334	0.678	0.139	10.5	0.205	0.297	0.239
Rt	µm	1.37	2.27	0.463	27	0.664	1.4	0.877
Ra	µm	0.0847	0.0339	0.0647	0.47	0.0755	0.0836	0.0792
Rq	µm	0.119	0.0951	0.0825	1.21	0.0935	0.113	0.101
Rsk		2.13	6.51	-47.7	49	-0.0117	1.74	0.31
Rku		36	116	2.08	1204	3.39	15.5	4.63
Material Ratio parameters - Roughness profile								
Rmr	%	76.1	40.7	0.249	100	67	99.9	99.8
Rdc	µm	0.159	0.0142	0.13	0.256	0.15	0.165	0.157

Tab. 28 - Statistical results of the sample C2 – Robust Gauss filter, Y axis

ISO 4287		Mean	Std dev	Min	Max	Lower Quartile	Upper Quartile	Median
Amplitude parameters - Roughness profile								
Rp	µm	0.502	0.638	0.19	7.71	0.278	0.526	0.339
Rv	µm	0.283	0.243	0.121	4.9	0.223	0.308	0.259
Rz	µm	0.785	0.714	0.403	8.2	0.528	0.813	0.623
Rc	µm	0.493	2.04	0.175	31.5	0.221	0.338	0.262
Rt	µm	1.89	2.76	0.63	31.5	1.02	1.89	1.3
Ra	µm	0.109	0.0329	0.0749	0.422	0.0891	0.118	0.105
Rq	µm	0.159	0.116	0.0915	1.46	0.115	0.167	0.143
Rsk		1.97	7.57	-44.9	60.6	-0.478	1.54	0.236
Rku		42.6	143	2.47	1236	4.8	16.6	7.85
Material Ratio parameters - Roughness profile								
Rmr	%	67.2	43.3	0.249	100	3.06	99.7	95.6
Rdc	µm	0.19	0.0128	0.157	0.221	0.18	0.2	0.19
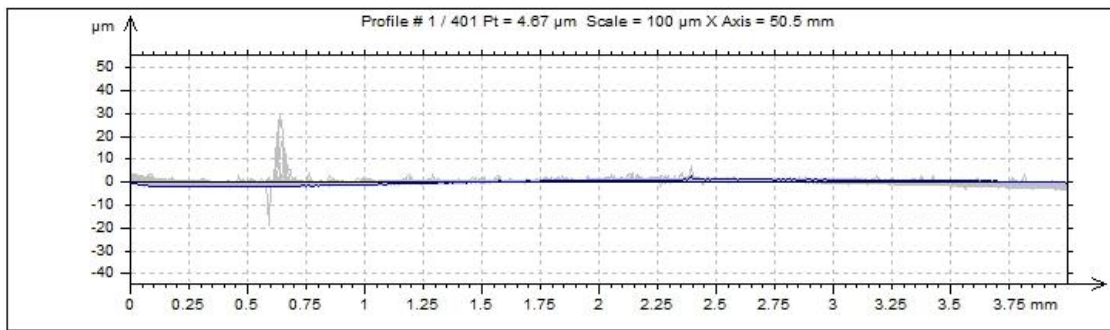
Graph 28 - Series of profiles of the sample C2, north - south direction (X axis)

Tab. 29 - Statistical results of the sample C2 – Gauss filter, X axis

ISO 4287		Mean	Std dev	Min	Max	Lower Quartile	Upper Quartile	Median
Amplitude parameters - Roughness profile								
Rp	µm	0.671	0.497	0.368	6.41	0.506	0.694	0.574
Rv	µm	0.202	0.15	0.106	2.73	0.157	0.209	0.178
Rz	µm	0.873	0.57	0.545	7.35	0.676	0.902	0.755
Rc	µm	0.493	1.55	0.159	26.4	0.235	0.443	0.302
Rt	µm	2.19	2.16	1.2	27.8	1.66	2.14	1.94
Ra	µm	0.0826	0.0345	0.0584	0.518	0.0716	0.0846	0.0772
Rq	µm	0.141	0.0858	0.09	1.21	0.115	0.145	0.127
Rsk		12.3	7.87	-68.7	61.7	8.75	14.5	11.3
Rku		149	162	26.7	1837	81.6	166	117
Material Ratio parameters - Roughness profile								
Rmr	%	3.12	8.23	0.249	83.1	1.05	1.87	1.33
Rdc	µm	0.108	0.019	0.076	0.258	0.0971	0.113	0.105

Tab. 30 - Statistical results of the sample C2 – Robust Gauss filter, X axis

ISO 4287		Mean	Std dev	Min	Max	Lower Quartile	Upper Quartile	Median
Amplitude parameters - Roughness profile								
Rp	µm	0.961	0.617	0.546	7.62	0.732	1.02	0.841
Rv	µm	0.245	0.244	0.088	4.77	0.175	0.265	0.211
Rz	µm	1.21	0.674	0.733	7.98	0.945	1.25	1.06
Rc	µm	0.762	2.28	0.212	31	0.319	0.741	0.426
Rt	µm	3.34	2.63	1.9	31.4	2.63	3.36	3.06
Ra	µm	0.114	0.0311	0.0795	0.467	0.0986	0.123	0.111
Rq	µm	0.211	0.101	0.129	1.42	0.174	0.221	0.197
Rsk		14.5	9.28	-87.6	96.9	11	16.9	14.1
Rku		162	238	29.1	3018	97.8	166	134
Material Ratio parameters - Roughness profile								
Rmr	%	1.13	0.444	0.249	3.74	0.738	1.25	0.977
Rdc	µm	0.15	0.0157	0.111	0.198	0.138	0.16	0.148

APPENDIX P I: RESULTS OF SAMPLE C1

Fig. 61 – Measuring places scheme – marking C1

Fig. 62 - Original and leveled plane of the sample C1


Graph 29 - Fractal dimension of the sample C1
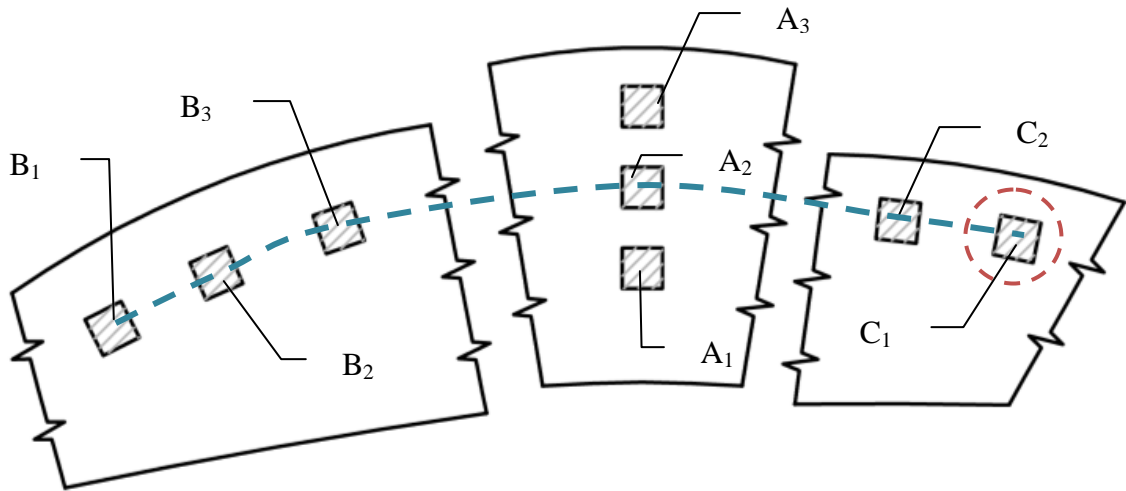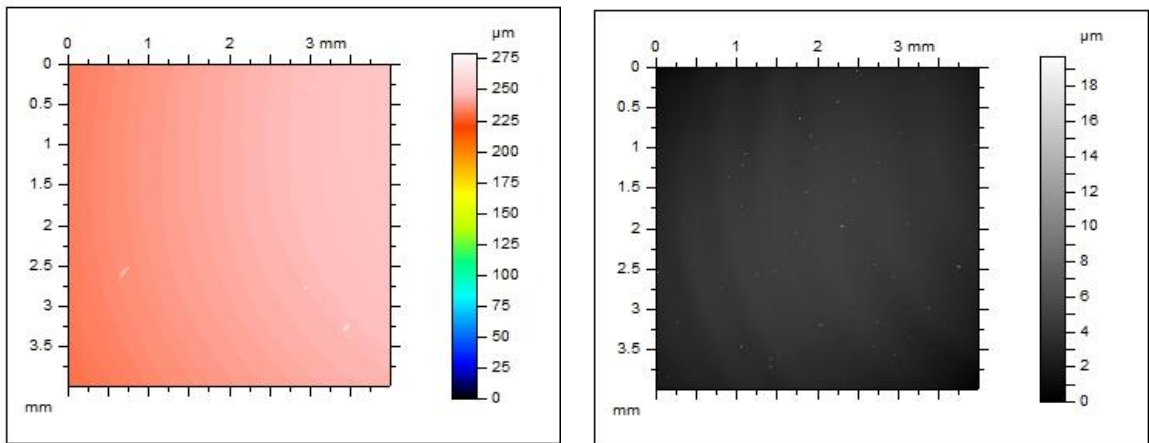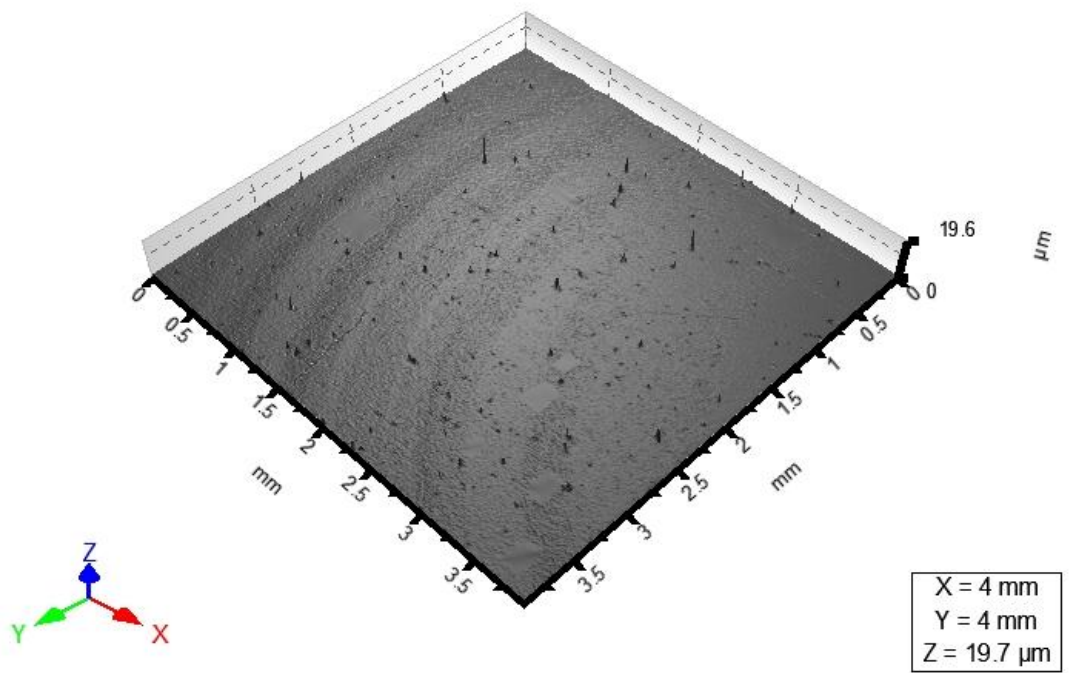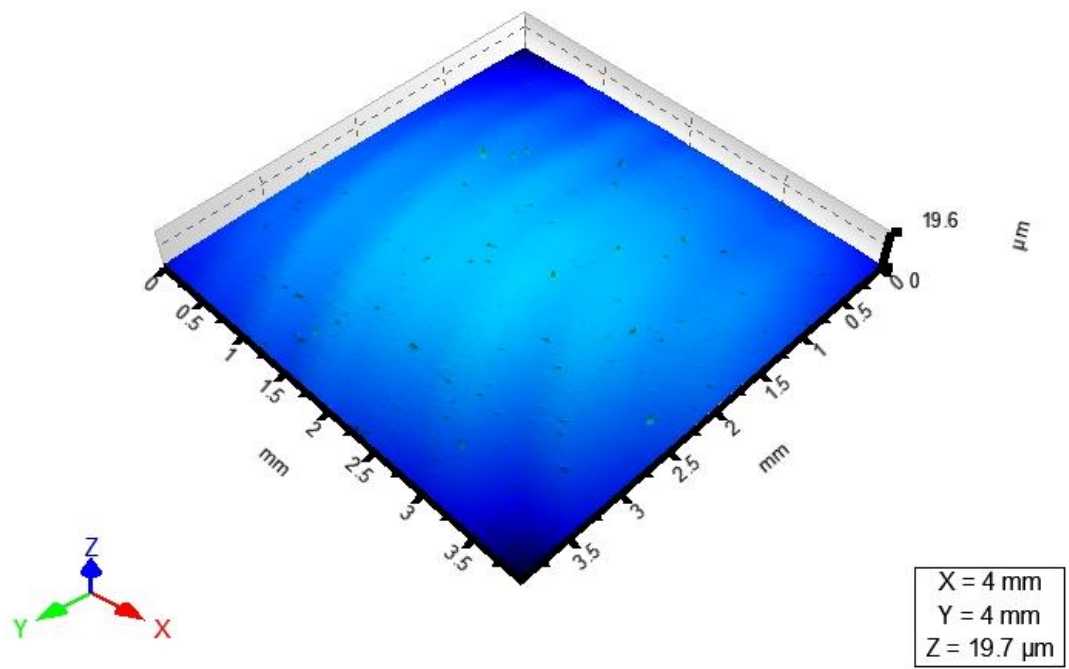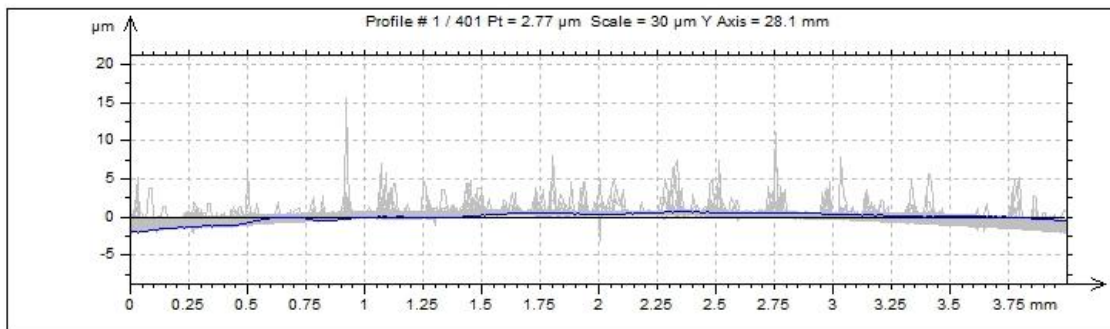
*Fig. 63 – 3D projection of the sample C1*

Graph 30 - Series of profiles of the sample C1, west – east direction (Y axis)

Tab. 31 – Statistical results of the sample C1 – Gauss filter, Y axis

ISO 4287		Mean	Std dev	Min	Max	Lower Quartile	Upper Quartile	Median
Amplitude parameters - Roughness profile								
Rp	µm	0.343	0.315	0.105	2.17	0.144	0.42	0.205
Rv	µm	0.153	0.0395	0.0939	0.47	0.129	0.165	0.145
Rz	µm	0.497	0.336	0.225	2.45	0.284	0.567	0.355
Rc	µm	0.27	0.285	0.0989	2.87	0.142	0.285	0.172
Rt	µm	1.3	1.25	0.312	8.63	0.488	1.67	0.762
Ra	µm	0.0616	0.015	0.0465	0.165	0.0527	0.0643	0.0567
Rq	µm	0.0905	0.0435	0.0555	0.351	0.0649	0.0983	0.0722
Rsk		5.68	10	-8.22	55.9	0.0574	6.39	0.758
Rku		92.2	194	2.6	1385	3.83	76.2	7.71
Material Ratio parameters - Roughness profile								
Rmr	%	68.9	45	0.249	100	0.883	99.9	99.8
Rdc	µm	0.114	0.0126	0.0877	0.167	0.106	0.119	0.112

Tab. 32 - Statistical results of the sample C1 – Robust Gauss filter, Y axis

ISO 4287		Mean	Std dev	Min	Max	Lower Quartile	Upper Quartile	Median
Amplitude parameters - Roughness profile								
Rp	µm	0.461	0.459	0.117	4.01	0.181	0.563	0.275
Rv	µm	0.178	0.0615	0.0848	0.984	0.147	0.188	0.166
Rz	µm	0.639	0.475	0.264	4.23	0.344	0.738	0.452
Rc	µm	0.31	0.416	0.103	5.56	0.15	0.324	0.188
Rt	µm	1.83	1.78	0.381	16	0.723	2.18	1.13
Ra	µm	0.0711	0.0138	0.0529	0.137	0.0619	0.0757	0.0677
Rq	µm	0.113	0.0569	0.0651	0.512	0.078	0.12	0.0905
Rsk		7.26	13.1	-17	86.4	0.161	8.26	1.53
Rku		135	306	2.42	2625	5.07	98.8	11.8
Material Ratio parameters - Roughness profile								
Rmr	%	60.5	47	0.249	100	0.473	99.9	98.6
Rdc	µm	0.139	0.0128	0.11	0.173	0.128	0.147	0.138
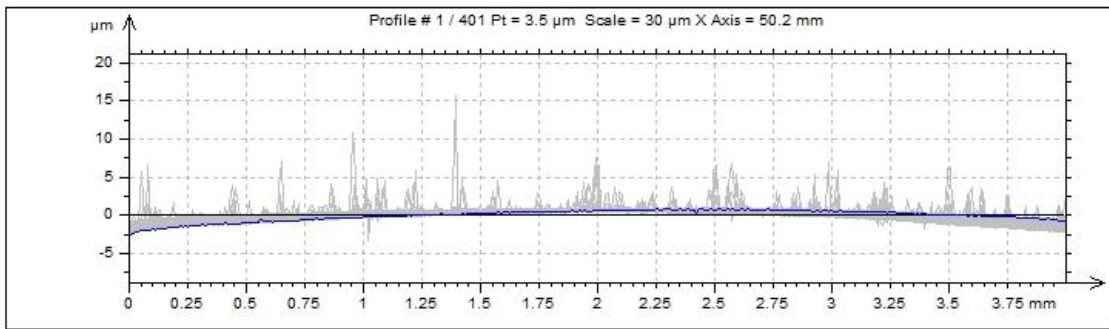
Graph 31 - Series of profiles of the sample C1, north - south direction (X axis)

Tab. 33 - Statistical results of the sample C1 – Gauss filter, X axis

ISO 4287		Mean	Std dev	Min	Max	Lower Quartile	Upper Quartile	Median
Amplitude parameters - Roughness profile								
Rp	µm	0.334	0.34	0.0684	2.42	0.112	0.434	0.2
Rv	µm	0.212	0.0592	0.0662	0.849	0.184	0.239	0.209
Rz	µm	0.545	0.37	0.145	2.79	0.317	0.647	0.4
Rc	µm	0.214	0.222	0.0657	1.98	0.106	0.214	0.133
Rt	µm	1.66	1.31	0.257	9.28	0.824	2.12	1.15
Ra	µm	0.0413	0.015	0.0234	0.14	0.0323	0.0439	0.0368
Rq	µm	0.0798	0.046	0.0354	0.366	0.0527	0.0876	0.062
Rsk		3	14.8	-16.3	77.9	-7.37	8.75	-2.29
Rku		178	243	5.43	2312	60.1	169	91.7
Material Ratio parameters - Roughness profile								
Rmr	%	65.7	46.6	0.249	100	0.565	99.9	99.4
Rdc	µm	0.0652	0.0115	0.0437	0.118	0.057	0.0712	0.0623

Tab. 34 - Statistical results of the sample C1 – Robust Gauss filter, X axis

ISO 4287		Mean	Std dev	Min	Max	Lower Quartile	Upper Quartile	Median
Amplitude parameters - Roughness profile								
Rp	µm	0.475	0.471	0.0699	4.16	0.171	0.594	0.294
Rv	µm	0.261	0.0811	0.0617	1.21	0.221	0.299	0.257
Rz	µm	0.736	0.497	0.193	4.47	0.43	0.867	0.558
Rc	µm	0.418	0.49	0.101	5.97	0.191	0.435	0.257
Rt	µm	2.32	1.8	0.367	16.4	1.15	2.89	1.66
Ra	µm	0.078	0.0158	0.0368	0.143	0.0689	0.0858	0.0769
Rq	µm	0.129	0.0569	0.0485	0.542	0.0957	0.139	0.111
Rsk		3.56	13	-10.1	75.5	-3.65	5.48	-1.6
Rku		133	263	3.29	2061	23	87.7	37.8
Material Ratio parameters - Roughness profile								
Rmr	%	54.4	47.6	0.249	100	0.277	99.5	88.3
Rdc	µm	0.141	0.0348	0.079	0.298	0.116	0.158	0.135